MODELS OF PREY CAPTURE IN LARVAL FISH

Promotor: dr. J.W.M. Osse, hoogleraar in de algemene dierkunde.
Co-promotor:dr. M. Muller, universitair docent m.b.t. de functionele morfologie
            en de biofysica.

Maarten R. Drost

MODELS OF PREY CAPTURE IN LARVAL FISH

INHOUD/CONTENTS

Cover: Wim Valen.

STELLINGEN

1

De energie gebruikt tijdens het opzuigen van een prooi is zeer laag. In een optimaal foerageermodel zijn energetische overwegingen om snel of langzaam te happen onbelangrijk, ook bij relatief kleine prooien.

Dit proefschrift

2

Voor visselarven is het essentieel om al vroeg in de larvale ontwikkeling nauwkeurig op een prooi te kunnen richten. Zonder nauwkeurig richten heeft het geen zin om snel te zwemmen of de kaken vooruit te steken (protrusie) tijdens de hap, hierdoor is het moeilijk snelle prooien te vangen.

Dit proefschrift

3

De grootte van structuren van visselarven kan niet nauwkeurig bepaald worden aan de hand van gefixeerd materiaal door de zeer grote en ongelijkmatige krimp tijdens fixatie.

Dit proefschrift

4

De theorie van 'punctuated equilibria' onderscheidt zich nauwelijks van fyletisch gradualisme met wisselende evolutiesnelheden.

Contra: S.J. Gould & N. Eldredge 1977. Punctuated equilibria:
The tempo and mode of evolution reconsidered. Paleobiology 3: 115-151.

5

De toegenomen invloed van beleidsgerichte academici op de natuurbescherming leidt tot een overdreven vereenvoudiging van doelstellingen, waarin 'zelfregulerende ecosystemen' ten onrechte de plaats dreigen in te nemen van bedreigde soorten of soorten-groepen.

6

Het nieuwe stelsel met AIO's (Assistenten In Opleiding) in plaats van wetenschappelijke assistenten leidt tot een degradatie van de academische promotie; gezien de salariëring lijkt de benaming 'Kandidaat Leerling Onderzoeker In Opleiding' beter dan AIO.

7

Gegeven de huidige formules voor het berekenen van de onderwijsbelasting voor docenten aan de LU, snijdt de docent van het Dierkunde practicum zich in zijn eigen vingers als hij er niet voor zorgt dat er genoeg deelnemers aan het 'niet-snijders' practicum zijn.

8

In de huidige biologie studie wordt geen aandacht besteed aan leren leiding geven, hoewel dit voor zeer veel banen essentieel is.

9

Vrouwen emancipatie is meer gebaat bij 'gedwongen' scholing, dan bij 'positieve' discriminatie.

10

De snelste en eenvoudigste manier om te bezuinigen op de collectieve sector is om uitgaven gewoon niet meer tot deze sector te rekenen.

11

De verplichting tot het toevoegen van stellingen aan een proefschrift kan het best afgeschaft worden: hoewel de stellingen ongetwijfeld het meest gelezen onderdeel van een proefschrift vormen, is hun rendement (in welke zin dan ook) zeer gering.

Inleiding

In dit proefschrift wordt de voedselopname door vislarven beschreven en geprobeerd een aantal processen ervan te begrijpen met behulp van fysische modellen. Dit proefschrift is een voortzetting van het onderzoek van Muller (1983) en van Leeuwen (1983), die de zuigende voedselopname bij volwassen vissen onderzochten met behulp van fysische modellen en de vergelijking van vissen met diverse typen van prooi opzuigen.

Het larvale stadium is het meest dynamische levensstadium van vissen. De morfologie verandert radicaal, de groei kan 5-30% per dag bedragen en de sterfte is hoog gedurende de eerste levensweken of maanden tot de metamorfose, al is over de exacte hoogte van de sterfte onder natuurlijke omstandigheden weinig bekend. Het is goed mogelijk dat in het larvale stadium bepaald wordt hoe groot de nieuwe jaarklasse wordt (Hunter, 1977). In de eerste dagen nadat ze uit het ei gekomen zijn, zijn de larven van de meeste soorten vissen nog zeer incompleet. Dit hangt af van o.a. de eigrootte. Hun energie krijgen ze uit de dooiervoorraad. Als de larve na een of enkele dagen het eerste voedsel uit het milieu kan opnemen, zijn de kaken en ogen functioneel en is de dooiervoorraad bijna opgebruikt.

Gedurende de eerste dagen van voedselopname verandert de larve sterk van vorm (allometrische groei). Toch moet het voedselopnameapparaat voortdurend functioneel zijn: vooral jonge larven kunnen maar kort vasten. Voor ansjovis (Engraulis mordax) neemt de maximale duur van de vastperiode voordat er sterfte optreedt, toe van 2,5 dag bij larven van 4 mm (eerste voedselopname) tot meer dan twee weken bij larven van 35 mm (Hunter, 1977). Bij het eten door vislarven kunnen we een aantal belangrijke deelprocessen onderscheiden (zie ook Blaxter (1986) voor een recent literatuuroverzicht): zwemmen (om het voedsel te bereiken), waarnemen (het voedsel ontdekken, meestal met de ogen (Blaxter,

1969)), voedselopname (het vangen van voedsel) en vertering. De eerste drie deelprocessen zijn vooral bij mariene larven bestudeerd, b.v. ansjovis, E. mordax (Hunter, 1972,1980) en haring, Clupea harengus (Blaxter & Staines, 1971). De beschrijvingen van voedselopname beperken zich tot het gedrag vlak voor de voedselopname. Door de korte duur van de hap (enkele milliseconden) en de geringe grootte van de larven (3-10 mm) is een gecompliceerde (dure!) opstelling met een filmcamera met hoge beeldsnelheid nodig is om betrouwbare waarnemingen te doen.

Over bouw en ontwikkeling van de darm (vertering) is wel veel onderzoek gedaan (b.v. Stroband, 1980).

De functionele morfologie onderzoekt de samenhang tussen bouw en functie in de biologie, voorzover deze vorm-functie relatie aanwezig is op grond van fysische principes. Deze relatie is ontstaan door evolutie en natuurlijke selectie. De vorm-functie relatie kan bestudeerd worden m.b.v. inductie: het vergelijken van vormen, of m.b.v. deductie: het opstellen van een fysisch model (Dullemeyer, 1974). Voor een functioneel morfologisch onderzoek is het ideaal als een aantal nauwverwante soorten of ontwikkelingsstadia van een soort voor een 'belangrijke' functie zowel verschillen in bouw als in uitoefening van die functie vertonen.

De voedselopname van visselarven vormt een dankbaar onderwerp voor functioneel morfologisch onderzoek:

1-de morfologie verandert sterk gedurende de larvale ontwikkeling (vormverandering);

2-Voedselopname is een vitale functie.

3-Tijdens de larvale ontwikkeling treedt een verandering in de manier van voedselopname op (functieverandering): bijna alle jonge larven zijn predatoren (jagers op relatief grote prooien), bij volwassen vissen komen ook allerlei andere typen van voedselopnames voor: filteren, predatie en voedselopname van

de bodem;

4-er treedt een grote sterfte op: er is dus de mogelijkheid voor selectie;

5-voedselopname stelt hoge mechanische eisen aan de vorm van de kop;

6-de hydrodynamische omstandigheden veranderen tijdens de groei (functie verandering).

De vraagstelling in dit onderzoek was:

-hoe verloopt de voedselopname bij larvale vissen (beschrijving)?

-wat is de oorzaak van het lage vangstsucces bij larvale vissen?

-wat is de invloed van de wrijving op voedselopname?

-kunnen we de vormverandering zoals die bij larven optreedt functioneel interpreteren?

-welke eigenschappen van prooien bepalen of ze door vislarven gevangen kunnen worden?

Proefdieren

Als proefdier is primair gekozen voor de karper, omdat daarvan een laboratoriumkweek aanwezig was, zodat gedurende het hele jaar larven aanwezig waren. Dit was van essentieel belang tijdens het ontwikkelen van de filmopstelling. Daarnaast is de snoek gebruikt omdat die gedurende zijn hele leven predatoir blijft, in tegenstelling tot de karper die na enkele weken overgaat op een langzamer type voedselopname, eten van de bodem. De prooiopname van snoeklarven van 14 mm, als ze voor het eerst eten, kon vergeleken worden met die van grote snoeken van bijna een halve meter. Door de grote range aan maten konden ook veranderingen die langzaam met de grootte van de vis optreden, bepaald worden. In deze studie is de prooiopname van slechts twee van de in totaal ongeveer 20.000 (Nelson, 1976) soorten vissen bestudeerd. Met behulp van modellen wordt geprobeerd uitspraken te doen die algemeen geldig zijn voor larven.

Modellen

Het gebruik van modellen maakt het mogelijk na te gaan welke parameters het belangrijkst zijn in een proces. Het maken van fysische modellen van biologische processen vraagt vaak een sterke versimpeling van de biologische complexiteit: in dit proefschift wordt de mondholte van een vislarve tijdens een hap voorgesteld door een expanderende cylinder. In werkelijkheid bestaat de wand van de mondholte uit een groot aantal botten, pezen en spieren, die op uiterst ingewikkelde manier bewegen. In de versimpelde voorstelling kan dan exact bepaald worden wat het effect van het veranderen van de ene (invoer) variabele is op een andere (uitvoer) variabele. Met het gebruikte hydrodynamische model van prooiopname kunnen we de maximale diameter van de bek vergroten, alle andere parameters constant laten en het effect op b.v. de watersnelheid bekijken. Het aangeven van optimale bewegingen bij een gegeven vorm van de gesimuleerde mondholte is vaak wel mogelijk, het aangeven van een optimale vorm moeilijker. Het terugvertalen van deze parameters naar echte structuren in de vis is zo moeilijk, omdat door de vereenvoudiging de afzonderlijke morfologische structuren (b.v. botten) niet als parameter in het model aanwezig zijn. Vandaar dat vaak alleen voor grote morfologische veranderingen aangegeven kan worden wat de effecten zijn op de prooiopname. Indien geen modellen gebruikt worden om te bepalen welke parameters belangrijk zijn, kan je 'alles' gaan meten zonder dat dit direct het inzicht vergroot (zie b.v. Hoda & Tsukahara, 1971 voor karperlarven). Als we willen weten wat een optimale beweging voor een vis bij een gegeven vorm van de mondholte is, zullen we dat moeten doen binnen reele beperkingen in de invoerparameters (b.v. de maximale kracht of het vermogen dat de vis op elk moment kan leveren). Tevens moet bekend zijn van welke parameters de prooivangst afhankelijk is: b.v. richten, snelheid van happen, volume van het opgezogen water of

vluchtbewegingen van prooien. De uitkomsten van modellen van deelprocessen geven vaak uitkomsten die wel goed interpreteerbaar zijn, b.v. de invloed op het vangstsucces van de nauwkeurigheid van het mikken op de prooi tijdens het happen.

Vislarven krijgen in het ei een bepaalde hoeveelheid energie mee. Deze kan worden aangewend voor de opbouw van verschillende functionele systemen: centraal zenuwstelsel, zintuigen, darm (verteringsapparaat), spieren of gebruikt worden voor voortbeweging. Naar de hoeveelheid energie die in elk ei aanwezig is kunnen we twee extreme typen in de reproductie onderscheiden: 'gokkers', met veel kleine eieren en 'op zeker spelers', met weinig grote eieren. De larven van gokkers zijn morfologisch nog weinig ontwikkeld als ze voedsel gaan opnemen. Gokkers lopen dus individueel aanzienlijke risico's, zoals het niet of te laat vinden van goed voedsel in een voldoende hoge concentratie, maar kunnen als populatie door het grote aantal nakomelingen een grote sterfte verdragen. De karper is een gokker, de snoek meer een intermediair.

Naast de voedselopname stellen ook zwemmen en waarschijnlijk ademhalen eisen aan structuren van de kop, zodat de aanwezige structuren een compromis vormen tussen tegenstrijdige eisen (Barel, 1985).

Prooiopname

Van de helft van de ongeveer 20.000 recente soorten vissen zuigen de volwassen exemplaren hun prooi op door een snelle expansie van de mondholte (b.v. de snoek). Deze expansie vindt meestal plaats binnen 100 ms en de prooien zijn relatief groot. Andere vissen vangen hun prooi door te filteren (b.v. de ansjovis), de prooien zijn dan vaak heel klein (algen en zooplankton); weer andere soorten nemen hun voedsel van de bodem op (bentische levenswijze), b.v. de karper. Hoewel in al deze gevallen een waterstroom wordt opgewekt, is deze veel trager dan bij de zuigende voedselopname. De larven van nagenoeg alle

vissoorten voeden zich tijdens de vroege larvale ontwikkeling met relatief grote prooien, die met een snelle zuigbeweging opgenomen worden (Hunter, 1980, voor mariene larven). Dit geldt dus ook voor de soorten waarvan de adulten filteren of de prooi vrij langzaam opnemen. Bij een karperlarve van 6 mm lengte wordt de prooi binnen 4-6 ms na het begin van bekexpansie opgenomen met een snelheid van ongeveer 0.3 m/s (50 lichaamslengtes per seconde). Ook tussen kleine larven komen echter al grote verschillen in voedselopname voor. Larven van vissen die ook als adult predator zijn, kunnen al jong overgaan op het eten van vis, bij Sphyraena (de barracuda) kan dit al bij een lengte van 5 mm plaatsvinden (Hunter, 1980). Een van de onderzochte vragen is of op fysische gronden aan te geven is dat voor kleine vislarven het opzuigen van prooien de enig mogelijke manier van voedselopname is.

Groei

Gedurende de larvale ontwikkeling treden sterke veranderingen op in de morfologie van de larve. Larvale en juveniele vissen zijn relatief eenvormig vergeleken met de uiteenlopende vormen zoals die voorkomen bij volwassen vissen (zie b.v. Russell, 1976). Tijdens de snelle groei treedt een sterke vormverandering op. In het algemeen geldt dat ze sterk lijken op de adulten, zodra ze ongeveer 20 tot 30 mm lang zijn. De verdere groei geschiedt voornamelijk zonder vormverandering (isometrische groei). Tevens worden de zintuigen en het zenuwstelsel beter ontwikkeld en treden verbeteringen op in de mogelijkheden voor voedselverwerking: bij de karper breken de keeltanden door op een leeftijd van 6-8 dagen en ook de enzymatische activiteit in de darm neemt toe.

Naast deze biologische veranderingen treden ook fysische veranderingen op door de groei. Voor zeer kleine vissen zijn wrijvingskrachten zeer belangrijk en traagheidskrachten van ondergeschikt belang. Voor grote vissen zijn de

traagheidskrachten overheersend. We kunnen zeggen dat larven in een 'stroperiger' omgeving leven dan grote vissen. Tijdens de groei veranderen dus de hydrodynamische eisen die aan de voedselopname gesteld worden.

Tijdens de eerste dagen van de larvale ontwikkeling kan de groei tientallen procenten per dag bedragen (60% per dag gedurende de eerste week bij karperlarven (Huisman, 1974)). Voor deze groei is een grote voedselopname nodig. Een geringe voedselopname kan leiden tot directe verhongering of via verzwakking tot verhoogde kans op predatie. Het aantal waargenomen prooien hangt af van de zwemsnelheid en van de afstand waarvan prooien kunnen worden waargenomen (ogen!). Het hangt natuurlijk ook af van de prooi-dichtheid en -zichtbaarheid). De fractie opgenomen prooien hangt onder andere af van het vangstsucces (fractie succesvolle happen). Dit vangstsucces neemt sterk toe gedurende de vroege ontwikkeling van vislarven. Een laag vangstsucces kan een gevolg zijn van slecht mikken of van het ontsnappen van de prooi.

Technische problemen

Als karperlarven beginnen te eten (2 dagen nadat ze uit het ei gekomen zijn), zijn ze ongeveer 5 mm lang en wegen ze 1 mg. Het zal duidelijk zijn dat geen druk- of snelheidsopnemers in de mondholte bevestigd kunnen worden, zoals bij volwassen vissen is gedaan (Osse, 1976; Muller & Osse, 1984; van Leeuwen & Muller, 1983 en referenties daarin). Er zijn snelle films (500-1150 beelden/s) gemaakt van etende larven. Er is gebruik gemaakt van een schaduw (silhouet) film techniek (Arnold & Nuttall-Smith, 1974). Hiermee kon de dieptescherpte een factor tien opgevoerd worden (tot 1 cm). Tevens kon ondanks de zeer korte belichtingstijden (tot 1/3000 s) met een 'normale' hoeveelheid licht volstaan worden. Hierdoor trad geen stress door te hoge lichtintensiteit op. M.b.v. een door de TFDL gemaakte filmtafel met spiegelopstelling kon gelijktijdig van onder en van opzij gefilmd worden. Uiteindelijk zijn films gemaakt waarbij de vis op

ware grootte op het negatief aanwezig was, zodat nauwkeurige metingen mogelijk waren. De prooi werd vastgeplakt aan een draadje (dikte 1/100 mm) en met een micromanipulator precies in het midden van het beeld gebracht. Een nieuwe methode werd beschreven om de volumeverandering van de mondholte nauwkeurig te bepalen aan de hand van filmbeelden (artikel 1).

Optimalisatie van prooivangst

Volgens de theorie van optimaal foerageergedrag moet een dier streven naar een maximale netto energieopname (zie b.v. Pyke, 1984). Er is alleen gekeken naar een optimaal hapgedrag, en b.v. het zoeken, verwerken en verteren van voedsel is niet mede beschouwd.

Een mishap kan het gevolg zijn van slecht mikken (de vis hapt op de verkeerde plaats) of van een vluchtreactie van de prooi (de vis hapt op de goede plaats, maar de prooi is daar niet meer) of een combinatie van deze twee. De strategie voor optimalisatie van de prooivangst hangt af van het relatieve belang van deze twee factoren. Een verbetering in de richtnauwkeurigheid van de larve vereist een goede waarneming van de prooi (ogen, zenuwstelsel) en een nauwkeurige beweging (spier-zenuwstelsel) om exact op die positie te happen. Beyer (1980) heeft met een mathematisch model het verband tussen onnauwkeurigheid van richten en het vangstsucces van larvale vissen op niet-bewegende prooien bepaald. Dit model is uitgebreid en de eerste metingen van de richtonnauwkeurigheid gedurende het happen van larven van karper en snoek worden gepresenteerd (artikel 3). Nauwkeurig richten is ook nodig om tijdens de prooiopname (hard) te kunnen zwemmen en de kaken vooruit te steken (protrusie), want beide zorgen voor een gerichte waterstroom. Deze snelle beweging en de hoge zuigsnelheid zijn vereist om het ontsnappen van prooien te voorkomen.

In hun morfologie vertonen karperlarven reeds vanaf de eerste voedselopname eigenschappen die waterstroom tijdens de voedselopname optimaliseren. De

kieuwspleet wordt tot het moment van het binnenspoelen van de prooi door het kieuwdeksel afgesloten (zodat daar geen instroom van water op kan treden) en de mondhoeken worden afgedicht door een roteerbaar maxillare (bovenkaak), zodat geen lekstroom langs de zijkanten van de mond optreedt (artikel 2). De invloed van grootte van de vis op het zuigproces is onderzocht in artikel 4. Omdat in het voor volwassen vissen ontwikkelde hydrodynamische model van voedselopname (Muller & Osse, 1978, 1984; Muller et al. 1982; van Leeuwen, 1984; van Leeuwen & Muller, 1984) de wrijving verwaarloosd is, kan het niet voor larven gebruikt worden. Daarom is het recent ontwikkelde programmapakket Odyssee van het Waterloopkundig Laboratorium gebruikt. Dit pakket neemt zowel instationaire effecten als de wrijving in beschouwing (beide effecten zijn zeer belangrijk in de waterstroom tijdens de voedselopname door larvale vissen). De biologische aannamen ('vertaling' van de vis in parameters van vorm en beweging) waren grotendeels gelijk aan de eerdere (zie Muller & Osse, 1984). De beschrijving van het model is gegeven in artikel 5. De invoergegevens zijn bepaald uit een snelle film (1125 beelden/s), waaruit beeld voor beeld de volumeverandering gemeten is. Het vermogen dat tijdens de hap door de larve geleverd wordt is berekend. Bij de gesimuleerde hap (naar de beweging van een karperlarve van 6,5 mm lengte) was de energie nodig om een bepaalde snelheid in de mondopening te halen 2,5 maal de energie die daarvoor zonder wrijving nodig geweest zou zijn. Met het model is ook het aanstroomveld voor de mond uitgerekend en daaruit de banen die waterdeeltjes daarin afleggen. We mogen aannemen dat prooien die zelf geen actieve bewegingen uitvoeren (vluchten), ongeveer de uitgerekende banen van waterdeeltjes volgen. Tevens zijn banen uitgerekend van deeltjes die wel actief bewegen: vluchtende prooien. De vluchtsnelheid die in het model gebruikt wordt, is zo gekozen dat hij lijkt op snelheden die echte prooien (watervlooien en roeipootkreeftjes) kunnen halen. Als de uitgerekende baan de mondopening

passeert, wordt de prooi opgenomen, anders kan hij ontsnappen. Op grond van deze berekeningen kan voorspeld worden welke typen prooien tijdens welke fase van de prooiopname nog actief aan een vislarve kunnen ontkomen (artikel 6)

Conclusies

1-Tijdens prooiopname door larvale vissen treden watersnelheden op, die in verhouding tot hun eigen grootte zeer hoog zijn: 0.3 m/s bij een larve van 6 mm.

2-Vanaf het moment van eerste voedselopname bezitten karperlarven morfologische aanpassingen aan het zuigen: de wangen kunnen naar buiten bewogen worden (abductie) en de mondbodem (hyoid) naar beneden, tevens worden de mondhoeken afgedicht door een roteerbaar maxillare en kan het kieuwdeksel dat de kieuwspleet tot na de prooiopname afsluiten.

3-De onnauwkeurigheid van mikken (in absolute maten) neemt toe tijdens de groei van de snoek. De relatieve onnauwkeurigheid (onnauwkeurigheid/lengte van de vis) neemt sterk af. Het vangstsucces op stilstaande prooien is een directe functie van de relatieve onnauwkeurigheid. Het berekende vangstsucces neemt bij snoek toe van 80% bij 12-14 mm lengte (net etend) tot 100% bij 60 mm. De relatieve onnauwkeurigheid van net etende karperlarven (6 mm) is veel groter dan van net etende snoeklarven (12-14 mm). Het berekende vangstsucces is daar 66%.

4-Er is geen oorzakelijk verband tussen de grootte van de prooi en de kans dat de prooi tijdens een hap gemist wordt, tenzij de prooi zo groot is dat hij niet door de mond past. Deze conclusie berust zowel op hydrodynamische gronden als op gemeten waarden van mik-onnauwkeurigheden en hun interpretatie met het model (artikel 3).

5-Zolang larven nog niet nauwkeurig kunnen mikken, moeten ze water ongericht aanzuigen, omdat ze de prooi dan ook nog aanzuigen als de prooi niet recht voor de bek is. Door hard zwemmen en protrusie ontstaat een gericht aanstroomveld.

Beide zijn in dit opzicht dus nadelig, het zijn echter de aangewezen manieren om prooien van een grotere afstand op te kunnen nemen (dit is vooral van belang bij prooien die (snel) kunnen ontsnappen). Uit films is gemeten dat protrusie afwezig is bij karperlarven die net beginnen met eten (6 mm), maar al duidelijk aanwezig is bij larven van 9 mm.

6-Jonge larven kunnen relatief het volume van de mondholte veel sterker vergroten dan volwassen vissen: dit kan beschouwd worden als een optimalisatie van prooivangst door het volume opgezogen water te vergroten: de kop van larven is relatief groot.

7-De energie die gebruikt wordt tijdens het opzuigen van een prooi is verwaarloosbaar klein ten opzichte van de energie die de larve verkrijgt als hij de prooi vangt (in de orde van 0,01% voor grote prooien tot 10% voor zeer kleine prooien). In een optimaal foerageermodel zullen energetische overwegingen dus onbelangrijk zijn in de strategie om langzaam of snel te zuigen.

8-Voor het genereren van hoge watersnelheden (ten opzichte van de mond) is het vermogen (energie per tijdseenheid) belangrijk, in deze context is de energie die tijdens het zuigproces gebruikt wordt wel belangrijk.

9-Slechts 40% van de geleverde energie tijdens het opzuigen van de prooi door een larvale karper van 6.5 mm is ooit in de waterstroom als kinetische energie aanwezig. De rest gaat direct verloren in wrijving.

10-Bij toenemende grootte van vissen neemt de invloed van de wrijving op het zuigen af. Gegeven de relatie tussen duur van het zuigproces en de grootte van de vis (gemeten bij snoek van 12 tot 485 mm lengte) is de spierspanning die nodig is om te happen minimaal bij de grootte waarop ze uit het ei komen. Voor nog kleinere vissen neemt deze spanning langzaam toe (bij steeds kleinere grootte), voor grotere vissen neemt deze snel toe (met toenemende grootte). Op grond van spierspanning is geen minimale grootte voor vissen aan te geven om het

voedsel zuigend op te nemen, eerder een maximale grootte. Bij het uit het ei komen lijkt de benodigde spierspanning voor het zuigen minimaal, zodat daar geen optimale vorm nodig is.

11-De interactie tussen vluchtende prooien en de zuigstroom van vislarven bepaalt welke typen prooien opgenomen kunnen worden. Bij jonge larven met een korte duur van het zuigproces (b.v. minder dan 10 ms) is het belangrijker dat ze laat door hun prooi ontdekt worden dan dat ze een maximale zuigsnelheid halen. Bij larven waarbij de hap langer duurt (b.v. 20 ms of meer) is een grote snelheid wel belangrijk. Dit komt omdat het ongeveer 10 tot 20 ms duurt voordat een watervlo of roeipootkreeftje de maximale snelheid bereikt.

12-Tijdens het opzuigen van de prooi door een karperlarve treden enorme versnellingen van het aangezogen water op (tot 800 m/s^2 in de mond opening). Als een prooi in het gebied van deze hoge versnellingen terecht komt kan hij niet meer ontsnappen.

13-Dit onderzoek biedt een basis voor de vergelijking van de verschillende soorten vislarven in het Nederlandse binnenwater en misschien voor de voedselopname van vislarven in kweekvijvers.

Literatuurlijst

Arnold, G.P. & Nuttall-Smith, P.B.N., 1974. Shadow cinematographyof fish larvae. Mar. Biol. 28: 52-53.

Barel C.D.N., 1985. A matter of space, constructional morphology of cichlid fishes. Proefschrift, Rijksuniversiteit Leiden.

Beyer, J.E., 1980. Feeding success of clupeoid fish larvae and stochastic thinking. Dana 1: 65-91.

Blaxter, J.H.S., 1969. Development: eggs and larvae. In: W.S. Hoar & D.J. Randall (eds.). Fish Physiol. 3: 177-252. New York: Academic Press.

Blaxter, J.H.S., 1986. Development of sense organs and behaviour of teleost larvae with special reference to feeding and predator avoidance. Trans. Am. Fish. Soc. 115: 98-114.

Blaxter, J.H.S. & Staines, M.E., 1971. Food searching potential in marine fish larvae. In: Crisp, D.J. (ed.) Fourth European marine Biology Symposium. Cambridge: University Press.

Dullemeyer, P., 1974. Conceps and approaches in animal morphlogy. Assen, the Netherlands: Gorcum.

Hoda S.M.S. & Tsukahara, H., 1971. Studies on the development and relative growth in the carp, Cyprinus carpio. J. Fac. Agr. Kyushu Univ. 16: 387-509.

Huisman, E.A., 1974. Optimalisering van de groei bij de karper (Cyprinus carpio L.). Proefschrift Landbouwhogeschool Wageningen.

Hunter, J.R., 1972. Swimming and feeding behavior of larval anchovy, _Engraulis_ _mordax_. Fish. Bull. U.S. 70: 821–838.

Hunter, J.R., 1977. Behavior and survival of northern anchovy _Engraulis_ _mordax_ larvae. Cal. Coop. Fish. Invest. Rept. 19: 138–146.

Hunter, J.R., 1980. The feeding behavior and ecology of marine fish larvae. In: Bardach, J.E., Magnuson, J.J., May, R.C. & Reinhart, J.M. (Eds). Fish behavior and its use in the capture and culture of fishes. ICLARM Conference Proceedings 5, 512 pp. ICLARM, Manilla, Philippines.

Leeuwen, J.L. van, 1983. Optimum prey capture techniques in fish. Proefschrift, Landbouwhogeschool Wageningen.

Leeuwen, J.L. van, 1984. A quantitative study of flow in prey capture by Rainbow Trout, with general consideration of the actinipterygian feeding mechanism. Trans. zool. Soc. Lond. 37: 171–227.

Leeuwen, J.L. van & Muller, M., 1983. The recording and interpretation of pressures in prey sucking fish. Neth. J. Zool. 33:425–475.

Leeuwen, J.L. van & Muller, M., 1984. Optimum sucking techniques for predatory fish. Trans. zool. Soc. Lond. 37:137–169.

Muller, M., 1983. Hydrodynamics of suction feeding in fish. Proefschrift, Landbouwhogeschool Wageningen.

Muller, M., & Osse, J.W.M., 1978. Structural adaptations to suction feeding in fish. Proc. Zodiac Symp. 'On adaptation'. Wageningen: Pudoc.

Muller, M., & Osse, J.W.M., 1984. Hydrodynamics of suction feeding in fish. Trans. zool. Soc. Lond. 37: 51–135.

Muller, M., Osse, J.W.M., & Verhagen, J.H.G., 1982. A quantitative hydrodynamical model of suction feeding in fish. J. theor. Biol. 95: 49–79

Nelson, J.S., 1976. Fishes of the world. New York: Wiley.

Osse, J.W.M., 1976. Mecanismes de la respiration et de la prise des proies chez _Amia calva_ L.. Abstract. Rev. Trav. Inst. Peches Marit. 40: 701–702.

Pyke, G.H., 1984. Optimal foraging theory: a critical review. Ann. Rev. Ecol. Syst. 15: 523–575.

Russell, F.S., 1976. The eggs and planktontic stages of British marine fishes. 524 pp. London: Academic Press.

Stroband, H.W.J., 1980. Structure and function of the digestive tract in the grasscarp. Proefschrift, Landbouwhogeschool Wageningen.

A simple method for measuring the changing volume of small biological objects, illustrated by studies of suction feeding by fish larvae and of shrinkage due to histological fixation

M. R. Drost and J. G. M. van den Boogaart

Department of Experimental Animal Morphology and Cell Biology, Agricultural University, Marijkeweg 40, 6709 PG Wageningen, The Netherlands

(With 1 plate and 5 figures in the text)

A simple method has been devised to determine dynamic changes in volume of biological objects of a 'smooth' form. The method requires two perpendicular views (side and bottom). The method can be used also in static volume changes. Differential changes in length, width and height can be quantified. The volume of the object is approximated by a series of ellipses. The length of the axes of the ellipses is determined from the two views. Possible sources of error are discussed. The method is applied in a study of static volume changes of fish larvae due to fixation and in a study of the dynamic volume change of the mouth cavity of carp larvae, increasing their head volume 30% in 8 ms, when sucking prey.

Contents

Introduction

It is difficult to determine dynamic volume changes, such as those occurring in a beating heart, a pulsating vacuole or the rapid changes in volume of the mouth cavity of fish larvae when sucking prey, the duration of the latter process being much less than 30 ms. We have developed an accurate method to determine these changes from movie films with simultaneous views from below and from the side. The method can be used also for static volume determination, e.g. the magnitude of the shrinkage during histological fixation. To our knowledge, no quantitative method exists for dynamic volume determination. For static volume determination, some alternatives exist, e.g. determination of volume by submersion, determination of volume from weight (and density) and reconstruction from microscopical serial sections (see e.g. Aherne & Dunnill, 1982). The advantages of our method compared to determination from submersion or weighing are: 1. the volume of a part of an object can be determined without damaging the object and 2. separate effects of length, height and width shrinkage can be determined and differential changes in height

and width of the object can be quantified. The advantage of the ellipse method compared to reconstruction are: 1. Effects of histological fixation are avoided (they may be very large, and not constant in all directions, see the section on 'Shrinkage') and 2. Reconstruction is much more laborious. The accuracy of the three alternatives will be slightly higher than with the ellipse method, e.g. the weight in fish larvae (40–310 mg) can be determined with a coefficient of variation of 1·14% (Lockwood & Daly, 1975).

Ellipse method

If the form of an object is 'smooth', i.e. without appendages or considerable surface irregularities, each of its cross-sections can be approximated by an ellipse. The error caused by deviation from the ellipse form ('type 1 error') is discussed in the section 'Errors'. The entire object thus consists of a series of ellipses. The length axis of the object has to be chosen carefully. In principle, it is possible to define a straight or a curvilinear length axis. For a straight axis, its origin and direction must be specified. For a curvilinear axis, one must define the axis over the whole length of the object, either analog by a mathematical function, or discrete by specifying the coordinates of many points. In our problems, the objects were well described with straight axes. We will further leave out curvilinear axes. Even with a straight axis (in a straight object!), it was sometimes difficult to determine its exact position.

The area of an ellipse is determined by the length of its 2 axes:

$$A = \pi \, r_s \, r_l$$

where A = area of ellipse; r_s—short radius = length of short axis of the ellipse; r_l—long radius = length of long axis of the ellipse.

To avoid confusion with the length axis of the object, we use 'short radius' for the length of the short axis of an ellipse and 'long radius' for the length of the long axis. Both radii of each ellipse can be determined from 2 views (photographs) perpendicular to each other and perpendicular to the length axis of the object, i.e. a side view and a bottom view (Fig. 1). It appeared practical to digitize the coordinates of the outline of the object with an x-y tablet and to determine at many points (e.g. 100) the 2 radii. Both radii are perpendicular to the length axis. The volume of the object is the integral of the area of the cross-sectional areas (= ellipses) over the length of the object.

Errors

There are three sources of error: 1. The assumption that the cross-sectional areas are ellipses; 2. Difficulty in aligning both views (see e.g. Fig. 1) and 3. Difficulty in making views exactly parallel to the radii of the ellipse.

Type 1. The magnitude of a type 1 error has to be estimated for each problem. This can be done by comparing the actual cross-sectional area with the cross-sectional area calculated with the ellipse method. From e.g. microscopical cross-sections, the actual cross-sectional area can be calculated with a digitizer or a point lattice. The radii of the ellipse can be measured from the same section.

Type 2. A type 2 error can be avoided by aligning structures based on clues visible in both views, for example chromatophores in our experiments using fish larvae.

Type 3. The magnitude of a type 3 error can be calculated. The error in the measurement of the radii of the ellipse is zero in perpendicular projection, as ideally occurs in both views in our method. The measured radius of a projected ellipse in non-perpendicular projection depends on the angle between the actual and ideal plane of projection, the 'deviation angle', and on the ratio of both radii. The relation between the measured radius and the deviation angle is given in Fig. 2a.
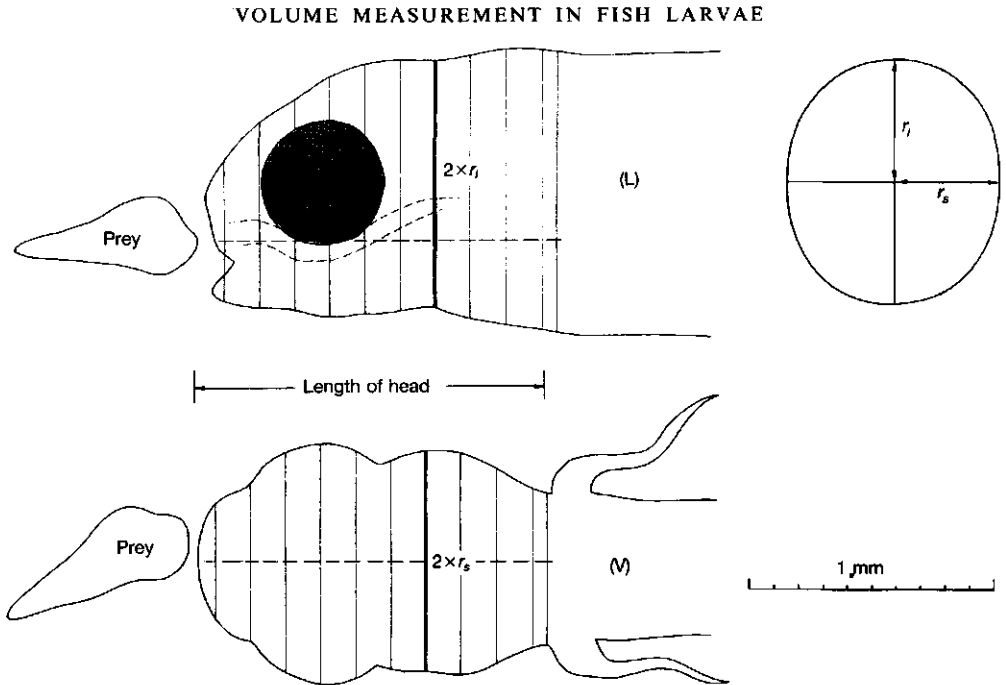
VOLUME MEASUREMENT IN FISH LARVAE

FIG. 1. Example of determination of volume from two perpendicular views (the head of a prey-sucking carp larva, drawn after Plate Ic). The short radius r_s of the i-th ellipse is measured in the ventral view (V), long radius r_l in lateral view (L). Total volume of the head is the integral of the cross-sectional areas over the length of the head. Normally, 100 cross-sectional areas are calculated from 0.5% to 99.5% of the length of the head. Here 10 pairs of radii are indicated, only the 7th ellipse is drawn. The pecked line is the length axis of the mouth cavity.

This relation is periodic with 180°. In most problems it will be possible to achieve a deviation angle less than 10°, in extreme cases perhaps 30°. Obviously, the magnitude of the error strongly depends on the ratio R (long radius/short radius). For $R = 1$ (i.e. a circle) the error is 0 for all deviation angles. The underestimation of the long radius increases from 1.5% ($R = 1.5$) to 3% ($R = 10$) for a deviation angle of 10°. The overestimation of the short radius is much greater for this deviation angle: 1.5% ($R = 1.5$), 3% ($R = 2$), 9% ($R = 4$), 27% ($R = 10$). If the views are absolutely perpendicular to each other (for example because they are made simultaneously, one direct and one via a mirror set at 45°), the relative error in calculated area (Fig. 2b) is less than the relative error in calculated short radius (Fig. 2a). This occurs because an overestimation of the short radius is coupled with an underestimation of the long radius, so the error is partly compensated. The calculated lengths of long and short radius are complementary, i.e. the calculated length of the long radius at a deviation angle a is equal to the calculated length of the short axis at a deviation angle 90°-a. So, the error in calculated area is periodic with 90°. Maximal error occurs at a deviation angle of 45°. For a deviation angle of 10°, the overestimation of area increases from 0.5% ($R = 1.5$), 1.5% ($R = 2$), 6.5% ($R = 4$) to 24% ($R = 10$). If both deviation angles are independent (i.e. both views are not made simultaneously with a mirror), the error in calculated area is dependent on both deviation angles. The error for each radius can be calculated from Fig. 2a; in these cases the error in the calculated area may be bigger or smaller than those indicated in Fig. 2b.
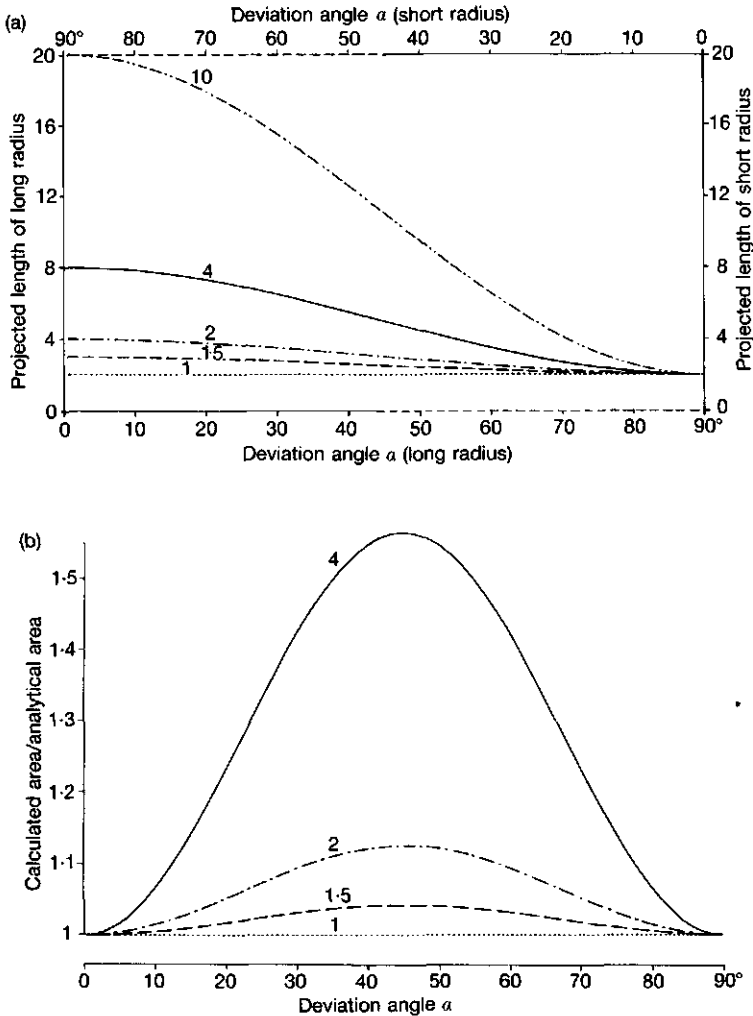
M. R. DROST AND J. G. M. VAN DEN BOOGAART

FIG. 2. Influence of non-perpendicular projection on the measured length of the radii (a) of the ellipse and its calculated area (b). Alpha (a) is the angle in which the angle of projection deviates from the ideal plane (deviation angle). An $a > 45°$ is not realistic, in fact the projection is then on the perpendicular plane with a deviation angle of $90°\text{-}a$. R is the ratio between the long and the short axis. Its value is indicated above each curve. It has a minimum of $R = 1$: a circle. (a) Calculated length of long radius (left y-axis) as function of the deviation angle (lower x-axis, left half) and calculated length of the short radius (right y-axis) as function of the deviation angle (upper x-axis, right half). The short radius is always taken with a length 2, the (non-projected) length of the longer radius varies with R (from 2-20). Non-realistic parts of x-axes are stippled. (b) Formfactor of the ellipse, i.e. (calculated area of the projected ellipse)/(analytical area of the ellipse), provided that both views are absolutely perpendicular. Overestimation of the short radius is partly compensated by underestimation of the long radius.

VOLUME MEASUREMENT IN FISH LARVAE

Example 1: shrinkage

Shrinkage of tissue during successive steps of fixation in Bouins fixative is determined for larval carp via the ellipse method. Photographs from above and from the side (not simultaneously) are made from alive anaesthetized (MS 222) larvae and from deep-frozen (in liquid nitrogen) or fixed larvae. Measurements were made on whole fish exclusive of head and fins. Due to different abduction of the walls of the mouth cavity, the volume of the head can increase by about a factor 2 in living larvae, as occurs during e.g. suction feeding.

Type 1 errors (deviation from ellipse form). Type 1 errors are measured to be less than 10%.

Type 2 errors (non-aligned views). The chromatophore pattern on the skin allowed accurate alignment of the views. Errors are virtually absent; they are estimated to be less than 1%.

Type 3 (deviation angle). Deviation angle was always less than 5°. This accuracy is easily obtained in static measurements. The ratio between long and short radius (R) was about 1·5 to 3, only in the tip of the caudal peduncle was it up to 10. Mean ratio R of a fish was always less than 3. So the error is less than 1%.

The measurements on frozen larvae are less accurate than the others, because the photographs had to be taken quickly (so the deviation angle was greater) and frost blurred, and to some degree enlarged, the outlines of the larvae.
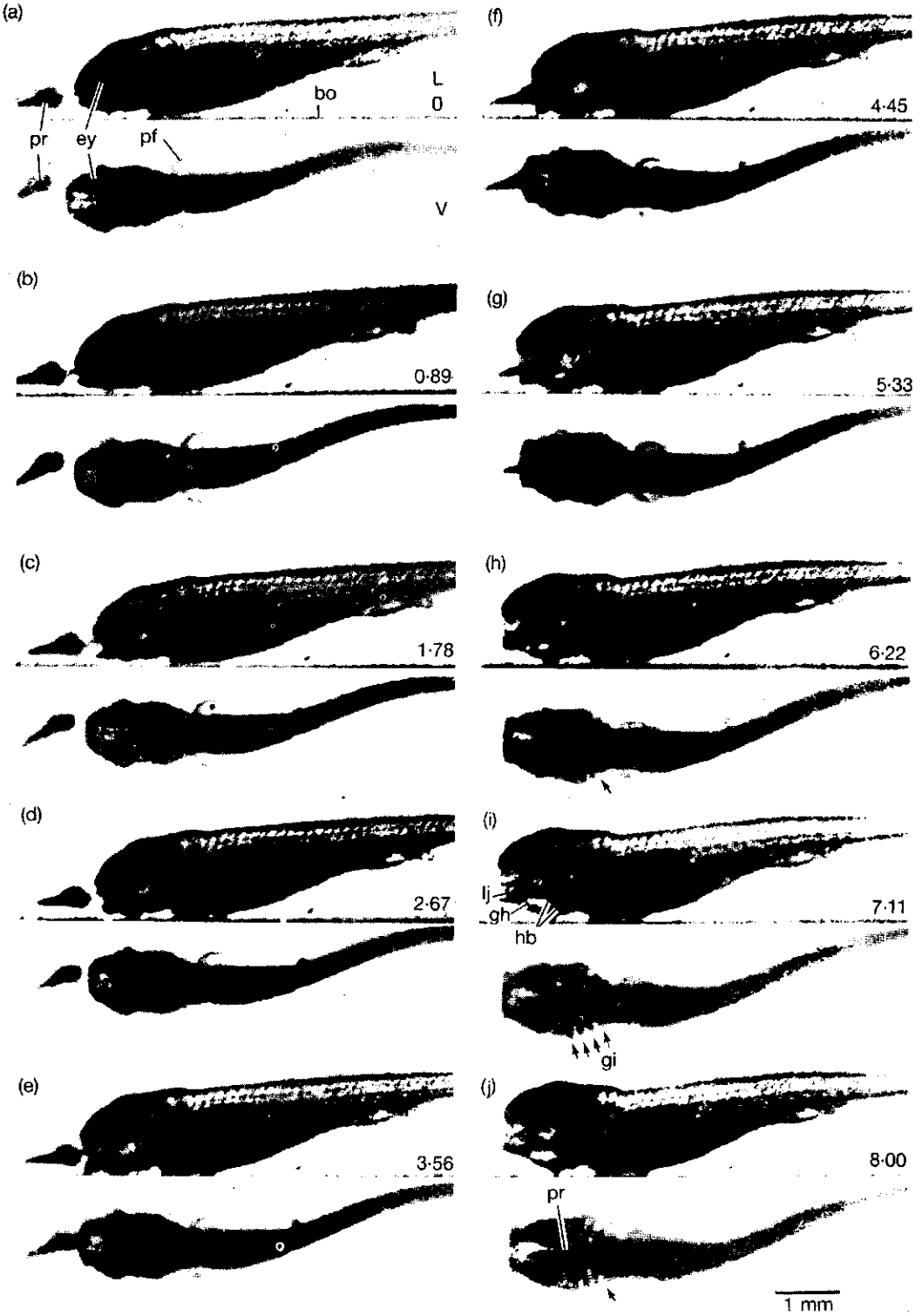
The results are given in Table I. The shrinkage after fixation is quite extensive for small larvae, about 60% in volume, and less for large larvae, about 30%. The shrinkage in cross-sectional area is approximately proportional to shrinkage in length to the second power. The shrinkage in width, however, is only about 30% of the shrinkage in height (range 17–41%). The explanation for this differential shrinkage is unclear. It causes a form distortion (change in ratio between width and height) of about 25%. Such form distortions cause serious errors in reconstructions after microscopical serial sections of fixed fish larvae. After freezing in liquid nitrogen, the cross-sectional area of large larvae increases (insignificantly) and their length decreases significantly (5%, Student's t-test), but with a large variation. The explanation of this difference is also unclear.

TABLE I
Percentage shrinkage relative to the live situation

	small larvae		large larvae		
	fixed $n = 10$	dehydrated $n = 10$	frozen $n = 5$	fixed $n = 5$	dehydrated $n = 5$
height	40·4± 8·6***	43·4± 5·3***	−5·8±5·0−	19·6±3·8***	21·9±6·0**
width	14·7±15·4**	17·6±10·4***	1·6±2·7−	3·4±2·9*	6·5±2·3**
area	44·6±11·5***	48·9± 5·9***	−2·6±5·4−	21·8±5·5***	26·0±6·5***
length	20·8± 4·9***	26·5± 4·8***	13·8±6·3**	9·7±2·4***	10·6±1·6***
volume	56·4± 8·0***	62·6± 4·0***	11·5±9·6*	29·3±5·7***	33·8±5·9***

Student's t-test – not significant; * 5%; ** 1%; *** 0·1%

Shrinkage of carp larvae exclusive of the head region calculated with the ellipse method. Small larvae ($n = 10$, SL $= 5·50±0·38$ mm) and half of the large larvae ($n = 5$, SL $= 13·07±0·82$ mm) were fixed in Bouins fixative, measured and afterwards dehydrated in alcohol (70%, 80%, 90%, 96%, 100%) and remeasured. Other large larvae ($n = 5$, SL $= 12·89±1·19$ mm) were frozen in liquid nitrogen. Percentage shrinkage in the tissues between the pectoral girdle and caudal peduncle is determined relative to the live, anaesthetized situation. Expansion is depicted negative. Mean height, width and area shrinkage per fish are calculated as the mean of the shrinkage of its 100 cross-sectional areas. Indicated values are inter-individual means and standard deviations.

(a) pr ey pf bo L 0 V

(b) 0·89

(c) 1·78

(d) 2·67

(e) 3·56

(f) 4·45

(g) 5·33

(h) 6·22

(i) lj gh hb gi 7·11

(j) pr 8·00

1 mm

VOLUME MEASUREMENT IN FISH LARVAE

Example 2: suction feeding

Calculation of the water velocity and the pressures in the mouth cavity (= buccal + opercular cavities) of a prey-sucking fish, with the hydrodynamical model of Muller and co-workers (Muller, Osse & Verhagen, 1982; van Leeuwen, 1984), is possible if the change of volume of the mouth cavity is known. They estimated this volume by determining the mouth radius and the distance between the operculars, assuming a conical profile. A considerably improved estimation of the flow volume can be made with the ellipse method.

Plate I presents a series of frames from a movie (1125 frames/s) of a carp larva (*Cyprinus carpio*, total length 6·5 mm), while sucking a nauplius of brine shrimp (*Artemia salina*). A shadowgraphic filming technique was used (Arnold & Nuttall-Smith, 1974). The fish is partly transparent: in Plate I the hyoid bar and the geniohyoid muscle can be seen in the lateral view, g–j; the gills in the ventral view, h–j; the prey can be seen moving inside the mouth cavity, f–j. In the beginning of the suction process the posterior (opercular) side of the mouth cavity is closed and only the mouth is open, so every change in volume of the mouth cavity invokes a flow through the mouth aperture. Later, the opercular valves open (Plate I, closed in h, see arrow; opening in i and open in j, see arrow). The mouth cavity is then open at both ends and volume flow through the mouth can no longer be calculated in a simple way, because the water can also flow through the opercular slits with an a priori unknown velocity. The volume of the head of the suction act of Plate I, calculated with the ellipse method, is given in Fig. 3a, the resulting flow rate in Fig. 3b.

The accuracy of the method depends on the magnitude of the three types of error.

Type 1 (deviation from ellipse form). The check for type 1 errors is whether 'ellipse areas' of microscopical serial sections of carp larvae correspond with measured areas. The 'ellipse area' was calculated by measuring the greatest horizontal and vertical distance in each slide. The real area of the outline was measured with a digitizer (Summagraphics supergrid) connected to a computer (Digital Minc 11). Figure 4 gives the results for a 15 mm carp. At most places, the difference between measured and calculated area is very small. At the eyes and at the posterior side of the mouth cavity, the ellipse method slightly overestimates the volume. Total overestimation is 3·3%. So the ellipse method produces reliable results in this respect.

Type 2 (non-aligned views). In the shadowgraphic movies (Plate I), no surface structures are visible, only outlines. Characteristic points, e.g. the eyes, are visible in all frames. We estimate type 2 errors to be less than 5%, with an important systematic component: the error from one frame to the next will be less than 1%, because successive frames are much alike.

Type 3 (deviation angle). Type 3 errors will be very small, because the ratio between the radii of each ellipse (R) varies between 1 and 2 (see Figs 1, 2b; Plate I). If the deviation angle is constant during the successive frames of the film, the relative error in the change in volume between two frames (resulting from deviation angle) is as big as the relative error in volume, i.e. it is a systematic

PLATE I. Selected frames of a shadowgraphic movie film (1125 frames/s) with a lateral (L) and a ventral (V) view of a carp (*Cyprinus carpio*) larva (total length 6·5 mm), when feeding on a nauplius of brine shrimp (*Artemia salina*). The fish is just above the bottom of the aquarium. The ventral view is obtained via a mirror set at 45°. Ventral and lateral view are thus absolutely synchronous. Time is indicated in ms, starting from the last frame with a yet closed mouth (frame a). Bar denotes 1 mm. The fish is partly transparent. The pectoral fins are visible in the ventral view (pf in a), not in the lateral view. They become adducted during the feeding sequence. The hyoid bars and the geniohyoid muscle are visible in frames g–j, lateral view; the gills in frames h–j, ventral view (arrows in i). The prey can be seen moving inside the mouth cavity in frames f–j, best in the ventral view (pr in j). hb–hyoid bar; gi–gill; gh–geniohyoid muscle; lj–lower jaw; pf–pectoral fin; pr–prey; ey–eye; bo–bottom.
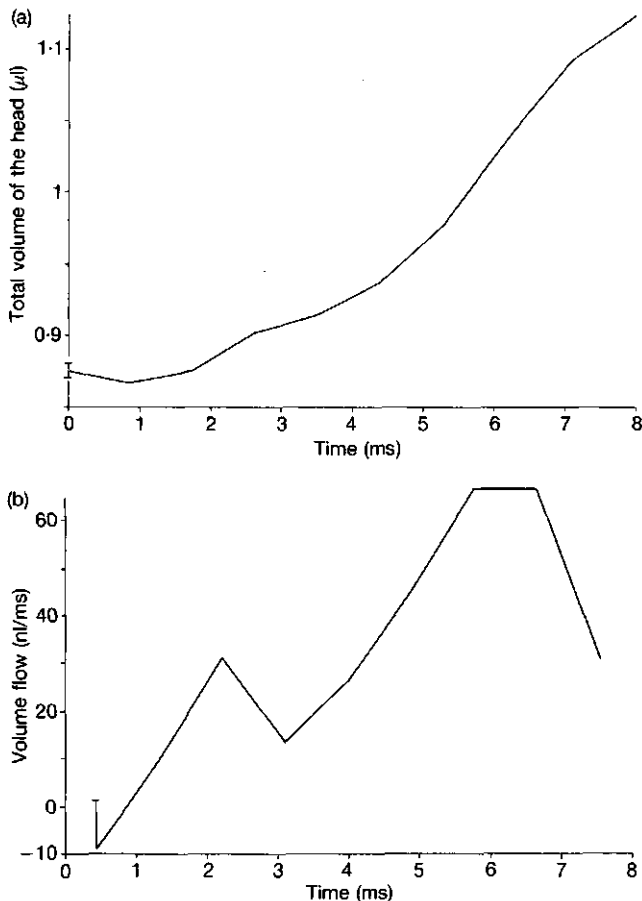
FIG. 3. Calculated volumes of the head (a) and flow rate (b) of the suction act of Plate I. The approximate error is indicated by a bar (the error is constant over the curve).

error. If the deviation angle varies between the successive frames, the absolute error in the volume change between two frames is as big as the absolute error in calculated volume (and the relative error of the change is thus much greater than the relative error of the volume). In the films, the angle of projection, mostly, changes little during a feeding sequence (compare Plate I).

To check the calculations, the measured velocity of the prey is compared with the calculated water velocity at the position of the prey. As the swimming velocity of an *Artemia* is negligible compared to the suction velocities of fish larvae, and their density is about the same as water, I assume that the prey moves as does the surrounding water. The internal width and height of the mouth aperture can be measured from the film. Assuming the mouth aperture to be an ellipse, its cross-sectional area can be calculated. Volume flow divided by cross-sectional area gives the mean water velocity at the mouth aperture (in the *moving frame*, i.e. relative to the centre of the mouth aperture). Water velocity in the *earth-bound frame* (i.e. relative to the aquarium) is velocity in the
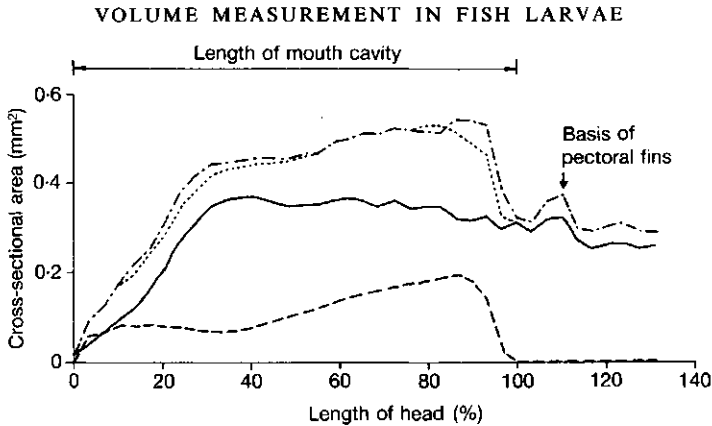
VOLUME MEASUREMENT IN FISH LARVAE

FIG. 4. Cross-sectional areas of the outlines of the head of a fixed carp larva (15 mm SL) as measured via a digitizer tablet ($\cdots$) and via the ellipse method ($-\cdot-$). The measured total area of water ($--$) and of tissue ($—$) are indicated. No correction for shrinkage is made.

moving frame plus swimming velocity of the fish (measured as the velocity of the centre of the mouth aperture). In front of the fish, the water velocity due to suction (earth-bound) rapidly falls off with increasing distance from the mouth aperture (Muller *et al.*, 1982: formula 34).

$$U = u_m \frac{h_1^3}{\sqrt{(h_1^2 + d_{mp}^2)^3}}$$

h_1—radius of the mouth (assumed to be circular)
d_{mp}—distance in front of the mouth at which the velocity is calculated
u_m—water velocity at the mouth aperture (earth-bound frame)
U—water velocity at the axis of the fish at distance d_{mp} in front of the fish (earth-bound frame).

The radius of the mouth is calculated as the geometric mean of height and width of the mouth. So the cross-sectional area is kept constant. The centre of the prey is calculated from the ventral view, assuming that the prey has rotational symmetry. So its centre of mass and not the centroid of its projection is determined. The swimming velocity of the fish was rather low in comparison to the errors of measurement. Therefore, it is taken as constant. The mean water velocity, at each length position inside the mouth cavity, is the volume flow through that cross-section divided by the cross-sectional area of water. The volume flow and the total cross-sectional area at each length position inside the mouth cavity can be calculated with the ellipse method. This total area consists of water and tissue. Due to unknown and differential shrinkage (see preceding section), it is impossible to calculate the tissue (and thus the water) cross-sectional area accurately. When the centre of mass of the prey has entered the mouth, the best approximation of the calculated prey velocity is the calculated water velocity at the mouth aperture. Due to friction, the water velocity at the walls of the mouth cavity will be lower and the velocity in the middle will be higher than the mean. In Fig. 5, the calculated mean water velocity at the mouth aperture in the moving and in the earth-bound frame, and the measured velocity of the prey and the calculated water velocity at the position of the centre of mass of the prey, are depicted. The suction act is the same as in Plate I and Fig. 3. Velocities are calculated between the frames; the used distances are the mean of the distances at the frames. The centre of mass of the prey passes the mouth aperture at $t = 4 \cdot 45$ ms, so calculated and measured velocities can be compared best till $t = 4 \cdot 89$ ms, i.e. only half a frame
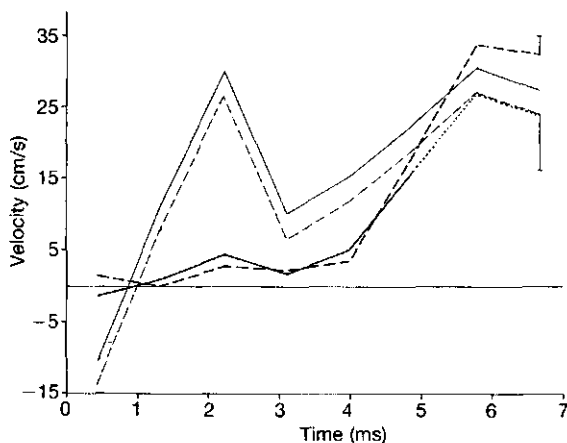
M. R. DROST AND J. G. M. VAN DEN BOOGAART

FIG. 5. Measured velocity of the prey (- -) and calculated water velocity at the place of the prey (—) of the suction act of Plate I and Fig. 3. After $t = 4\cdot89$ ms, the calculated water velocity is less accurate (see text), it is then dotted. Also indicated are calculated water velocity at the mouth aperture in the moving (- -) and in the earth-bound (- -) frame. Further explanation in the text. Approximate errors in measured and calculated prey velocity are indicated by a bar.

later. Both velocities agree fairly well. The high water velocity at the mouth aperture at $t = 2\cdot23$ ms results from a rather high volume flow (see the small bump at $t = 2\cdot67$ ms in Fig. 3a), together with a still small mouth aperture.

Summary

A simple method has been devised to determine dynamic changes in volume of biological objects having a smooth form. The method requires two perpendicular views (side and bottom). The volume of the object is approximated by a series of ellipses. The radii of the ellipses are determined from the two views. Possible sources of error are discussed. Depending on the form of the object and the obtained perpendicularity of the views, an error of 5-10% is obtainable, of which a large part is systematic.

A first example is the shrinkage of small carp larvae during histological fixation. Not only the mean shrinkage, which can be obtained also in other ways, but also differential length, width and height shrinkage are determined. Mean volume shrinkage in carp larvae (total length 5·5 mm) due to fixation in Bouins fixative is 60%; the form distortion (change in ratio of width and height) is 25%.

The method is also applied in a study of the dynamic volume change of the mouth cavity of carp larvae, increasing their head volume 30% in 8 ms, when sucking prey. The water velocity, calculated from volume flow measured with the ellipse method, corresponds quite closely to the measured velocity of the prey.

VOLUME MEASUREMENT IN FISH LARVAE

REFERENCES

Aherne, W. A. & Dunnill, M. S. (1982). *Morphometry*. London: Edward Arnold.

Arnold, G. P. & Nuttall-Smith, P. B. N. (1974). Shadow cinematography of fish larvae. *Mar. Biol., Berlin* **28**: 51-53.

Leeuwen, J. L. van (1984). A quantitative study of flow in prey capture by Rainbow trout, *Salmo gairdneri* with general consideration of the actinopterygian feeding mechanism. *Trans. zool. Soc. Lond.* **37**: 171-227.

Lockwood, S. J. & Daly, C. de B. (1975). Further observations on the effects of preservation in 4% neutral formalin on the length and weight of O-group flatfish. *J. Cons. int. Explor. Mer.* **36**: 170-175.

Muller, M., Osse, J. W. M. & Verhagen, J. H. G. (1982). A quantitative hydrodynamical model of suction feeding in fish. *J. theor. Biol.* **95**: 49-79.

The energetics of feeding strikes in larval carp (Cyprinus carpio)

M.R. Drost & J.G.M. van den Boogaart
Dept. of Experimental Animal Morphology and Cell Biology,
Agricultural University, Marijkeweg 40, 6709 PG Wageningen, The Netherlands

ABSTRACT

The prey intake of larval carp is described from high speed (200-1250 fr/s) films with synchronous lateral and ventral views. Even in first feeding carp larvae the operculars are functional in sealing effectively the opercular slit till the moment of prey intake and the maxillaries close off the corners of the mouth, preventing leak flow. In reducing the distance between larva and prey during attack the relative importance of sucking the prey towards the mouth and swimming forward is variable; overall they are about equally important. The volume and the velocity of the water sucked into the mouth cavity during prey uptake are calculated. The energy costs of suction (i.e. accelerating the water sucked into the mouth cavity) during prey intake are estimated from these values. The energy costs of suction and swimming are in the same order of magnitude. Together they form only a fraction of a percent of the energetic content of the prey. So considerations about energy expenditure seem unimportant in a strategy to optimize the prey attack. During searching however, they will be important. Also considerations about power requirements during attack may be important.

I Introduction

Predation and starvation are the dominant causes of the extensive mortality of fish larvae (e.g., Blaxter, 1969), predation seemingly the more important (Oiesfed, 1984). The feeding behaviour and food consumption of first feeding larvae has been studied for some species (e.g., Hunter, 1972 for the anchovy, Engraulis mordax). This paper presents the first description for carp larvae. Special reference will be given to the actual attack phase lasting less than 20 ms in first feeding carp larvae.

Fish larvae can adjust their kinematics and thus their energy expenditure of the attack to the type of prey (e.g., Vinyard, 1982). The importance of energetics of prey capture for larval carp is discussed.

II Material and methods

II.1 Filming setup

To investigate larval feeding, 30 snaps of larval carp (<u>Cyprinus</u> <u>carpio</u>) were filmed with a Hadland Hyspeed camera (500-1150 fr/s, exposure time respectively 0.8-0.35 ms) with a standard 135 mm Nikon lens on 16 mm Kodak 2X negative film (25 DIN/250 ASA). Framing rate was monitored with a 250 or 500 Hz calibration signal, recorded by a light pulse on one margin of the film. So the framing rate could also be determined accurately for still accelerating films. Shadow cinematography was used (Arnold & Nuttall-Smith, 1974), using 75W Xenon lamps (Osram XBO 75W2) as point sources (the effective diameter of this lightsource is about 0.5 mm). Each lamp was placed in the focus of a 200 mm optical quality, achromatic lens (Spindler & Hoyer). The resulting effective diaphragm is f/400 (the Nikon lens was fully opened (f/2.8)). At the used magnifications (1/3 to 2) this resulted in a depth of field of about 40 to 7 mm. The filming set-up is outlined in Fig. 1. Synchronous lateral and ventral views are obtained by three surface coated mirrors. To make the working distance in the lateral
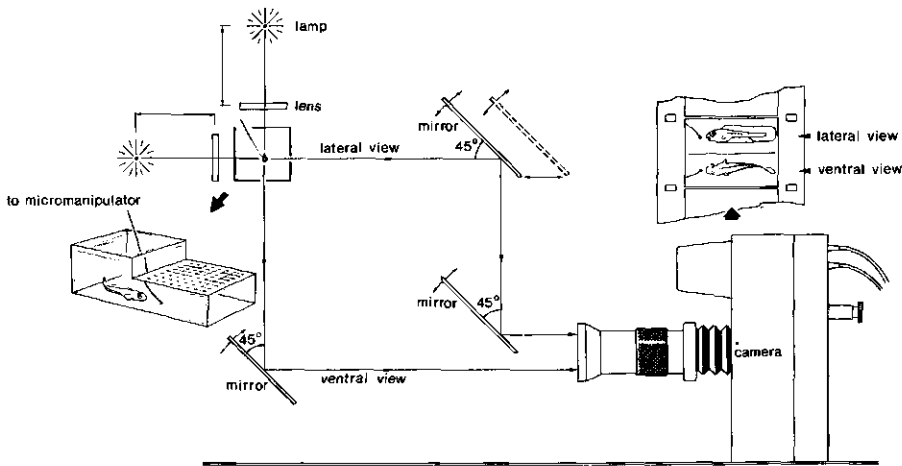

Fig. 1. Schematic drawing of the filming setup, not drawn to scale. A horizontal and a vertical beam of parallel light are obtained each from a Osram XBO 75W2 Xenon arc lamp in the focus of a +200 mm achromatic lens. The beams are projected into the lens of the camera via three surface coated mirrors (50.50 mm). Differences in working distance in lateral and ventral view are corrected by moving the upper lateral mirror horizontally while slightly adjusting the angles of the mirrors. The top of the filming aquarium is covered with an eye piece graticule (see inset). In some experiments the prey is glued to a 12 μm nylon thread (length about 0.5 cm). This thread is connected to a micromanipulator via a human eye lash. Camera, mirrors, lamps and lenses are mounted on an optical bench. The filming aquarium is placed on a XYZ table.

and ventral view exactly equal, the upper mirror can be moved horizontally 0-30 mm relative to the lower. The upper side of the filming aquaria was covered with glass to prevent refraction by a curved water surface. The use of parallel light beams prevented perspectivic distortion. An eye piece graticule provided an absolute scale. Illumination strength was about 800 lux. During the experiments the fishes were never visibly stressed from the lights.

Small carp larvae (6-8 mm SL) were fed free swimming nauplii of Artemia salina, larger larvae (10-15 mm SL) restrained Artemia nauplii or Daphnia. Prey were restrained by glueing them with superglue (cyanoacrylate) to a 12 μm nylon thread (length 5-10 mm) which was glued to a human eye lash. The lash was connected to a micromanipulator in order to be able to position the prey exactly in the middle of the field of view. Artemia nauplii swim for only about 5 min after being glued; Daphnia for more than a day. Restrained Daphnia can swim away several mm and than drift back into focus. Artemia nauplii are too weak to swim away. The suction currents generated by feeding carp larvae are so strong (maximal velocity more than 0.25 m/s for first feeding carp larvae) that the nylon thread scarcely hinders the movement of the prey in the suction flow, unless the thread is firm. Carp were bred in our laboratory at 23 C. The smaller larvae were fed once or twice a day on Artemia, the larger were given a mixture of zooplankton, consisting mainly of Daphnia.

II.2 Ellipse method

A simple method to calculate changes in volume of the head of a fish is given in Drost & van den Boogaart (1986). The head of the fish is approximated by a series of ellipses. The area of each ellipse is determined by the length of its two axes. The length of these axes can be measured from cine films with simultaneous lateral and ventral views. The volume of the head is the integral of the cross sectional areas over the length of the head. The volume of the head consists of the (constant) volume of tissue, and of the (rapidly changing) volume of the mouth cavity. So, measured changes in volume of the head correspond to equal changes in volume of the mouth cavity. In the beginning of the suction process the opercular (posterior) side of the mouth cavity is closed and only the mouth is open. So, the volume flow through the mouth is the change in volume of the mouth cavity. After the moment the opercular valves open (at about 8 ms after the onset of suction for 6-8 mm carp larvae), water can also flow through the opercular slit. Direction and velocity of this flow are not a priori known. The volume flow through the mouth aperture can thus be determined only till the moment of the opening of the valves. Possible sources of errors

of the ellipse method are discussed in Drost & van den Boogaart (1986).

III Results and discussion

III.1 Suction process

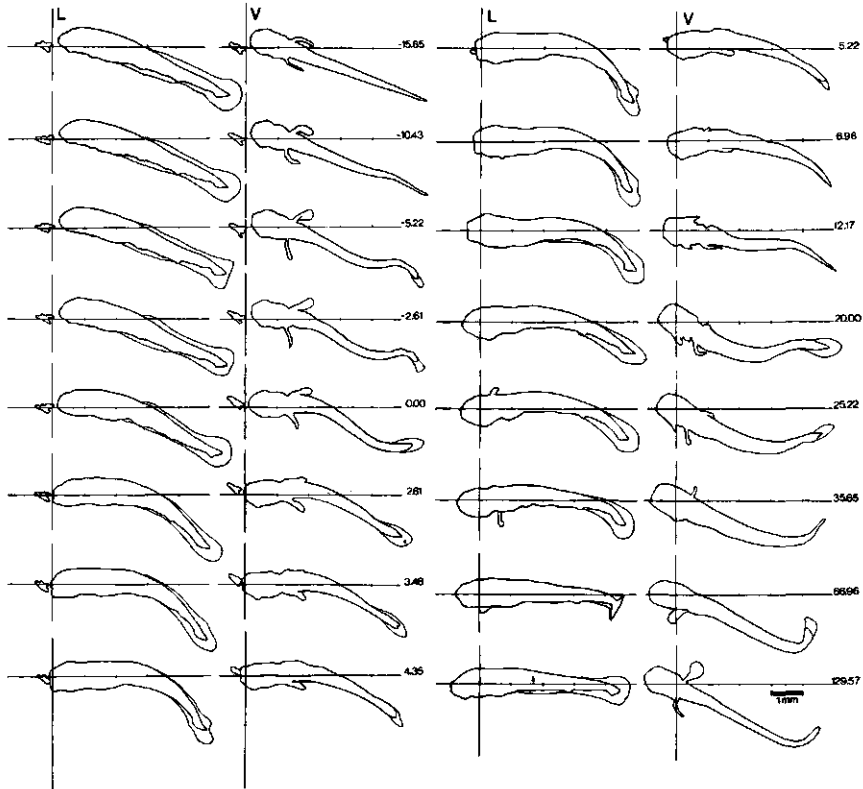Searching for prey, carp larvae swim intermittently. Periods of 0.1 s of activ-

Fig. 2. Selected tracings of a film (1150 fr/s) showing the movements of a carp larva (SL 5.8 mm) and its prey (a nauplius of Artemia salina) in a lateral (L) and a ventral (V) view relative to a stationary grid. The outlines of the body and of the finfold and pectoral fins are traced. Due to a slight rotation only a small part of the finfold is visible in the lateral view after t=2.61 ms. Bar and divisions on the horizontal axes denote 1 mm. Time is indicated in ms, relative to the onset of suction.
The snap starts at t=-15.65 ms by movements of the pectoral fins and a bending of the body. Swimming forward starts at t=-2.61 ms. The start of mouth opening is at t=0. Besides a lateral flexure, as is normal in swimming fish, also a dorso-ventral flexure of the body starts to develop at t=0. Maximal flexure is 55° at the moment of prey intake. The maximal velocity of the prey, relative to the grid (earth bound frame) is 0.28 m/s. About 2/3 of the inital prey distance is covered by swimming, only 1/3 by suction. At the moment of prey intake the pectoral fins are folded against the body. The opercular valves open at t=6.96 ms. At t=12.17 ms a new swimming movement with body and pectoral fins starts. The mouth is closed at t=20 ms; the valves close about t=60 ms. The snap has ended after about 100 ms, although it is difficult to define an exact end.

ity of the pectoral fins often accompanied by flexing the body are alternated with periods of rest. These periods of rest mostly take about 0.3 s, but also longer periods often occur. When a larva spots a prey, it fixates the prey by turning both eyes inward. Positioning is accomplished by one or more periods of activity (as in searching). Before the actual attack no S shaped attack posture is formed (as does occur in e.g. clupeoid (Hunter, 1972) and pike larvae (Braum, 1963)). The movements during attack of a 5.8 mm carp larva feeding on an Artemia nauplius are given in Fig. 2. The prey passes through the mouth aperture 20 ms after the start of attack and only 5 ms after the onset of suction. Chewing takes about 1 second, then the prey enters the intestine
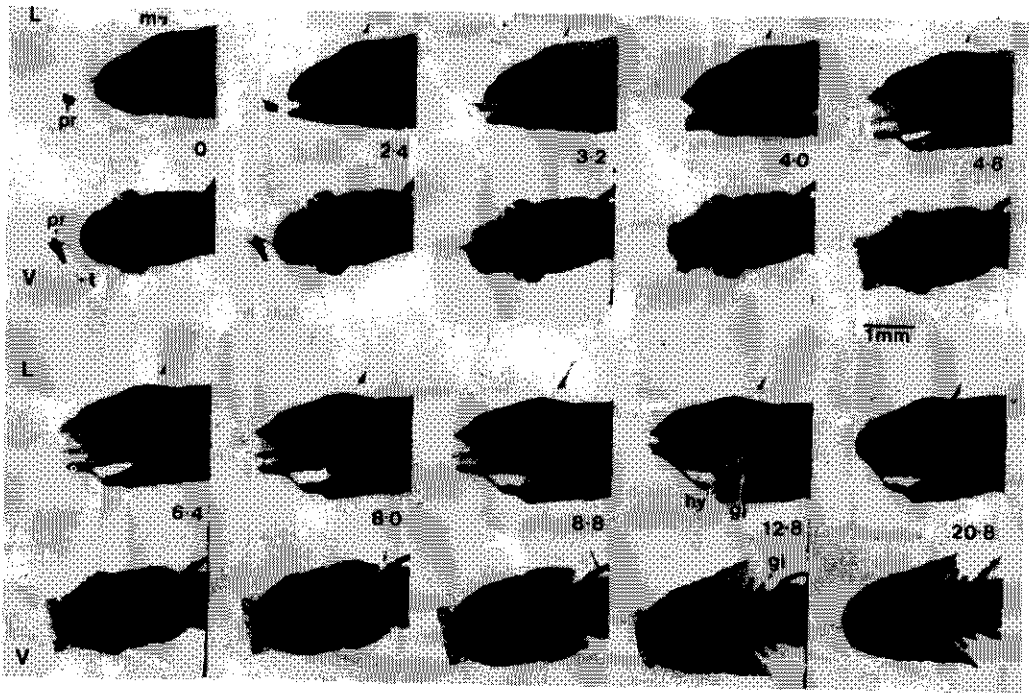
Fig. 3. Selected frames of a shadowgraphic film (1250 fr/s) showing the movements of the head of a carp larva (SL 9.5 mm) and its prey (pr, a nauplius of Artemia salina) in a lateral (L) and a ventral (V) view. The Artemia is glued to a 12 um nylon thread (t, faintly visible) connected to a micromanipulator (m). Time is indicated in ms. The fish is partly transparant: hyoid (hb) and gill bars (gb) can be seen. The upper jaw protrudes 0.12 mm (3.8% of the length of the head between t=4.8 ms and t=8 ms). A round suction tube is formed, without notches. The prey is small relative to the larva. It is taken in before maximal mouth aperture, the latter time being normal for bigger prey. The opercular valves open at t=8 ms (arrow).

(determined from video films). The body of the larva does not only flex later-ally, as usually occurs during swimming, but also to a large extent dorso-ven-trally. In this snap the maximum flexure between head and end of the notochord is 55°.

Early in the suction process notches in the mouth aperture are visible in the lateral view and a curved frontal side in the ventral view (Fig. 3). Both conditions are unfavorable hydrodynamical conditions, inducing leak flow (Osse, 1969; Muller & Osse, 1984). Even in the smallest larvae filmed (5.8 mm) a flat frontal plane of the mouth is formed: the notches were closed of and the ante-rior margin of the mouth cavity was straightened by rotation of the maxil-laries. Protrusion of the premaxillaries is absent (at least not detectable) at the 5.8 mm stage. In the 9.5 mm larvae maximal protrusion is already 3.8% of the length of the head. In older larvae the circular mouth aperture seems to be reached relatively earlier than in smaller larvae (compare Figs. 2 and 3).

In adult fishes the opercular and branchiostegal valve is important in sealing the opercular slit and preventing backflow (Osse, 1969; van Leeuwen, 1984; Muller & Osse, 1984). Even in the smallest larvae the opercular valve is func-tional: the opercular slit is closed till approximately the moment the prey enters the mouth. The opercular abduction is still rather small at valve open-ing. During growth mean time delay between prey intake and valve opening in-creases to about 5 ms in 15 mm larvae (there is some variability in the rela-tive timing, even at a length of 15 mm valve opening sometimes precedes prey capture). Opercular abduction at the moment of valve opening increases during growth. This partly causes the increase in volume of water sucked before valve opening (Table 1).

III.2 Flow and energy

The changing volumes of the heads and flow rates through the mouth aperture of carp larvae when sucking prey are given in Fig. 4. Total volume ingested till the moment of opening of the valves increases rapidly during growth (Table 1). During a snap energy is required for sucking water into the mouth cavity ('suc-tion energy') and for swimming ('swimming energy'). Both suction and swimming energy consist of energy lost to friction and of acceleration (increase in kinetic energy). The frictional term of the suction energy can only be esti-mated with a hydrodynamical computer model solving the complete Navier Stokes equation in 2-D.

Kinetic energy is given by:

$$E_k = \frac{1}{2} \cdot m \cdot v^2 \tag{1}$$

Table 1. Kinetic energy of the water sucked into the mouth cavity of carp larvae when sucking prey and the required power (W/kg body weight). Volumes are calculated with the ellipse method. The film of the 15 mm larva was too slow (400 fr/s) to measure the velocity of the prey. More explanation is given in the text.

SL (mm)	volume (mm^3)	velocity (m/s)	energy (nJ)	body mass (mg)	duration (ms)	power (W/kg body weight)
5.8	0.20	0.28	39	1.2	4	8.1
6.5	0.25	0.35	77	2.0	6	6.5
9.5	1.97	0.43	910	10.6	8	10.7
15.0	7.23	-	-	78.9	12.5	-
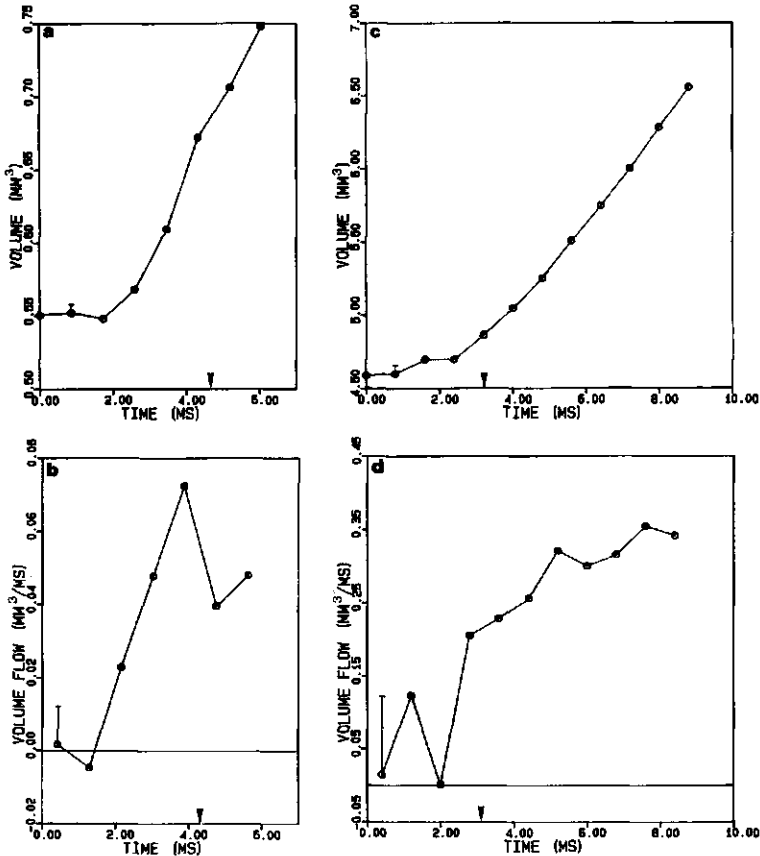
Fig. 4. Changes in the volume of the head of carp larvae while sucking prey and the rate of change of the volume of the head, both as determined with the ellipse method. The approximate error is indicated with a bar; only one side of each error bar is drawn. Within one curve all measurements have the same error. Arrows indicate the moment of prey intake.
a-volume of the head (SL 5.8 mm).
b-volume flow through the mouth aperture of Fig. 4a.
c-volume of the head (SL 9.5 mm; same sequence in Fig. 3).
d-volume flow through the mouth aperture of Fig. 4c.

In the calculation of kinetic energy all velocities must be measured in the earth bound frame (i.e. relative to the aquarium). In discussing the chance of prey capture it is often easier to use the moving frame, i.e. relative to the centre of the mouth aperture of the fish.

Ideally the kinetic suction energy should be determined by integrating the kinetic energy of each volume element over the total field of flow.

When fish create a suction current, the largest velocities occur near the mouth aperture (Muller et al., 1982; Muller & Osse, 1984). For adult fishes the earth bound velocity of the water near a point of the X-axis and the distance to the mouth aperture, d, has been calculated (Muller et al., 1982: formula 34). At distances larger than one mouth diameter in front of the mouth aperture this relation is roughly:

$$v \sim d^{-3} \qquad (2)$$

The region near the mouth aperture will thus make the largest contribution to the total kinetic suction energy. The mass (volume) of the water accelerated till the moment of valve opening can be calculated with the ellipse method. In adult trout (Salmo gairdneri) the greater part of the volume entering the mouth aperture enters **after** the moment of valve opening (82%, van Leeuwen, 1984). As an approximation I use 80% for larval carp. This may be an overestimation because swimming, which tends to increase this percentage, is relatively more important in adult trout than in larval carp. It is assumed that the maximal velocity of the water is equal to the velocity of the prey (which is easily determined from film). Calculated suction kinetic energy for snaps of carp larvae of different size are given in Table 1.

Swimming energy consists of increase in kinetic energy of the body and the water which is used to accelerate and of energy lost in friction. The following calculation of the swimming energy is modified after Webb (1975).

For symbols see appendix 1.

Assuming the added mass is 0.2 m, the body kinetic energy, E_k, is:

$$E_k = \frac{1}{2} \cdot 1.2 \cdot m \cdot v^2 \qquad (3)$$

We assume that the acceleration, a, is constant and that the frictional drag force, D, can be calculated from standard hydrodynamic equations:

$$D = \frac{1}{2} \cdot \rho \cdot S_w \cdot v^2 \cdot c_D \qquad (4)$$

S_w is surface wetted area, ρ is the specific gravity.

Transition from a laminar to a turbulent boundary layer occurs at $Re_L = 10^5$. Re_L for swimming larvae is less than 10^3. So the boundary layer is laminar so that (Bird et al., 1960):

$$c_D = \frac{1.33}{\sqrt{Re_L}} \tag{5}$$

The work against drag, WD, from x=0 to x=s is:

$$WD = \int_0^s F\ dx \tag{6}$$

Insertion of Eqs. 4 (the drag force) and 5 (the drag coeficient) in Eq. 6 gives:

$$WD = \frac{1}{2} \cdot \rho \cdot S_w \cdot L^{-1/2} \cdot \nu^{1/2} \cdot \int_0^s v^2 \cdot 1.33 \cdot v\ dx \tag{7}$$

From standard Newtonian mechanics follows that for uniform acceleration (a) from a speed v=0 to v=v:

$$v = \sqrt{2 \cdot a \cdot x} \tag{8}$$

Inserting Eq. 8 in Eq. 7, followed by integration gives:

$$WD = \frac{1}{2} \cdot \rho \cdot S_w \cdot L^{-1/2} \cdot \nu^{1/2} \cdot (2a)^{3/2} \cdot \frac{4}{7} \cdot x^{7/4} \tag{9}$$

For the snap of the 5.8 mm carp larva $a = 8.5 m/s^2$, s=0.7 mm, $S_w = 12.4\ mm^2$. So the calculated friction is 1.6 nJ. The drag of an oscillating body is higher than of a rigid body. At high Re this factor is about 5 (Webb, 1975 quoting the Lighthill model). At low Re, where the viscous forces dominate, this factor is much closer to one. According to Aleyev (1977) the transition between low and high Re occurs at about 5000 in the case of swimming animals (e.g. fishes). For the 5.8 mm carp larva maximal Re during the snap is 640 (L=5.8 mm, $v_{max}=0.11$ m/s). We use a factor two, because the actual Re is rather close to the transition. This may however be an overestimate. Taking a factor two, total drag is 3.2 nJ. The body kinetic energy is 8.7 nJ. Total swimming energy thus equals about 12 nJ.

Energy costs of suction (39 nJ) and swimming (12 nJ) are in the same order of

magnitude. The power needed for swimming is delivered during 15 ms (7 ms forma-
tion of body curvature and 8 ms acceleration phase), making power needed for
swimming lower than for suction.

The energetic content of an Artemia nauplius is 40 mJ (Hunter, 1977), the costs
of one snap are 51 nJ for a 5.8 mm carp larva (see above). Assuming a 10%
digestive efficiency, a 75% Froude efficiency and a 10% muscular efficiency
(Alexander, 1977; Webb, 1971), the costs for snapping at an Artemia nauplius
are only 0.016% of the energetic gains for a 5.8 mm larva. For a 9.5 mm carp
larva this has increased to only 0.4%.

If the 5.8 mm larva snaps with the same movements at prey 10 times smaller in
linear dimensions than an Artemia, the costs of snapping are 16% of the gains.
At this size the catch success (successful snaps/total snaps) of carp larvae
feeding on Artemia nauplii is about 50%. Assuming an equal capture success for
smaller particles the speed of attack at these smaller particles will affect
the net gain of energy per snap.

According to data of Hunter (1977) anchovy (Engraulis mordax) larvae of about 6
mm length do not grow on a diet of Gymnodium splendens ($\emptyset$ 30 μm, energetic
content 0.21 mJ). They can be grown to metamorphosis on larger prey, e.g.
Artemia. Assuming that the energetic costs of snapping of a carp larva and
anchovy larva are equal at equal size, the growth of anchovy larvae becomes
retarded when feeding on a prey of a size that the cost of snapping becomes a
large fraction of the energetic content of the prey.

If the snap is carried at twice as fast, all energies become roughly four times
as big and are even then only 0.06% of the gains for a 5.8 mm larva and 1.6%
for a 9.5 mm larva. So, the net energetic gain is almost independent on the
speed of attack. The optimum speed of attack at a certain prey might not depend
on the energy balance between energetic costs of snapping and the energetic
gains of capturing the prey, but on the balance between prevention of active
prey escape by lunging and sucking fast and missing a prey due to inaccurate
aiming. We suppose that there is a negative correlation between speed and
accuracy.

To check the accuracy of these energy estimations we will compare the required
power of the muscles, calculated from these energies with values of maximal
power output for fish muscle.

Suction energy is 39 nJ for 5.8 mm carp larva. By far the greatest part of it
will be delivered in the first 4 ms of the suction process: the time that
active expansion of the mouth cavity with closed valves occurs and the water is

accelerated from rest to maximal velocity. Given that no energy storage (e.g. in tendons) occurs, mean power output during these 4 ms is 9.8 μJ/s. On the basis of 12 carp larvae (SL between 6 and 12 mm) a length (L in mm) weight (W in mg) relation $W=0.0005 \cdot L^{4.42}$ is determined. So the calculated weight of a 5.8 mm larva is 1.2 mg. Mean specific power is 8.1 W/kg body weight. Most of the power during suction feeding is delivered by the axial muscles (Osse, 1969). About 27% of the body mass of a 6 mm carp larva consists of muscle (determined from serial cross sections of one individual, fixed in Bouin's fixative. Assuming that all muscles contract synchronously, the mean specific power is 30 W/kg muscle. Although total energy expenditure during snapping is very small, the power output is rather high. It is most probable that in increasing the velocity of the prey the larvae are limited by their maximal power output (cf. Muller & Osse, 1984).

Inaccuracy in determination of body weight, of duration of power delivery and of suction energy and the neglection of power needed for swimming can cause serious errors. Given the crudity of the calculations, the values are surprisingly close to calculated maximal values for white muscle of cod (Gadus morhua): 16 W/kg muscle and blue marlin (Makaira nigricans): 37.2 W/kg at 15 C and 57.2 W/kg at 25 C (Johnston & Salamonski, 1984) and adult carp (Cyprinus carpio): 19.3 W/kg muscle (Johnston et al., 1985). Maximum work per unit muscle volume, delivered in one contraction is independent of the size of an animal. The rate of shortening however increases with decreasing size. Hence power output is scaled to increase with decreasing body size (Schmidt-Nielsen, 1984). Our calculations are not accurate enough to decide whether power output of the muscles of carp larvae during suction feeding is higher or lower than the maxima as found for adult fish.

CONCLUSIONS

Even in first feeding carp larvae the opercular valve is functional in sealing the opercular slit till approximately the time of prey intake and the maxillaries close the corners of the mouth off, both preventing leak flow. During growth the maximal abduction niveau of the operculars with sealed slit increases. In reducing the distance between larva and prey during attack, the relative importance of sucking the prey towards the mouth and swimming forward is variable; overall they are about equally important.

The energy costs of the actual attack are only a fraction of a percent of the energetic content of the prey; the energy costs of suction and swimming being in the same order of magnitude (the energy costs of searching and manoeuvering

are ignored). The power output during the attack is very high. Considerations about energy expenditure during snapping seem unimportant in a strategy to optimize prey attack; considerations about power output however are important.

ACKNOWLEDGEMENTS

REFERENCES
Aleyev, Y.G., 1977. Nekton. The Hague: Junk.
Alexander, R. McN., 1977. Swimming. In: Alexander, R. McN. & Goldspink (Eds.). Mechanics and energetics of animal locomotion. London: Chapman and Hall. 346 pp.
Arnold, G.P. & Nuttall-Smith P.B.N., 1974. Shadow cinematography of fish larvae. Mar. Biol. 28: 52-53.
Bird, R.B., Stewart, W.E. & Lightfoot, E.N., 1960. Transport phenomena. New York: Wiley.
Blaxter, J.H.S., 1969. Development: eggs and larvae. In: W.S. Hoar & D.J. Randall (eds). Fish Physiol. 3: 177-252. New York: Academic Press.
Braum, E., 1963. Die ersten Beutefanghandlungen junger Blaufelchen (Coregonus wartmanni Bloch) und Hechte (Esox lucius L.). Zeitschr. f. Tierpsychol. 20: 257-266.
Drost, M.R. & Boogaart, J.G.M. van den, 1986. A simple method for measuring the changing volume of small biological objects, illustrated by studies on suction feeding by fish larvae and of shrinkage due to histological fixation. J. Zool. Lond. (A) 209: 239-249.
Hunter, J.R., 1972. Swimming and feeding behavior of larval anchovy Engraulis mordax. Fish. Bull., U.S. 70: 821-838.
Hunter, J.R., 1977. Behavior and survival of northern anchovy Engraulis mordax larvae. Cal. Coop. Fish. Invest. Rept. 19: 138-146.
Johnston, I.A. & Salamonski, S., 1984. Power output and force-velocity relationship of red and white muscle fibres of the Pacific Blue Marlin (Makaira nigricans). J. exp. Biol. 111: 171-177.
Johnston, I.A., Sidell, B.D. & Driedzic, W.R., 1985. Force velocity characteristics and metabolism of carp muscle fibres following temperature acclimation. J. exp. Biol. 119: 239-249.
Leeuwen, J.L. van, 1984. A quantitative study of flow in prey capture by Rainbow trout, Salmo gairdneri, with general consideration of the actinopterygian feeding mechanism. Trans. Zool. Soc. Lond. 37: 171-227.
Muller, M., Osse, J.W.M. & J.H.G. Verhagen, 1982. A quantitative hydrodynamical model of suction feeding in fish. J. theor. Biol. 95: 49-79.
Muller, M. & Osse, J.W.M., 1984. Hydrodynamics of suction feeding in fish. Trans. Zool. Soc. Lond. 37: 51-135.
Oiested, V., 1984. Predation on fish larvae as regulatory force, illustrated in mesocosm studies with large groups of larvae. NAFO Sci. Coun. Stud. 8: 25-32.
Osse, J.W.M., 1969. Functional morphology of the head of the perch (Perca fluviatilis L.); an electromyographic study. Neth. J. Zool. 19: 289-392.
Schmidt-Nielsen, K., 1984. Scaling, why is animal size so important?. Cambridge: Cambridge University Press.
Vinyard, G.L., 1982. Variable kinematics of Sacramento perch (Archoplites

interruptus) capturing evasive and nonevasive prey. Can. J. Fish. Aquat. Sci. 39: 208-211.

Webb, P.W., 1971. Swimming energetics of the trout: II oxygen consumption and swimming efficiency. J. exp. Biol. 55: 521-540.

Webb, P.W., 1975. Hydrodynamics and energetics of fish propulsion. Bull. Fish. Res. Bd. Can. 190. 158 pp.

Appendix 1

Symbols

a	-acceleration.
c_D	-drag coefficient.
d	-distance between the the centre of the mouth aperture and a point on the axis of the mouth cavity.
D	-drag force.
E_k	-kinetic energy.
m	-mass.
Re	-Reynolds number.
Re_L	-Reynolds number based on length.
s	-distance covered.
S_w	-surface wetted area.
v	-velocity (in the earth bound frame).
v_{max}	-maximal velocity (earth bound).
WD	-work done against drag.
ν	-kinematic viscosity.
ρ	-specific gravity.

The relation between aiming and catch success in larval fishes

M.R. Drost
Dept. of Experimental Animal Morphology and Cell Biology,
Agricultural University, Marijkeweg 40, 6709 PG Wageningen
The Netherlands

Abstract

The accuracy of aiming on prey by fish larvae is estimated. The measured param-eter is the **aiming inaccuracy**, i.e. the standard deviation of the distance between the centre of mass of the prey and the length axis of the mouth cavity. Distances are measured from high speed films with synchronous lateral and ventral views. In pike the aiming inaccuracy increases from 0.28 mm for 14 mm larvae to 0.73 mm in 62 mm juveniles, in 6-8 mm carp larvae it is 0.22 mm. A mathematical model provides the relation between aiming inaccuracy and catch success on stationary prey. Theoretical and measured catch success agree for larval carp feeding on Artemia nauplii, which are nearly immobile during the 5-20 ms of an attack of a larva. For larval pike feeding on Daphnia, the model adequately predicts the measured success from aiming. Escape movements of the prey however cause more unsuccessful snaps. The relative influence on catch success of the accuracy of aiming of the predator and escape possibilities of various prey can be estimated. This relative influence is important in inter-preting the rapid morphological changes and the rapid increase in catch success occurring during the ontogeny of fishes.

I Introduction

I.1 Rate of feeding

It is widely believed that predation and starvation are the dominant causes of the extensive mortality of fish larvae (e.g., Blaxter 1969), predation seemingly the more important (Oiested 1984). The feeding behavior and food consumption of first feeding larvae has been studied by e.g. Hunter (1972). The actual attack of a prey by a larva lasts very short, less than 15 ms in first feeding larval carp (Drost & van den Boogaart 1986b). This paper analyses the food intake in larval carp and pike and relates the increasing catch success during ontogeny to better aiming.

At a given prey density, the rate of feeding depends on two independent processes: a) the rate of encounter with prey and b) the efficiency of capture and ingestion of encountered prey. The rate of encounter with prey depends on the distance within which the prey is detected and reacted to (reactive distance) (Braum 1967; Confer & Blades 1975) and mean swimming velocity (Braum 1967; Hunter 1972). The efficiency of capture of encountered prey depends on the possibility to approach the prey close enough to start the strike (Braum 1967), accuracy during the strike (Beyer 1980) and the rapidity of the strike in relation to the "escape properties" of the prey (Drenner et al. 1978; Winfield et al. 1983; Mills et al. 1984). These properties are maximal (and actual) escape velocity and acceleration and reaction distance.

A review of feeding behavior of marine fish larvae is given in Hunter (1980).

A snap is defined as a lunge forward, while increasing the volume of the mouth cavity rapidly; if a feeding sequence ends with a snap it is called finished (Blaxter & Staines 1971). Catch success is the percentage successful snaps of the total number of snaps. It is also called feeding success (e.g. Hunter 1980), capture success (Mills et al. 1984) or capture efficiency (Meyer 1986). Rosenthal & Hempel (1970) determine success relative to the number of prey encountered. Catch success increases rapidly during growth of fish larvae: see Table 1. Larvae which are larger at hatching have a higher initial catch success (e.g. pike); also some small larvae have a high initial catch success (big eye and bay anchovy). Larvae have often different catch successes for different prey (e.g. northern anchovy feeding on Brachionus and on Artemia) even on prey of equal size (Meyer 1986).

An increase of catch success of a larva feeding on a certain prey can result from better aiming or a higher speed:

1- Aiming: the larvae become relatively more accurate in aiming at the prey.

Table 1. Catch success of fish larvae. Success is percentage successful of all snaps. Age is given relative to hatching, ff is first feeding. Standard length (SL) is indicated in mm, ?? if not given. Prey are: A- nauplii of _Artemia salina_; B- _Brachionus_; D- _Daphnia_ of equal size to _Artemia_ nauplii; MZ- mixed zooplankton; MZS- mixed zooplankton passing through a 110 µm and retained by a 53 µm mesh sieve.

Species		success	age	SL (mm)	prey	ref.
Engraulis mordax	northern anchovy	10	ff (3 days)	3.8	B	1
		81	17 days	8.3	B	1
		17	17 days	8.3	A	1
Clupea harengus	herring	7*	ff	??	A	2
		95*	7 weeks	??	A	2
Esox lucius	pike	30	0-3 days since ff	??	MZ	3
		80.5	15 days since ff	??	MZ	3
Coregonus fera	Weissfelchen	4.8	0-8 days since ff	??	MZ	3
		18.3	9-16 days since ff	??	MZ	3
C. wartmanni	Blaufelchen	3.2	0-8 days since ff	??	MZ	3
		21.6	9-16 days since ff	??	MZ	3
Anchoa mitchilli	bay anchovy	36.5	ff (2 days)	2.7	MZS	4
		51.6	8 days	3.9	MZS	4
A. lamprotaenia	big eye anchovy	50.3	ff (2 days)	3.6	MZS	4
		70.0	8 days	5.5	MZS	4
Alosa sapidissima	American shad	43	6 days	10.3	A	5
		50	12 days	10.5	A	5
Cichlasoma managense		70	ff	9.2	A	6
		6-7	ff	9.2	D	6
Cyprinus carpio	common carp	51.2	ff (2 days)	5.7	A	7
		88.5	5 days	7.4	A	7

*These values are calculated from their Fig. 5 as successful of total finished as opposed to the more quoted values of successful of total (finished + unfinished) snaps. References. 1: Hunter, 1972; 2: Blaxter & Staines, 1971; 3: Braum, 1963; 4: Chitty, 1981; 5: Wiggins et al., 1985; 6: Meyer, 1986; 7: this study.

Aiming can be distinguised in three perpendicular directions: left-right, vertical and parallel to the length axis of the larva. I take left-right and vertical aiming together as **perpendicular aiming.** Aiming parallel to the length axis is called **parallel aiming.** Left-right aiming is called horizontal aiming. Parallel and perpendicular aiming are both **distances.** The direction of aiming is given by the ratio of perpendicular and parallel aiming. To my knowledge no data on aiming of feeding fish larvae have been published;

2- Speed: the prey has less possibilities to escape, either due to an increase in mouth radius of the predator involving an increase of the required escape distance and/or a faster suction event, thus reducing the time to escape; see section IV.5 for a discussion about escape movements of the prey.

These two aspects are however not independent for it is reasonable to assume that for a given size of predator an increase in speed causes an increase in

aiming inaccuracy.

To be able to relate the extensive change in form of fish larvae during onto-geny with the increase in catch success, it is important to know whether this increase is due mainly to an increase in speed or to better aiming. If increase in speed is the more important factor the changes in form during ontogeny might be regarded as hydrodynamical optimizations to a higher catch success. Hydro-dynamical models, e.g. Muller et al. 1982, van Leeuwen & Muller 1984, are then useful to interpret the changes in morphology and in kinematics during attack, optimizing the velocity of the prey (i.e. the water). However, if the effects of aiming on catch success are the more important, the investigations should be focussed on the improvement of the senses and the muscular coordination during ontogeny.

It is known that adult fishes adjust the kinematics of prey intake to the type of prey (Nyberg 1971; Elshoud-Oldenhave & Osse 1976; Liem 1978). Also fish larvae can adjust the kinematics of prey intake to the type of prey: Sacramento perch larvae have different attack strategies for sluggish and for elusive prey (Vinyard 1982).

In this study the relative contribution of aiming of the predator and escape movements of the prey on the catch success of fish larvae is determined.

II Materials and methods

II.1 Filming setup

In total 30 snaps of larval and juvenile pike (Esox lucius) and carp (Cyprinus carpio) were filmed with a Teledyne DBM 54 camera (200-400 fr/s) or a Hadland Hyspeed camera (500-1150 fr/s). Shadow cinematography was used (Arnold & Nuttall-Smith 1974; cf. Drost & van den Boogaart 1986b for details). Illu-mination strength was about 800 lux. The fishes were never visibly stressed from the lights. Synchronous lateral and ventral views are obtained by three surface coated mirrors. The films were projected with a single frame projector (Analector 6, Oldelft) and analysed on a digitizer (Summagraphics supergrid) connected to a computer (Digital MINC 11).

II.2 Experimental animals and prey

Carp were from our laboratory stock at 23 C. Larvae were reared in 10 l aqua-ria with stagnant water. Oxygen supply and filtering ocurred with an air water lift and a filter (Tetra Briljant). Carp were fed once or twice a day nauplii of brine shrimp (Artemia salina). The eggs of pike were kindly supplied by the OVB (Dutch Organisation for Improvement of the Inland Fisheries), collect-ed from pikes in ponds. Pike larvae were kept in 15 l aquaria at 16-18 C. They

were fed once or twice a day a mixture of zooplankton, consisting mostly of Daphnia. From about 30 mm SL they were fed carp larvae.

Carp larvae (6-8 mm) were fed free swimming Artemia nauplii, pike larvae (14 mm) free swimming Daphnia (length 0.8-1 mm, excluding spine) in all experiments, in which distances were measured. In the experiments with pike juveniles (62 mm), prey fish were tied to a 0.1 mm nylon thread. With restrained prey a greater magnification could be achieved. Restrained prey were positioned exactly in the middle of the field of view by means of a micromanipulator. They were less active than free swimming prey. To stimulate the feeding of the fish and to prevent habituation to restrained prey, 1-2 free swimming prey were released in the filming aquarium when a restrained prey was introduced. In experiments with free swimming prey, width and height of the aquarium were at least equal to the total length of the fish. The length of the aquarium was at least twice the length of the larva. When a prey was restrained in its movements, all dimensions were at least 1.5 times bigger.

To make reliable measurements the magnification on the negative must be high. With free swimming prey, the aquaria had to be small to have at least some snaps in the field of view. With restrained prey the magnification can be high, irrespective of the size of the aquarium. The fish fed easily.

II.3 Measurements of aiming inaccuracy

In this study only perpendicular aiming is considered. The reason to leave out parallel aiming is treated in section IV.4. The method to determine the accuracy of aiming of a snap is summarized in Fig. 1a. The position of the centroid of the projection of the prey is determined at the frame before the mouth starts to open. The **length axis** is the length axis of the mouth cavity, unless otherwise indicated. The length axis is a line in the main direction of the mouth cavity passing through the middle of the mouth aperture. For successful snaps the position of the length axis is determined at the frame the prey enters the mouth; for failed snaps it is determined at the frame of maximal mouth aperture, because this moment coincides with prey uptake in adult fishes (Muller & Osse 1984). The distance between the centroid of the prey and this length axis is called the **projected perpendicular uptake position** (ppup). It can be positive (prey left of or above the length axis) or negative. For each snap a vertical and a horizontal projected perpendicular uptake position can be measured. The **perpendicular uptake distance** (pud) is the pythagorean sum of vertical and horizontal ppup.

Even if the prey does not move actively, it is moved by the suction flow to-
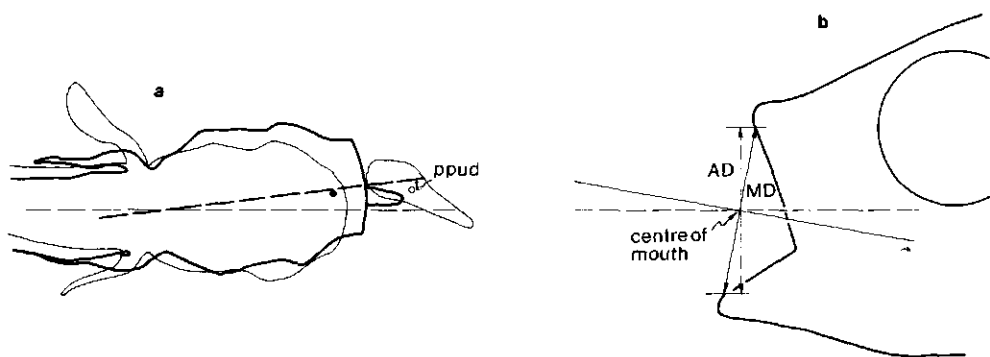
Fig. 1. a-*The* accuracy of aiming is determined from the film as shown in this example of the ventral view of a carp larva (5.8 mm). The position of the larva and the prey at the frame just prior to the start of mouth opening is indicated in light lines; o is the centre of mass of the projection of the prey. Positions at the frame the centre of mass of the prey passes the mouth aperture are in bold lines, **o** is the centre of mass of the projection of the prey. The pecked line is the length axis of the mouth cavity: the line in the main direction of the mouth cavi·ty, passing through the centroid of the mouth. The projected perpendicular uptake distance (ppup) is the distance between the centroid of the prey at the frame just before the start of mouth opening (o) and the length axis at the frame of prey uptake (- - -).
b-If the mouth aperture is not perpendicular to the length axis of the mouth cavity (- - -) two errors occur. First the mouth radius is overestimated: compare the measured distance (MD) with the real distance (AD), a difference of 2.5% in this situation. Projected perpendicular uptake position (ppup) should be measured relative to the length axis of the mouth cavity (- - -), but is measured relative to ---. The latter error increases with increasing measured distance parallel to length axis of the fish between prey and centre of mouth.

wards the length axis of the mouth cavity (Muller & Osse 1984; Muller & van Leeuwen 1985). A later determination of the position of the prey would underestimate the ppup; if the prey actively moves the ppup would be overestimated. I assumed that the fish aims just prior to the onset of suction and that it does not adjust its movements later, even if the prey makes escape movements. Large changes during the suction process will be almost impossible due to its short duration (Osse & Muller 1980).

II.4 Accuracy of the measurements

In small carp larvae (6-8 mm SL), the lateral and dorso-ventral head movements during a snap are very extensive (see e.g. Figs. 4 and 5); in pike larvae the movements of the head perpendicular to the swimming direction are low compared to the movement parallel to it. For carp the measured position of the axis of the mouth cavity is thus strongly dependent on the exact time of measurement.

The precision of measurements of the ppup for carp is therefore less than for pike. The pike juveniles were fed fish, which are elongate. Many prey fish were grasped between the pike's teeth, so there is no direct need to aim at the centre of mass. Measuring the aiming distance in the ventral view poses no problems, because the fish's movements and morphology are symmetrical. In the lateral view two problems exist. The first is that the line from the tip of the upper jaw to the tip of the lower jaw is not exactly perpendicular to the length axis (Fig. 1b). In the measurements the length axis is considered to be perpendicular to line from the tip of the upper jaw to the tip of the lower jaw, although that is not correct. This introduces an error in the measurements. This error increases with increasing distance, parallel to the length axis, between the mouth aperture and centre of the prey. Fortunately this distance is mostly very small (less than 0.5 mouth radius). The effective mouth radius is also slightly (less than 10%) overestimated. The second problem is that the centre of the mouth aperture moves laterally because upper and lower jaw move asynchroneously. So also the vertical ppup is susceptible to the exact time of measurement. The position of the prey is considered to be the centroid of its projection in lateral or ventral view. Strictly spoken, this is wrong, because the mass distribution in the third dimension is neglected. I think that the error is negligible for the ovoid Daphnia; small for Artemia and larger for fish.

III Results

III.1 Suction process of the pike

Prior to the suction act itself, a first feeding larva (SL 12-15 mm) slowly approaches the prey, mostly by movements of the pectoral fins. It then forms a S shaped attack posture. Its duration is dependent on the type of prey. Feeding on very sluggish prey (e.g. nauplii of Artemia salina) it is virtually absent; feeding on evasive prey (calanoid copepods) it was prominent and lasted for several seconds. In older larvae the attack posture is not longer distinct, but becomes integrated in the swimming movements. Suction starts when the larva straightens and almost simultaneously increases the volume of its mouth cavity by opening its mouth. In first feeding pike larvae, the prey enters the mouth within 15-20 ms after the beginning of the mouth opening or it is missed. This time increases with fish-length.

Fig. 2 depicts a lateral view of an unsuccessful snap of a 14 mm pike larva on a Daphnia. The speed of the centroid of the mouth aperture is first mainly due to swimming, but later to an increasing extent to a relative movements of
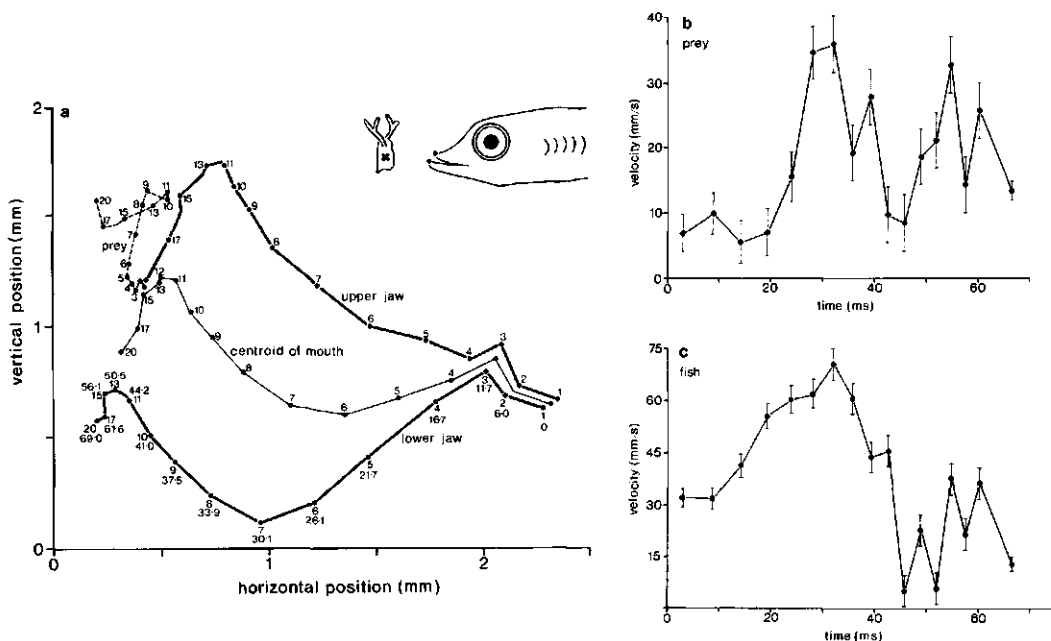
Fig. 2. Example of an unsuccessful suction act of a 14 mm pike larva feeding on a Daphnia. The film is accelerating from approximately 170 fr/s in frame 1 to 400 fr/s in frame 20.
a-Movements of upper and lower jaw, centroid of the mouth and centre of mass of the prey in lateral projection. Numbers indicate successive frames. Time for each frame is indicated near the curve of the lower jaw, starting from the last frame in which the mouth is just closed (frame 1). Note that the aiming was very accurate: the projected perpendicular uptake position (ppup, length axis determined at frame 9: maximal mouth aperture) is very small.
b-Velocity of the prey. First the prey is stationary (frame 1-4). Then it jumps away (frame 5-9): maximal acceleration 5.2 m/s^2 (error 1.7 m/s^2), the maximal velocity is 34 mm/s (e. 4 mm/s). At frame 9 the centre of mass of the prey is just in front of the fish's upper jaw. Between frame 9 and 10 it is sucked toward the mouth aperture. In frame 11 it has collided with the upper lip and is pushed forward. At frame 20 the prey starts a second jump and definitively escapes, not drawn in this figure.
c-Velocity of the middle of the mouth aperture. It accelerates from 0.03 m/s to 0.07 m/s and then decelerates. The stark oscillation in the velocity after t=45 ms is surprising: there is no reason for an increase in inaccuracy of measurement.

upper and lower jaw. The pike starts to open its mouth at a distance of about 2 mm from the prey. First the prey is stationary. Then it jumps away: the maximal acceleration is 5.2 ($\pm$ 1.7) m/s^2, the maximal velocity 34 ($\pm$ 4) mm/s. Because only movements in the plane of projection are considered, all values are minimum estimates. Unfortunately, in this snap no ventral view was made. At the end of the jump the centre of the prey is just in front of the upper jaw. The
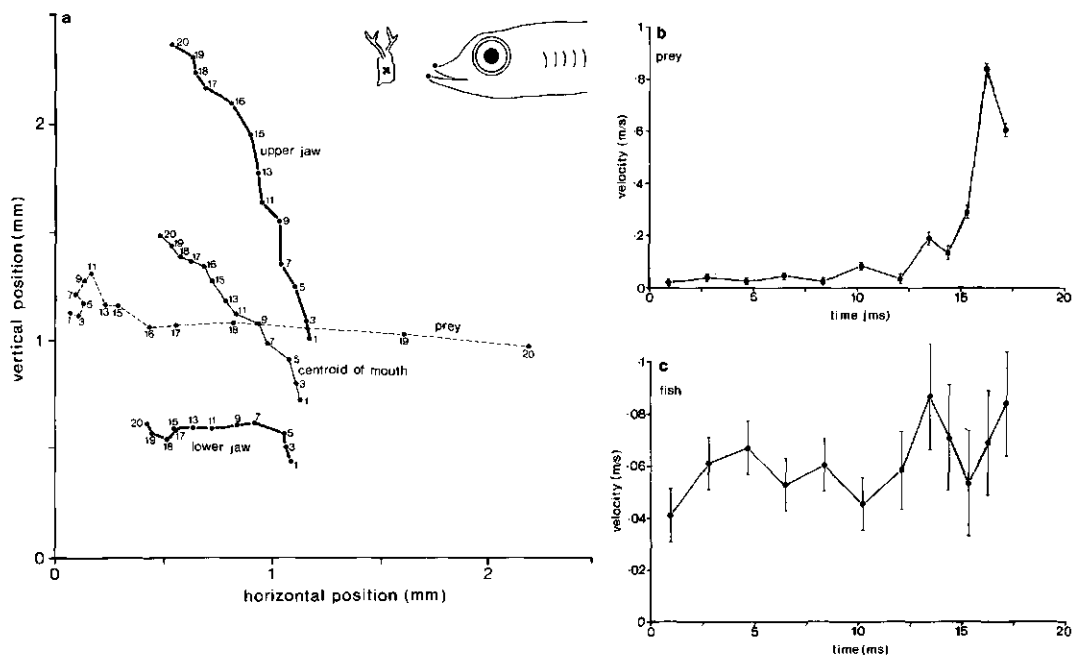
Fig. 3. Example of a successful suction act of a 14 mm pike larva feeding on a Daphnia. The filmspeed is 1077 fr/s. First every second frame is measured, later every frame.
a-Movements of upper and lower jaw, centroid of the mouth and centroid of mass of the prey in lateral projection. Numbers indicate successive frames. Time for each frame is indicated near the curve of the upper jaw, starting from the last frame in which the mouth is still closed (frame 1). Only the opening phase of the mouth is given. Aiming is worse than in Fig. 2: the projected perpendicular uptake position (ppup, length axis determined at frame 17: prey intake) is higher.
b-Velocity of the prey. The prey makes no escape movements. The measured velocity is first about 0.04 m/s. It is accelerated by the suction current, its maximal velocity being 0.84 m/s (earth bound).
c-Velocity of the centre of the mouth aperture. Within the accuracy of the measurements the velocity of the fish is almost constant.

prey finally escapes with a second jump. Note that the aiming was very accurate: the projected perpendicular uptake position at frame 11 (at maximal mouth aperture) is very small (Fig. 2a). The failure of the snap is due only to the movements of the prey. Measured maximal velocity of a prey during uptake by 12-15 mm pike larvae is 0.84 ($\pm$ 0.05) m/s (the velocity of the suction flow is thus 60 BL/s; see Fig. 3).

III.2 Suction process of the carp

While searching for prey, carp larvae (SL 6-8 mm) swim intermittently. Periods of 80-160 ms of activity, consisting of about 2 beats of the pectoral fins
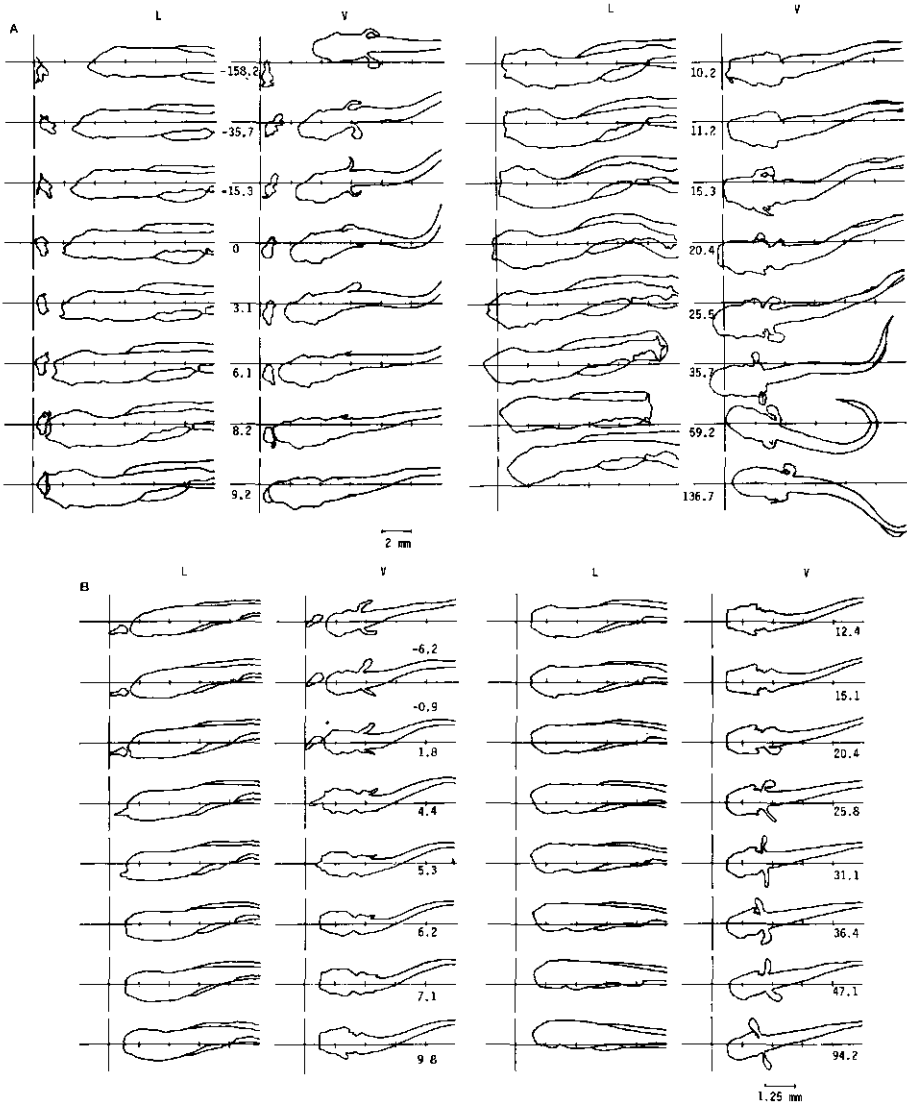
Fig. 4. Traces from high speed movies of larvae while sucking prey. Corresponding lateral (L) and ventral (V) views are depicted next to each other. Time, relative to the last frame the mouth is still closed, is indicated near the axis of the frame. Movements can be seen relative to the stationary frame. If the finfold shows its maximal size in the lateral view and is invisible in the ventral view, the fish is not rotated; if else the degree of rotation can be estimated from the relative apparent size of the finfold in lateral and ventral views. The posterior region of the larvae is not always in view, and the lateral and ventral views may be slightly translated relatively to each other. In evaluating the relative distance covered by suction and swimming, it must be noted that, even if no earth bound suction velocity occurs, suction is important in preventing stagnation (van Leeuwen, 1984).

In both snaps the pectoral fins become folded against the body (folded completely at the actual intake).

a- Pike, SL 12.5 mm, feeding on a restrained copepod. The bending of the body (S posture) and movements of the pectoral fins start about 150 ms prior to the onset of suction. Apart from extensive lateral bending (maximal at 0 and 60 ms) a dorso-ventral bending occurs: maximal at 15.3 ms. A possible explanation is that contraction of the epaxial muscles causes levation not only of the neurocranium, but also of the tail region. So contraction of the epaxial seems stronger than of the hypaxial musculature. The prey is almost stationary in the earth bound frame.

b- Carp, SL 6.5 mm, feeding on an Artemia nauplius from just above the bottom. This snap is not very intensive, compare the intensive snap of a 5.8 mm carp larva in Drost & van den Boogaart (1986b). The bending of the body and rotation of the length axis of the mouth cavity is small. In other snaps of carp larvae head and tail are moving upwards as in the snap of the pike larva in Fig. 4a. About 2/3 of the initial prey distance is covered by suction, only 1/3 by swimming.

often accompanied with low amplitude oscillations of the body, are alternated with periods of rest (often 0.2 to 0.4 s, but also frequently much longer). The velocity during activity is several BL/s, during rest it is very low, less than 0.1 BL/s. After a burst of activity, larvae decelerate rapidly (a length of 7 mm and a maximal velocity of 15 mm/s results in a Reynolds number of about 100). A typical attack sequence lasts about 400 ms. Before snapping, the larva fixes the prey by turning both eyes symmetrically forward. No real S shaped attack posture is formed, only one or two vigorous half oscillations of the body are made (see Fig. 4b) accompanied by vigorous movements of the pectoral fins. The pectoral fins become folded against the body at the moment of actual prey intake and opening of the opercular valve. Possible explanations of this moment of folding are that the outflow of water from the opercular slit would be hindered by spread pectoral fins, that the velocity of the fish at the moment of prey intake is maximized by synchronizing of the end of the power stroke of the fins with prey intake and that it is the start of the gliding phase in which the drag should be minimized. Suction starts when the mouth begins to open, all times are relative to the last frame the mouth is closed. Maximal angular velocity of the length axis of the mouth cavity is up to ca 10 ^{o}/ms during 5 ms (see Drost & van den Boogaart 1986b: Fig. 2). This is lower than in the Mauthner initiated startle response in larval zebra fish: up to 20 ^{o}/ms during 10 ms (Kimmel et al. 1980). The start of swimming precedes about 10 ms the onset of suction. The prey enters the mouth within 4-6 ms after the onset of suction or it is missed. In some movies the prey can be seen moving inside the mouth cavity through its transparant walls. The entrance of the esophagus is reached within 20 ms. The food enters the esophagus after about 1
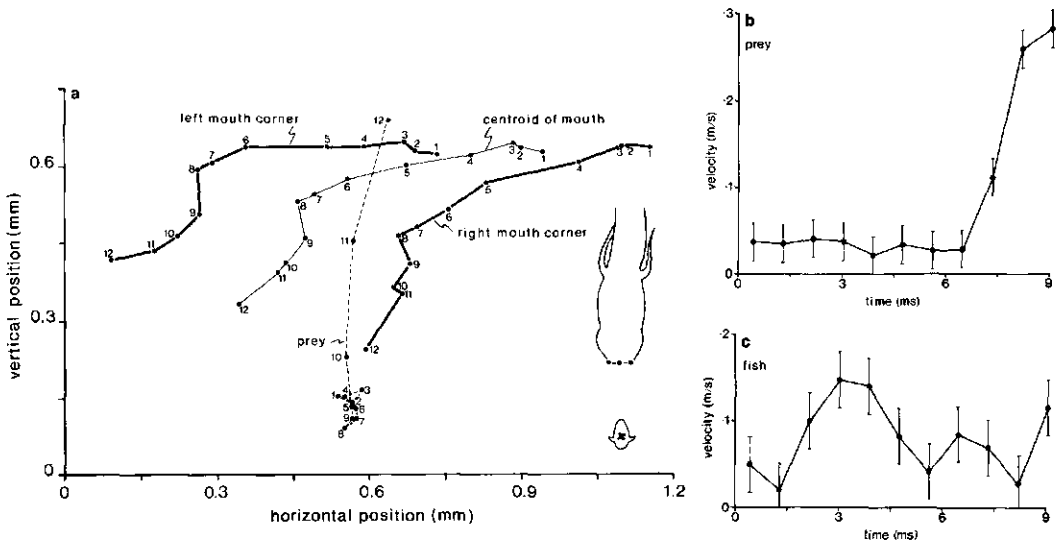
Fig. 5. Example of the suction act of a 5.8 mm carp larva feeding on an Arte-
mia nauplius (traces from this very intensive feeding act are given in Drost &
van den Boogaart (1986b). Filmspeed is 1150 fr/s.
a-Measured positions of left and right corner of the mouth and their middle and
the position of the centroid of the prey in ventral projection. A small suction
velocity towards the axis of the mouth cavity is visible. The movement of the
centroid of the mouth is not parallel to the mouth axis as we would expect in
swimming, but almost perpendicular to it (76°). The axis of the mouth cavity
rotates about 5°/ms during the first 5 ms.
b-Velocity of the prey. The prey is stationary first (velocity less than 0.04
m/s) and then sucked into the mouth cavity, with a maximal velocity of 0.26
m/s.
c-Velocity of the centre of the mouth aperture. This velocity shows no clear
trend in time.

s. The branchiostegal valve opens after about 8 ms, so the prey is captured
with still closed valves.

Fig. 5 gives the movements of a 6 mm carp larva sucking at an Artemia nauplius
in a vental view. The direction of the movement of the centre of the mouth
aperture is almost perpendicular to the length axis of the mouth cavity (76°).
The prey does not make active movements during the snap. Maximal velocity of
the prey during uptake is 0.26 (+ 0.03) m/s (so the larva creates a suction
current of 45 BL/s).

III.3 Strike accuracy

Prior to constructing a model for the relation between aiming and catch suc-
cess, the following notions are defined. The **aiming goal** is the mean of the
measured ppups, the **aiming inaccuracy** its standard deviation. According to

Table 2. Measured distance between the centre of the mouth aperture and the centre of mass of the prey. Positive values indicate that the centre nof mass is above (lateral view) or left of the the centre of the mouth (seen from above). Values are means + SE (number of measurements).
The mean is also called aiming goal, the standard deviation aiming inaccuracy.

	vertical	horizontal
Pike 14 mm	-0.38+0.26 (5)	-0.12+0.30 (6)
Pike 62 mm	-0.18∓0.72 (8)	-0.27∓0.74 (8)
Carp 6-8 mm	-0.15∓0.24 (9)	-0.01∓0.20 (10)

assumption 2 (section I.2), that the fish aims at the centre of mass of the prey, the expected value of the aiming goal is zero. The aiming inaccuracy is also called aiming accuracy (Beyer 1980). The latter terminology is avoided because a higher value of the aiming accuracy corresponds then to a less accurate aiming fish. In Table 2 the mean and standard deviation of vertical and horizontal ppup for pike larvae (SL 14 mm) and juveniles (62 mm) and carp larvae (SL 6-8 mm) are given.

In all three cases, vertical and horizontal values were not significantly different at the 5% level (Student's t-test). Contrary to our expectations however (section I.2), the aiming goal (= mean) differed significantly (5%) from the centre of the prey (=zero) for pike larvae in the lateral view. The same holds almost significantly for small carp. Both aimed too high: the prey enters through the lower half of the mouth aperture. For pike juveniles the difference was very small and not significant. In the ventral views, the aiming goal did not deviate significantly from the centre of mass of the prey. Vertical and horizontal aiming inaccuracies are almost the same in all three cases. During the ontogeny of pike aiming inaccuracy increases from 0.28 mm at a length of 14 mm to 0.73 mm at a length of 62 mm. The aiming inaccuracy relative to the standard length decreases from 2% to 1.2%: larger pikes aim relatively better. Aiming inaccuracy of 6-8 mm carp larvae is 0.23 mm. The relative aiming inaccuracy of these carp larvae is greater than of pike: 3.5%.
Maximal mouth radius during prey intake increases from 0.25-0.30 mm for a 6 mm, to 0.35-0.40 mm for a 8 mm carp larva. So mean maximal mouth radius did not increase relative to the length of the larvae (4.6% at 6 mm; 4.7% at 8 mm). Mouth width is 0-20% bigger than maximal mouth height. I combined the data of the 6-8 mm larvae to have more observations in one class.

IV Discussion

IV.1 Model construction

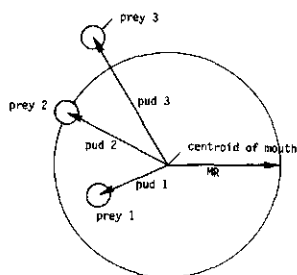The relation between aiming inaccuracy and catch success on approximately

Fig. 6. For a successful attack in the model the perpendicular uptake distance (pud) must be less than the mouth radius (MR). Prey 1 will be taken in ($pud_1<MR$); prey 3 will be missed ($pud_3>MR$). Prey 2 is the boundary ($pud_2=MR$).

spherical prey can be calculated with a mathematical model (Beyer 1980), assuming the following simplifying approximations:

1- The vertical and horizontal ppups are distributed normal, with a mean of zero and equal standard deviations;

2- Vertical and horizontal ppups are independent;

3- The prey enters the mouth if the perpendicular uptake distance is less than the mouth radius (see Fig. 6). The mouth aperture is assumed circular and aiming in the length direction is assumed optimal.

The following critical remarks about these assumptions can be made.

1- In principle this condition can be tested with the measured ppuds. I made however not enough measurements to test normality. In the ventral views, the mean did not deviate from zero, in the lateral view carp and pike larvae aimed too high. The assumption is thus not fulfilled. The influence of this deviation can be seen in Fig. 12b.

2- If we would assume a constant inaccuracy in strike **angle**, aiming inaccuracy increases linearly with strike distance. The vertical and horizontal ppups would then not be independent. In Fig. 7 absolute values of corresponding vertical and horizontal ppups are plotted against each other for carp larvae. The correlation coefficient (r) equals 0.47 ($r^2=0.22$), which is not significantly different from zero at the 5% level (Sokal & Rohlf 1969). A part of this correlation may result from a correlation between length of the carp larva and both horizontal and vertical ppup. The number of observations is however rather low (9). I suppose that 0.5 is a reasonable value for the parametric correlation, but this assumption is not statistically sound.

Model predictions were also calculated with a correlation of 0.5 and 0.9 between vertical and horizontal ppup (Fig. 12a). A more extensive treatment of
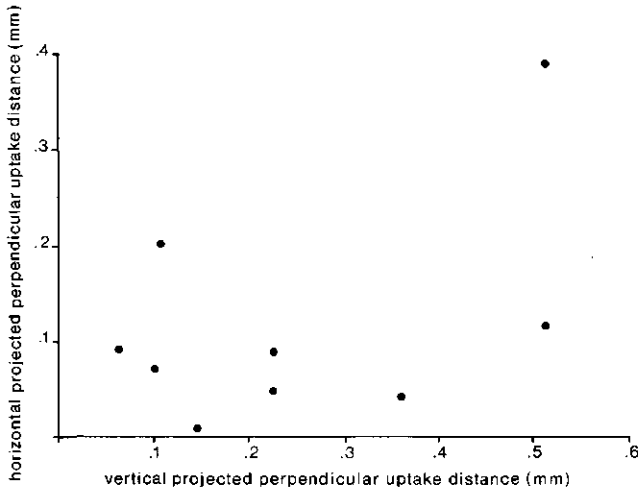
Fig. 7. To determine whether vertical and horizontal aiming are independent (condition 2, section IV.1), absolute values of vertical and horizontal projected perpendicular uptake positions (see section II.3 and Fig. 1 for an explanation) of a snap are plotted against each other. This is done for 9 snaps of 6-8 mm carp larvae. The distances are measured from high speed movies with synchronous lateral and ventral views. Calculated correlation: r=0.47. This is not significantly different from zero (at the 5% level, with this rather low number of measurements).

these calculations will be given later in this paper. For the correlation of 0.5 the influence on the calculated catch success is very small; even with a correlation of 0.9 no important deviations do occur.

3- During the suction process, water 'velocity has a radial component towards the centre of the mouth. The relative magnitude of this radial component depends on the ratio between swimming velocity and suction velocity (Muller & Osse 1984; Muller & van Leeuwen 1985). So, also a prey outside the mouth radius can be sucked in depending on the exact position of the dividing streamline. Possible effects of friction on the postion of the dividing streamline are neglected. In the model however, sucking is treated as filtering: so no prey more than one mouth radius from the length axis can be taken in.

Although this condition is not fully fulfilled, this is assumed to have only a minor influence.

Although the assumptions are only partly fulfilled, the deviations are small enough to continue with the model. A theoretical frequency distribution of the (vertical) projected perpendicular uptake position is given in Fig. 8a: a normal distribution, the mean being the centre of the prey. It is assumed that the horizontal ppup has the same frequency distribution (same mean and standard deviation, Fig. 8b). Vertical and horizontal ppup of Fig. 8 are combined to
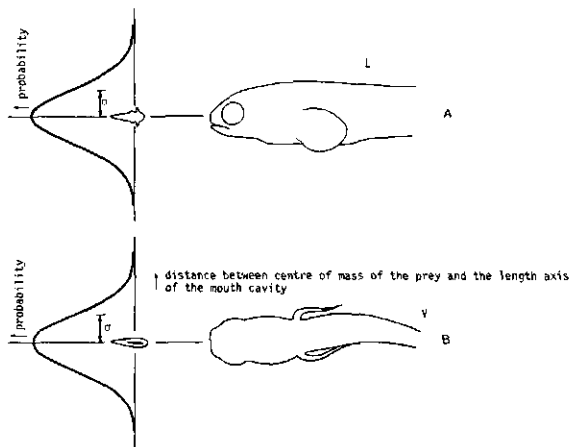
Fig. 8. a- Theoretical probability density distribution for the vertical projected perpendicular uptake position, i.e. the distance between the centre of mass of the prey and the length axis of the mouth cavity in a lateral view. The position of the prey is determined at the start of the snap, the postion of the length axis during prey intake or maximal mouth aperture, see also section II.3 and Fig. 1. The projected·perpendicular uptake position is taken positive if the prey is above, negative if it's below the length axis. Larva and prey are drawn from the frame of the start of mouth opening. The distance parallel to the axis between prey and mouth aperture is not considered in the model. The distribution is assumed to be normal (Gaussian), the mean being zero, i.e. the centre of mass of the prey. The standard deviation (σ) is called aiming inaccuracy.
b-Idem for the ventral view (horizontal ppup).

give a 2-D frequency distribution of the perpendicular uptake position, i.e. the position of the centre of mass of the prey relative to the length axis of the mouth cavity, terminology as explained in section II.3. This distribution is called the bivariate normal frequency distribution. Starting from the frequency distribution of the perpendicular uptake **position** (relative to the length axis (Fig. 9), the frequency distribution of the perpendicular uptake **distance** (to the length axis) can be calculated (Fig. 10a); the way of calculation is explained in Fig. 10b. Fig. 11 presents the cumulative frequency distribution of the perpendicular uptake distance; it shows the probability

that the pud is less than a given value. I assumed (condition 3, section IV.1) that the prey enters the mouth if the pud is less than the mouth radius. Therefore the ratio of mouth radius and aiming inaccuracy is put on the abscissa in Fig. 11 and the expected catch success on the ordinate. The measured data for aiming inaccuracy and catch success are also indicated in this figure.
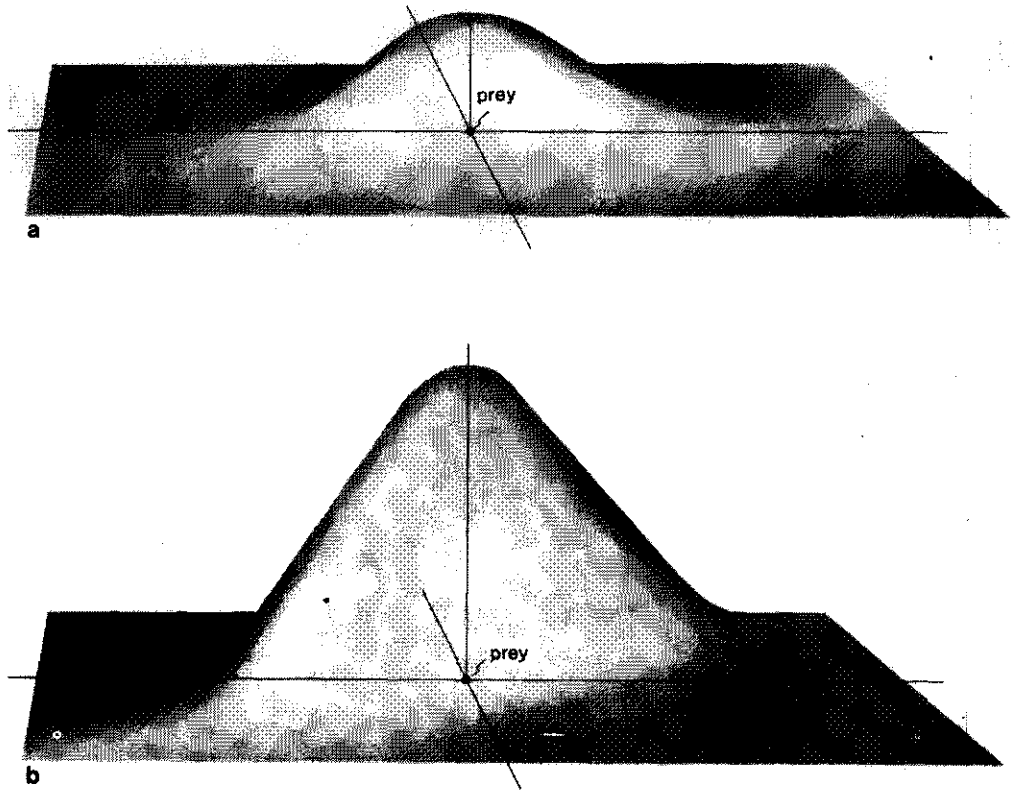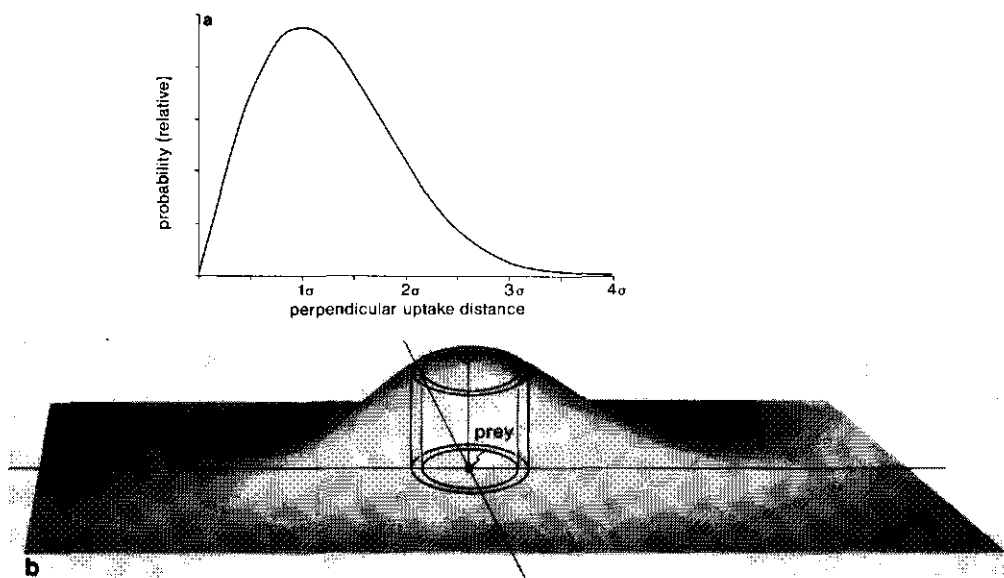In Fig. 12   the effect on the calculated catch success of violation

Fig. 9. Theoretical probability density distribution of the perpendicular uptake position, i.e. the position of the centre of mass of the prey relative to the length axis of the mouth cavity in 2D. The position of the centre of mass of the prey is determined just prior to the onset of suction; the position of the length axis is determined at the frame of actual prey intake or maximal mouth aperture (see for details section II.3 and Fig. 1). Vertical and horizontal projected perpendicular uptake position (ppup) are assumed independent and to have a mean of zero and equal standard deviations (a, see also Fig. 8). This distribution is the bivariate normal frequency distribution. If vertical and horizontal perpendicular uptake position are correlated ($r^2 > 0$) or both standard deviations are unequal the probability density function becomes elongated (b).

of the simplifying approximations 1 and 2 of section IV.1 are given.

Fig. 12a shows the effect of the magnitude of the parametric correlation on the calculated catch success. At a medium correlation (0.5, compare the calculated value of 0.47 for small carp larvae: Fig. 7) the calculated catch success

Fig. 10. a- Theoretical probability density distribution of the perpendicular uptake distance (pud), i.e. the distance between the centre of mass of the prey and the length axis, both determined according to Fig. 1a. This (Fig. 10a) distribution is calculated from the probability density distribution of the perpendicular uptake position in Fig. 9 according to Fig. 10b. The distribution gives the probability that the pud has a certain value.
b- Theoretical probability density distribution of the perpendicular uptake position (mound, as Fig. 9). Total volume under the mound is 1. The probability that the perpendicular uptake position is greater than r and smaller than r+dr is given by the volume of the cylinder skin.
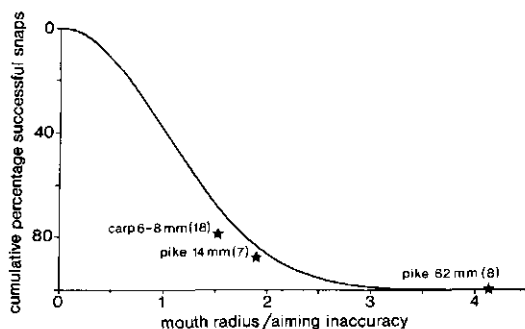
Fig. 11. Theoretical probability density distribution of the cumulative perpendicular uptake distance. It shows the probability that the perpendicular uptake distance (pud) is less than the given value. If we read on the abscissa the ratio of maximal mouth radius/ aiming inaccuracy, the ordinate gives the percentage successful snaps as calculated with the model. Observed catch success for pike and carp larvae measured from high speed movies is also indicated (number of observations in brackets).
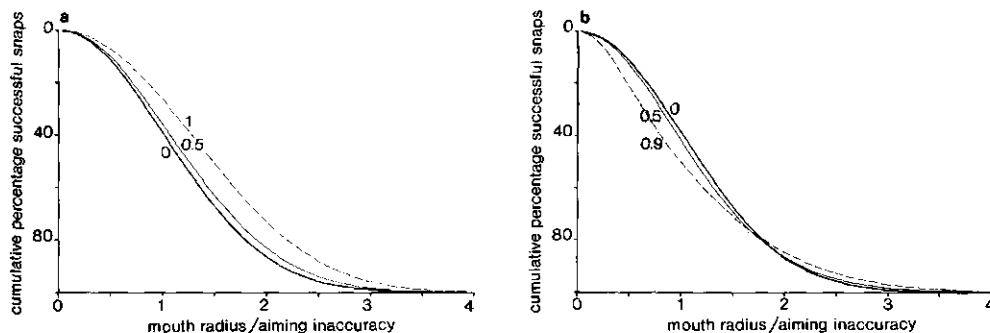
Fig. 12. Theoretical probability density distribution of the cumulative perpendicular uptake distance. The curves are constructed by sampling by computer 2×10^6 pairs out of a standard normal distribution. The standard deviation is always taken 1; mean was zero for the ventral view. The mean in the lateral view and the parametric correlation between vertical and horizontal projected perpendicular uptake position (ppup) could be varied. The resulting perpendicular uptake distance (pud) was calculated (Pythagoras). The values were divided in 100 classes of width 0.04 times the aiming inaccuracy.
a-Different values for the parametric correlation between horizontal and vertical ppup: 0, 0.5 and 0.9; both means are 0. The difference in calculated catch success between a correlation of 0.5 and 0 is very low: e.g. a increase of catch success at a ratio of mouth radius and aiming inaccuracy of 1 of 39% (correlation is 0) to 42% (correlation is 0.5). A correlation of 0.9 influences the calculated catch success appreciably: to a catch success of 50% under the same conditions.
b-Different values for the mean (aiming goal) in the lateral view. Parametric correlation is taken 0. The calculated catch success at a given value of the ratio mouth radius/aiming inaccuracy decreases with increasing aiming goal (as expected). The influence of an aiming goal of 0.5 aiming inaccuracy is rather small: e.g. at a ratio of mouth radius and aiming inaccuracy of 1 the calculated catch success decreases from 39% (aiming goal is zero) to 35%; the influence of an aiming goal equal to the aiming inaccuracy is bigger: calculated catch success under the same conditions is then 27%.

differs only slightly from the zero correlation situation. Only at high values of parametric correlation the calculated catch success is influenced appreciably.

In Fig. 12b the horizontal aiming goal is zero, i.e. the fish does not deviate systematically to the left or to the right; the vertical aiming goal is varied. If the vertical aiming goal is 0.5 times the aiming inaccuracy, the calculated catch success does not differ much from the both zero aiming goal situation. If the vertical aiming goal is equal to the aiming inaccuracy, the influence is much larger. According to Table 2 the vertical aiming goal is about 0.5 times the aiming inaccuracy for the carp larvae, and greater than the aiming inaccuracy for 14 mm pike larvae. The calculated catch success in Fig. 11 thus

overestimates the catch success of carp and small pike larvae.

IV.2 Aiming inaccuracy: comparison of observed and predicted catch success

Measured ratio of mouth radius and aiming inaccuracy of the 14 mm pike larvae is 1.89. According to Fig. 11 this corresponds to a catch success of 80%. Of the 8 filmed snaps 5 were successful, in one the Daphnia escaped by a jump perpendicular to the suction (Fig. 2), in one the prey was just sucked in, but swam out of the mouth aperture a little later and in one case a larva missed a non moving prey. The observed percentage of missing due to aiming is thus 12.5%. In view of the low number of observations (8), expected and observed percentage are in the same range. For these pike larvae escape reactions of the prey (Daphnia) caused more failures than bad aiming.

For the snaps of the juvenile pike the ratio mouth radius/aiming inaccuracy was 4.13, which corresponds (Fig. 11) to an expected catch success of 100%. All eight filmed snaps indeed were successful. Catch success was also determined visually for pike juveniles (60-70 mm), feeding on larval carp. Of the 159 snaps 153 were successful (96.2%). In three snaps the failure obviously was caused by very bad parallel aiming; in two other failures the prey swam vigo-rously. The observed failure percentage due to perpendicular aiming is thus maximally 3.8%, and more probably 1.9% if the three failures probably due to parallel aiming are discarded and possibly only 0.6% if also the two failures with prey movement are attributed to escape movements. The observed and calcu-lated catch success due to perpendicular aiming thus closely agrees for pike juveniles.

For carp larvae 10 snaps were measured (9 lateral, 10 ventral). The ratio between mouth aperture and aiming inaccuracy was 1.54. According to Fig. 11 this corresponds to a catch success of 66%. Another 8 snaps of 6-8 mm carp larvae were filmed (300-400 frames/s). The magnification of these films was too low to measure ppups. Fourteen of the 18 snaps were successful (78%). Expected and observed percentage agree well. I never saw an Artemia perform escape movements. All failures were caused by bad aiming.

Capture success was also determined visually for carp larvae feeding on Artemia nauplii. It increased from 51.2% for 5.7 mm larvae to 88.5% for 7.4 mm larvae.

IV.3 Influence of prey size on catch success

In my model the size of the prey has no influence on the calculated catch success: the prey is taken in if the centre of mass is in front of the mouth aperture. Beyer (1980, also regarding spheres) assumed that the prey is only taken in if even its outer margin is in front of the mouth aperture, so the

size of the prey is important for expected catch success. To settle this problem, I have calculated from my raw data the expected catch success assuming Beyers 'outer margin' condition. I have considered an <u>Artemia</u> nauplius to be a sphere with a radius of 0.1 mm. For carp the relative aiming inaccuracy is then 92.5%. This corresponds to a catch success (Fig. 11) of 44%. The expected catch success under the first view (66%) is much closer to the observed catch success (78%). So, the model interpretation of my measurements does not indicate a relation between catch success and prey width for relatively small prey; obviously, this will change when the prey width approaches maximal mouth diameter. Catch success of anchovy larvae (age 17 days) dropped from 80% to 40%, when the prey was changed from the (small, diameter 0.133 mm) <u>Brachionus</u> to (larger, diameter 0.236 mm) <u>Artemia</u> nauplii (Hunter 1972). Beyer (1980) explains this by the greater radius of the nauplii. My suggestion is that the larvae suck faster to the nauplii, the increase in velocity causing an increase in aiming inaccuracy. To decide this issue aiming inaccuracy should be measured from high speed movies of larvae, while feeding on sluggish and on fast prey.

IV.4 Aiming in the length direction

In the plane perpendicular to the length axis of the predator, the centre of mass of the prey is a logical assumption for the target of aiming. Van Leeuwen & Muller (1984) gave predictions for optimal movements of fish when sucking prey, based on theoretical considerations. The prey should be taken in at maximal mouth aperture and the water (i.e. prey) velocity should be maximal at that moment. To determine the optimal prey distance with given movements of the larva is a slightly different problem, because maximal gape and maximal water velocity need not to coincide in actual snaps. This velocity can be calculated from accurate motion curves of the mouth cavity (Drost & van den Boogaart 1986a), but it is laborious and the results are hardly accurate enough. Therefore aiming in the length direction (parallel aiming) has not been taken into account. However bad parallel aiming might also cause unsuccessful snaps. As my model neglects these failures, its predicted catch success will thus be an overestimation of total success from aiming.

Nyberg (1971) found in a high speed movie study of large mouth bass (SL 58-349 mm) that 8 of the 85 snaps in which the prey did not move, failed. Seven failures were due to "opening the mouth to soon" or "not soon enough", i.e. aiming in the length direction in my terminology. One was due to an "error in direction", i.e. perpendicular aiming. According to Webb & Skadsen (1980) the most

common cause for a failed strike in hybrid tiger muskie was "striking above or below (the prey)", i.e. perpendicular aiming.

IV.5 The influence of escape movements of the prey on the catch success

The movement required for the prey to escape from being sucked into the mouth cavity, is just the mouth radius of the larva, under the following three conditions:

1-the prey starts at the onset of the strike to move perpendicular to the strike direction (this direction seems to minimize the chance of being captured);

2-the aiming inaccuracy is zero, i.e. the predator aims exactly at the centre of mass of the prey;

3-once started, the larva does not adjust its strike in concordance with sensory input in these few milliseconds.

The following remarks about these assumptions can be made.

1- Some prey (species) jump away before the snap has started (e.g. calanoid copepods), other never jump away (e.g. Artemia nauplii). Knowledge of the reaction field of zooplankters is required to evaluate this condition. Whether or not this condition is fulfilled depends on the species preyed upon.

2- If the perpendicular uptake position has a bivariate normal frequency distribution with a non-zero standard deviation (=aiming inaccuracy; see Fig. 11) the distance required for the prey to come outside of the radius of the mouth aperture is a complex function. It can be calculated from the mouth radius and the aiming inaccuracy, assuming that all escape directions perpendicular to the length axis of the predator are equally probable. The assumption that the aiming inaccuracy is zero greatly simplifies the calculations and causes only slightly different solutions. Furthermore the aiming inaccuracy is not well known. So condition 2 is only for mathematical convenience.

3- Swimming, especially accelerating, induces considerable wobble of the head for fish larvae, due to the curvature of the whole body (Fig. 4). As larvae swim vigorously during attack, the head does not move in a straight line in a ventral view, even if the prey does not move actively (see Fig. 5). In a lateral view the centre of the mouth aperture moves as a function of the opening of lower and upper jaw, which do not move synchroneously. Therefore, it is impossible to decide whether or not a larva has adjusted its strike axis during the strike to a rapidly accelerating prey. Given the short duration of the attack (less than 15 ms for a first feeding carp larva), it is reasonable to think that the movements are rather stereotyped, once they are started (see

Table 3. Movement data for zooplankters. Measured maximal acceleration and distance covered in the first 20 ms of the movement. Data are measured from multiflash photographs (escape of Cyclops scutifer) or high speed films (other data).
References. 1: Lehman 1977; 2: Strickler 1977; 3: Strickler & Ball 1973; 4: Gilbert 1985.

Species	max. acceleration (m/s^2)	dist. covered (mm)	movement type	reference
Copepoda				
Diaptomus franciscanus	15	2.25	escape	1
Cyclops scutifer	12	0.74	hop and sink swimming	2
C. scutifer	-	1 (in 5 ms)	escape	3
Cladocera				
Daphnia pulex	6.5	0.8	escape	1
Rotifera				
Polyarthra vulgaris	-	0.7*	escape	4

*During the escape movement the velocity changed erratically. The distance covered is calculated from the mean velocity.

also Nyberg 1971; Osse & Muller 1980).

For a 14 mm pike larva maximal mouth radius is about 0.7 mm and strike time about 20 ms, although the start of the strike time is rather arbitrarily. Movement data for zooplankters from the literature are given in Table 3. It suggests that Daphnia might just be able to escape from a prey-sucking pike larva by velocity, Diaptomus and Cyclops amply.

IV.6 Feeding strategy of larval fish

An important question is whether there exists a strategy which maximizes the net energetic gains of a fish larva once it has encoutered a prey. One choice might be to maximize the chance that each encountered prey is captured, an other is to minimize the energy expenditure during a suction act, allowing some prey to escape. To minimize the chance that a prey tries to escape by jumping away, the larva has to minimize the time that it is within the detection range of the prey. The detection range of plankton for approaching fish is not known. The detection range of Temora longicornis, a copepod, is more than 4.5 mm for slow water currents (Gill & Crisp 1985). The attack distance of small pike larvae is about 5 mm. With a given detection range of the prey, the strategy of the predator depends on the relation between maximal velocity and acceleration of both predator and prey and the attack time and distance of the predator: the predator has to start swimming outside the detection range in order to to minimize the time it is within this detection range. It is possible that sucking very fast decreases the accuracy of aiming. This can be studied on

larvae trained on sluggish and on fast prey.

The energy that is used in a suction act consists of energy used for swimming and energy used for sucking. The required energy during a snap of a 6 mm carp larva is less than 0.02% of the energetic content of an Artemia nauplius (Drost & v.d. Boogaart 1986b). The error in this estimation is estimated to be less than a factor 10. Energetic considerations will thus be unimportant in deciding to suck fast or slow.

CONCLUSIONS

1-From the inaccuracy of aiming in the plane perpendicular to the length axis of the fish the percentage failed snaps due to bad perpendicular aiming can be predicted using a model.

2-During the ontogeny of pike, both aiming inaccuracy and mouth radius increase their ratio, however, and thus the failure percentage decrease. The model adequately predicts the catch success due to perpendicular aiming. For 14 mm larvae feeding on Daphnia escape movements however cause more failure than bad aiming.

3-Also during the ontogeny of larval carp the measured increase in catch success agrees with the calculated increase in catch success due to an increase of the ratio between mouth radius and aiming inaccuracy.

4-Catch success is determined by the ratio of mouth radius and aiming inaccuracy and by the 'speed' of prey and larva, but seems independent of the size of the prey (when smaller than the mouth aperture). Smaller catch success on larger prey may result from better escape movements of the prey.

5-The maximal velocity in the water flow created by carp larvae (SL 5.8 mm) when sucking prey is 0.26 m/s (45 BL/s); pike larvae (14 mm SL) 0.84 m/s (60 BL/s); this is much higher than the escape velocities of even calanoid copepods.

6-The importance of aiming in catch success suggests that a very early completion of the sensors for detecting the position of the prey is required. This hypothesis must be tested in future research.

ACKNOWLEDGEMENTS

66

REFERENCES

Arnold, G.P. & P.B.N. Nuttall-Smith (1974). Shadow Cinematography of Fish Larvae. Mar. Biol. 28: 51-53.

Beyer, J.E. (1980). Feeding success of clupeoid fish larvae and stochastic thinking. Dana 1: 65-91.

Blaxter, J.H.S. (1969). Development: eggs and larvae. In: W.S. Hoar & D.J. Randall (eds.). Fish Physiol. 3: 177-252. Academic Press. New York.

Blaxter, J.H.S. & Staines, M.E. (1971). Food searching potential in marine fish larvae. In: Crisp, D.J. (ed.) Fourth European Marine Biology Symposium. Cambridge: University Press. pp. 467-485.

Braum, E. (1963). Die ersten Beutefanghandlungen junger Blaufelchen (Coregonus wartmanni Bloch) und Hechte (Esox lucius L.). Zeitschr. f. Tierpsychol. 20: 257-266.

Braum, E. (1967). The survival of fish larvae with reference to their feeding behaviour and the food supply. In: S.D. Gerking (Ed.). The biological basis of fish production. pp. 113-131. Oxford: Blackwell Scientific Publishers.

Chitty, N. (1981). Behavioral observations of the feeding of the larvae of bay anchovy, Anchoa mitchilli and bigeye anchovy Anchoa lamprotaenia Rapp. P.v. Reun. Cons. Explor. Mer, 178: 320-321.

Confer, J.L. & Blades, P.I. (1975). Omnivorous zooplankton and planktivorous fish. Limnol. Oceanogr. 20: 571-579.

Drenner, R.W., R. Strickler & W.J. O'Brien (1978). Capture probability: the role of zooplankter escape in selective feeding of planktivorous fish. J. Fish. Res. Board Canada 35: 1370-1373.

Drost, M.R. & Boogaart, J.G.M. van den (1986a). A simple method for measuring the changing volume of small biological objects, illustrated by studies of suction feeding by fish larvae and of shrinkage due to histological fixation. J. Zool. 206: 239-249.

Drost, M.R., & Boogaart, J.G.M. van den (1986b, in press). The energetics of feeding strikes in larval carp (Cyprinus carpio). J. Fish Biol.

Elshoud-Oldenhave, M.J.W. & J.W.M. Osse (1976). Functional morphology of the feeding system of the ruff, Gymnocephalus cernua (L. 1758) (Teleostei, Percidae). J. Morph. 150: 399-422.

Gilbert, J.J. (1985). Escape response of the rotifer Polyarthra a high speed cinematographic study. Oecologia (Berl.) 66: 322-331.

Gill, C.W. & D.J. Crisp (1985). Sensitivity of intact and antennule amputated copepods to water disturbance. Mar. Ecol. Prog. Ser. 21: 221-227.

Hunter, J.R. (1972). Swimming an feeding behavior of larval anchovy Engraulis mordax. Fish. Bull., U.S. 70: 821-838.

Hunter, J.R. (1980). The feeding behavior and ecology of marine fish larvae. In: J.E. Bardach, J.J. Magnuson, R.C. May & J.M. Reinhart (eds.). Fish behavior and its use in the capture and culture of fishes. ICLARM Conference Proceedings 5, 512p. ICLARM, Manilla, Philippines.

Kimmel C.B., Eaton, R.C. & Powell, S.L. (1980). Decreased fast start performance of zebrafish larvae lacking Mauthner neurons. J. Comp. Phys. 140: 343-350.

Leeuwen, J.L. van (1984). A quantitative study of flow in prey capture by the Rainbow trout, Salmo gairdneri with general consideration of the actinopterygian feeding mechanism. Trans. zool. Soc. Lond. 37: 171-227. .I -3

Leeuwen, J.L. van & M. Muller (1984). Optimum sucking techniques for predatory fish. Trans. zool. Soc. Lond. 37: 137-169.

Lehman, J.T. (1977). On calculating drag characteristics for decelerating zooplankton. Limnol. Oceanogr. 22: 170-172.

Liem, K.F. (1978). Modulatory multiplicity in the functional repertoire of the feeding mechanism in cichlid fishes. J. Morph. 158: 323-360.

Meyer, A. (1986, in press). First feeding success with two types of prey by the fry of the central American cichlid fish, Cichlasoma managuense, morphology and behavior. Env. Biol. Fish.

Mills, E.L., Confer, J.L. & Ready, R.C. (1984). Prey selection by young yellow perch: the influence of capture success, visual acuity and prey choice. Trans. Am. Fish. Soc. 113: 579-587.

Muller, M. & J.L. van Leeuwen (1985). The flow in front of the mouth of a prey-capturing fish. In: H.R. Duncker & G.Fleisher (Eds.). Vertebrate Morphology. Gustav Fisher Verlag. Stuttgart, New York. Fortschitte der Zoologie 30.

Muller, M. & J.W.M. Osse (1984). Hydrodynamics of suction feeding in fish. Trans. zool. Soc. Lond. 37: 51-135.

Muller, M., J.W.M. Osse & J.H.G. Verhagen (1982). A quantitative hydrodynamical model of suction feeding in fish. J. Theor. Biol. 95: 49-79.

Nyberg, D.W. (1971). Prey capture in the Largemouth Bass. Am. Midl. Nat. 86: 128-144.

Oiested, V. (1984). Predation on fish larvae as regulatory force, illustrated in mesocosm studies with large groups of larvae. NAFO Sci. Coun. Studies 8: 25-32.

Osse, J.W.M. & Muller, M. (1980). A model of suction feeding in teleostean fishes with some implications for ventilation. In: Ali, M.D. (ed.). Environmental physiology of fishes: 335-352. Nato-Asi series A, Life sciences. New York: Plenum Pub. Co.

Rosenthal, H. & Hempel, G. (1970). Experimental studies in feeding and food requirements of herring larvae (Clupea harengus). In: Steele, J.H. (Ed.). Marine food chains.

Strickler, J.R. (1977). Swimming of planktonic Cyclops species (Copepoda, Crustacea): patterns, movements and their control. In: T.Y.T. Wu, C.J. Brokaw & C. Brennen (eds). Swimming and flying in nature (2): 599-613. 917p. Plenum Press. New York, London..

Strickler, J.R. & A.K. Ball (1973). Setae of the first antennae of the copepod Cyclops scutifer (Sars): Their structure and importance. Proc. Nat. Acad. Sci. USA, 70: 2656-2659.

Sokal & Rohlf (1969). Biometry. Freeman New York.

Vinyard, G.L. (1982). Variable kinematics of Sacramento perch (Archoplites interruptus) capturing evasive and nonevasive prey. Can. J. Fish. Aquat. Sci. 39: 208-211.

Webb, P. & Skadsen (1980). Strike tactics of Esox. Can. J. Zool. 58: 1462-1469.

Wiggings, T.A., Bender, T.R., Mudrak, V.A. & Coll, J.A. (1985). The development, feeding, growth and survival of cultured American Shad larvae through the transition from endogenous to exogenous nutrition. Prog. Fish-Cult. 47: 87-93.

Winfield, I.J., G. Peirson, M. Cryer & C.R. Townsend (1983). The behavioural basis of prey selection by underyearling bream (Abramis brama (L.)) and roach (Rutilus rutilus (L.)). Freshwater Biology 13: 139-149.

Hydrodynamic limitations of feeding in larval fish

M.R. Drost & J.H.G. Verhagen
Dept. of Experimental Animal Morphology and Cell Biology
Agricultural University
Marijkeweg 40, 6709 PG Wageningen, The Netherlands.

ABSTRACT

Most fish larvae take their food in by suction. The food is taken in within about 5 ms after the start of the suction. A simplified hydrodynamical model is constructed to obtain a picture of the importance of friction during this food intake. In some simulations the mouth cavity is schematized as lying between two parallel plates in other simulations as part of a flow pipe. A sudden pressure gradient is introduced on the profile. The plate model gives a good description of the start of the suction process, the flow pipe of the later stages. The calculated increase in power required to overcome friction is 45% for a first feeding carp larva. Combination of the model results with data of the relation between larval size and duration of the suction process for pike indicate that the muscle tension required for feeding is almost minimal at hatching. The slopes of increase of this tension are weak with decreasing size, but much steeper with increasing size (i.e. growth).

INTRODUCTION

Larvae of most fish species show considerable similarity in the form of the body and the head (see e.g. Russell, 1976); at least they are much more alike than adult fish (the term larvae is used loosely for both larvae and juveniles sensu Balon (1975). During ontogeny the form of many species of fish larvae changes markedly, up to a length of about 20-30 mm, exact size depending on species. The end of this rather gradual change in form is frequently called metamorphosis. At metamorphosis the young fish have become miniature adults and further growth involves little change of form. Adult fishes have many feeding types, the most important being filtering, ambush or pursuit predation on large prey and benthic feeding. Most fish larvae are predatory with a relatively large mouth (Blaxter, 1969). They feed on relatively large organisms at first (particulate feeding) obtained by suction.

The process of suction feeding in larval carp and pike is described by Drost & van den Boogaart (1986b). A first feeding carp larva (length about 6 mm) fixates a prey, then rapidly accelerates and after about 10 ms starts to suck by enlarging the volume of the mouth cavity. The volume is first enlarged by lifting the upper jaw and depressing the lower jaw; later the abduction of suspensoria (the cheeks) and the opercula becomes more important. The prey enters the mouth cavity within about 5 ms after the start of suction. The suction process is highly unsteady. In larval carp a water velocity of 0.3 m/s is reached within 5 ms (Drost & van den Boogaart, 1986a), so large local accelerations do occur (>60 m/s^2), see also Muller et al. (1982) and Muller & Osse (1984) for adult fishes. Given the dimensions of the larvae also viscous effects will be important.

One group of species changes during their ontogeny to smaller items of prey obtained by filtering: e.g. *Cetengraulis mysticetus* (Bayliff, 1963), *Engraulis anchoita* (Ciechomski, 1967), *Sardinops caerulea* (Hand & Berner, 1959), *Brevoortia tyrannus* (June & Carlson, 1971), *Sardina pilchardus* (Andreu, 1960), see Blaxter & Hunter (1982) for a more extensive bibliography. Other species change from predatory to benthic feeding: e.g. the cyprinids (Stankovitch, 1921). A third group remain predatory during their whole life, e.g. the pike *Esox lucius*.

In this paper the influence on friction of the possible options for food intake in larval fishes is considered.

To estimate the relation between larval size and friction during the (unsteady) suction process, a model is chosen in which the form of the fish is roughly schematized. In this model the influence of changing size is easily modelled. In the model of Drost et al. (in prep.) the form of the mouth cavity is much better approximated (an expanding cylinder). That model is fitted to calculate one snap in detail.

In the start of the suction process the mouth cavity is considered to consist of two plates lying close together (Fig. 1b). Between mouth and opercular a pressure gradient is introduced suddenly and the initial flow is considered. In later stages the mouth cavity is approximated as the part of a flow pipe (Fig. 1a).

II FLOWPIPE MODEL

Fig. 1. The mouth cavity of a fish while sucking prey can be approximated by an expanding cylinder (a) or by two plates, initially lying close together and moving away from each other (b).

The mouth cavity of the larva is considered to be part of a flowpipe of infinite length (Fig. 1). Over the flowpipe suddenly a pressure gradient is introduced to simulate the start of suction of the fish (i.e. the start of mouth opening). The solution of the Navier-Stokes equation for this system is given in textbooks on hydrodynamics (e.g. Bird et al., 1960).

A flowpipe is rather a strong abstraction of the head of a fish while sucking prey. The following reductions of the mouth cavity occur:

1. The walls are stationary
2. The walls are parallel
3. Obstacles in the flow are absent
4. No entry flow occurs
5. The cross sectional area is circular.

The following critical remarks about these reductions can be made:

1. In fact the walls of the mouth cavity do move radially: this causes the water flow. This will introduce a serious error. Calculations can only be used to study the influence of variation of parameters. Although the model is quantitative, the results can be interpreted only qualitative for fish: indicating trends. Power, energy and friction in an expanding cylinder are calculated quantitatively in Drost et al. (in prep.).

2. The walls of the mouth cavity are more or less parallel at the onset of suction; later in the suction process the mouth cavity is cone like, due to the different phase and amplitude of the movements of mouth and operculars (e.g. Muller & Osse, 1984, for adult fish; Drost & v.d. Boogaart, 1986b, for larval fish). The widening or tapering of the mouth cavity over its length may have considerable effects on the thickness of the boundary layer.

3. The gills and gill arches with their large surface areas are neglected (Fig. 2). They increase the surface/volume ratio and thus the effects of friction. They also might affect the flow seriously by partly dividing the mouth cavity in separate buccal and opercular cavities (Lauder, 1983; but see also Muller et al., 1985). Gills and gill rakers are however still poorly developed in larvae.
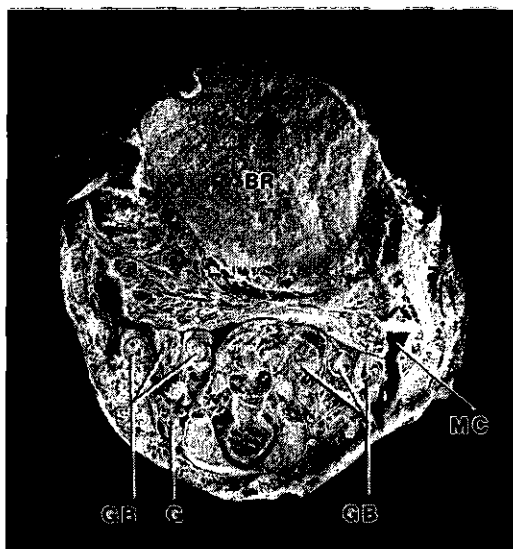
BR-brain
G -gill
GB-gill bar
MC-mouth cavity

Fig. 2. Cryo-scanning electron microscopical photograph of a 7 mm carp larva: a cross section shortly caudal of the eyes. The larva is anaestisized (MS 222), frozen in liquid nitrogen and cut with a scalpel. The specimen is gold sputtered in a Hexland Biochamber and, still frozen, examined in a Philips 505 Scanning Electron Microscope. In this way shrinkage is minimal. This figure gives an example of size and form of the mouth cavity in the beginning of the suction process (maximally adducted). Only one wider part of the mouth cavity is indicated.

4. Entry flow occurs at the mouth aperture. In the model the thickness of the boundary layer is constant over the length of the tube, in the mouth cavity the boundary layer is very thin at the lips and thicker rearwards (in this latter reasoning possible effects of unsteadyness and of the motions of the walls upon the boundary layer are not considered, see Drost & Osse (in prep.) for the changing (calculated) size of the boundary layer during the suction of a 6.5 mm carp larva).

5. Early in the suction act the mouth cavity is well described by two plates lying close together (Fig. 1b); later better by a cylinder (Fig. 1a). The plate situation is dealt with in the section "plates".

To compare the velocity distributions independently of the size of the radius and the applied pressure gradient, a dimensionless velocity is defined: the reduced velocity. The reduced velocity is the actual velocity at a certain time and radial position divided by the maximal, steady state velocity at the center of the tube, taking the effects of friction into account. For the cylinder model the distribution of the reduced velocity including the effects of friction ($V_{rf}(r,t)$ and ignoring the effects of friction ($V_{rp}(t)$)) as a function of time and radial position in the pipe are given by:

$$V_{rf}(r,t) = 1-(\frac{r}{R})^2 - 8 \sum_{n=1}^{\infty} \frac{J_o(\alpha_n \cdot \frac{r}{R})}{\alpha_n^3 \, J_1(\alpha_n)} \cdot e^{-\alpha_n^2 \cdot \tau_c} \tag{1}$$

$$V_{rp}(t) = 4 . \tau_c \tag{2}$$

$$\tau_c = \frac{\mu t}{\rho R^2} \tag{3}$$

$V_{rf}(r,t)$ is dependent on τ_c, which is equal to 1/Re (Reynolds number). We choose to use τ_c instead of Re, firstly because τ_c increases during the suction process, as does the real time, while Re decreases; and secondly Re is interpreted easily in steady flow, but difficultly in unsteady flow and might give wrong (i.e. steady) associations.

$V_{rp}(t)$ is constant over the radius of the pipe; and a constant acceleration in the time occurs (Fig. 3). $V_{rf}(r,t)$ is always zero
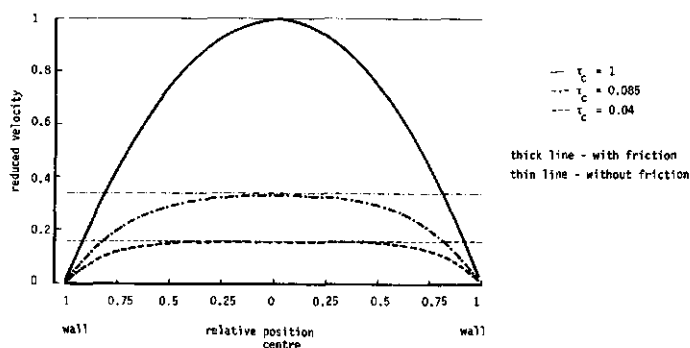
Fig. 3. Radial distribution of the reduced velocity (dimensionless) in the flow pipe for some values of τ_c ($\mu t/\rho R^2$). Reduced velocity is calculated velocity ($V_{rf}(r,t)$) divided by maximal velocity at the centre of the tube including the effects of friction (Poiseuille velocity). Calculated velocities neglecting the influence of friction ($V_{rp}(t)$) have a constant acceleration in time; calulated velocities taking friction into account ($V_{rf}(r,t)$) approach a steady state situation (Poiseuille profile). This is almost reached at $\tau_c=1$. The corresponding reduced velocity without friction is 4. Note the fourfold reduction in velocity.

at the wall (no slip condition). At an early time (e.g. $\tau_c=0.04$ in Fig. 3) $V_{rf}(r,t)$ is equal to $V_{rp}(t)$ also in the centre of the tube. Later frictional effects spread from the walls to the centre (Fig. 3, $\tau_c=0.085$). The distribution of $V_{rf}(r,t)$ will reach a steady state (Poiseuille profile), which is almost reached at $\tau_c=1$; $V_{rp}(t)$ is 4 at $\tau_c=1$ (not indicated in Fig. 3).
The flow rate is the integral of the velocity over the cross sectional area of the pipe. The flow rate for each value of τ can be calculated with neglection of friction and taking friction into account. The *relative flow rate* is the flow rate including frictional effects divided by the corresponding flow rate ignoring them. Its maximal value is one: friction has no effect on the flow; its minimal value approaches zero: friction almost prevents flow.

The power required for the generation of a water flow through the pipe is: pressure times flow rate. To make meaningful comparisons of required power with and without frictional effects (at the same value of τ_c) the flow rates in both situations should be equal. This can be achieved by increasing the pressure gradient (relative to the friction free situation) over the pipe proportional to the calculated decrease in relative flow rate due to frictional effects. Proportional increase in required power and pressure are thus equal. Both are a measure for the influence of friction. The relation between required pressure to maintain a given flow rate and τ_c is given in Fig. 4. For $\tau_c<0.01$ friction is not important,
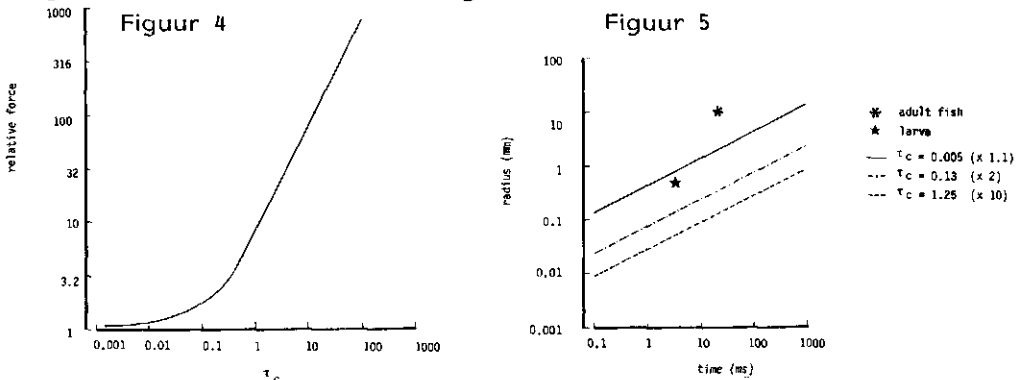
Fig. 4. Proportional increase due to friction of the force required to create a given flow rate relative to the force needed to create this flow ignoring frictional effects. Forces are a function of τ_c (reduced time: $\mu t/\rho R^2$). Forces are calculated using the cylinder model. Flow rate with friction is calculated with equation 1.
For $\tau_c<0.01$ friction is unimportant; for $0.01<\tau_c<1$ the boundary layer is developing; for $\tau_c<1$ it is fully developed.

Fig. 5. Iso-τ lines ($\tau_c=\mu t/\rho R^2$ constant) connect combinations of radius (R) and time (T) with a constant influence of the friction as calculated with the cylinder model.
To use the cylinder model for suction feeding fish, maximal mouth radius is taken as characteristic radius, time to open the mouth from 10% to 90% of its maximal opening as characteristic time. For a generalised adult fish (✱, R=10 mm, T=20 ms) calculated influence of friction is less than 1% (this value can be obtained from Fig. 4). For a 7 mm carp larva (✶, R=0.3 mm, T=5 ms) relative force increase due to friction is 45% (see Fig. 4).

for $\tau_c > 1$ the boundary layer is fully developed, in between these values the boundary layer is developing.

Combinations of radius and time resulting in the same value of τ_c and so in the same influence of friction are called *iso* τ *lines* (Fig. 5). In Fig. 5 three iso τ lines are drawn, for $\tau_c = 0.005$ (for instance a time of 10 ms and a radius of 1.4 mm) pressure increase relative to the frictionless situation is 10%, for $\tau_c = 0.13$ a factor 2, for $\tau_c = 1.25$ a factor 10.

For the suction proces, time from start of mouth opening to maximal mouth aperture is taken as characteristic time and maximal mouth radius as characteristic radius. For a generalized adult fish, e.g. the lionfish, *Pterois russelli*, a mouth opening phase of 20 ms and a maximal mouth radius of 10 mm are reasonable values (Muller & Osse, 1978). According to Fig. 5 ($\star$) this results in a very small influence of friction (<1%, compare Fig. 4). For a first feeding carp larva the duration of the opening phase is 4 ms and the maximal mouth radius 0.26 mm (Drost & van den Boogaart, 1986a). The calculated increase in pressure required to overcome friction is 45% (compare Fig. 4).
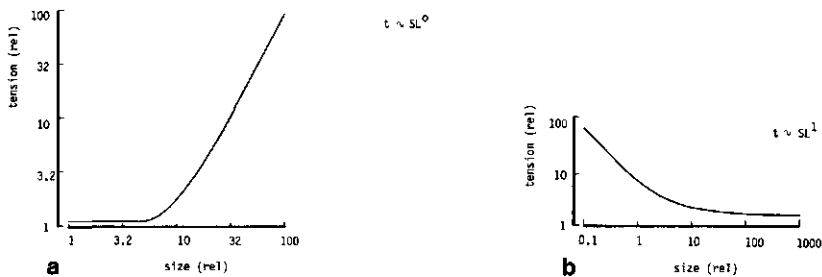
Fig. 6. Scaling of muscle tension required to create a certain suction velocity as a function of size. Increase in work spilled to friction is calculated with the cylinder model. The relation between duration of the suction process and the size of the fish can be varied independently, changes in velocity, maximal radius of the mouth (R), and of τ_c are calculated using dimension analysis. Form of the fish is assumed constant, so maximal deliverable power scales to L^3, maximal deliverable force to L^2.

a- Time (i.e. duration of the suction process) is constant ($t \sim SL^0$).

b- Time is proportional to length ($t \sim SL^1$).

The change during ontogeny in relative power (power/kg body weight) required for the suction process is calculated with dimension analysis, the influence of friction being estimated with the cylinder model. All parameters are assumed to change isometrically; only the relation between the length of the fish and the duration of the suction process can be varied independently. Fig. 6 gives the calculated relation between required muscle tension for a prey sucking fish and its length.

In Fig. 6a the duration of the suction process is taken constant. In the region where friction is not important, tension increases with length to the square; in the region where the friction is fully developed, tension is independent of length. This calculated increase of required tension with length results in an upper limit for fish-length as result of maximal power or tension delivery, not in a lower limit. Due to the assumption of isometric growth, muscle mass scales to fish length to the third power, physiological cross sectional to length to the square. The low calculated required tension at small lengths might give freedom for architectural changes there.

Fig. 6b gives the equivalent relation for a situation where the duration of the suction process is proportional to the length of the fish. In the area where frictional effects are negligible, required tension and power/unit muscle weight are independent of length. In the region where the friction is fully developed they decrease linearly with length increase. Where friction is developing the direction coefficient changes from -1 to zero. Given this relation, maximal obtainable tension or power determine a minimal length for fish larvae to be able to catch their food by suction feeding.

The duration (t_{ds} in ms) of the opening phase of the mouth (from 10% to 90% of maximal mouth aperture) in pike as a function of standard length (SL, in mm) measured from high speed film of prey uptake is given in Fig. 7. Regression analysis gives a relation $t_d = 12.9 \cdot SL^{0.28}$. With this relation the relation between muscle tension and size is calculated for the pike (Fig. 8, heavy line). The area between the thin lines indicates the calculated tension for durations within a factor 1.41 of the measured duration. The calculated tension is minimal around hatching length (10 mm) and increases during growth.

Figuur 7

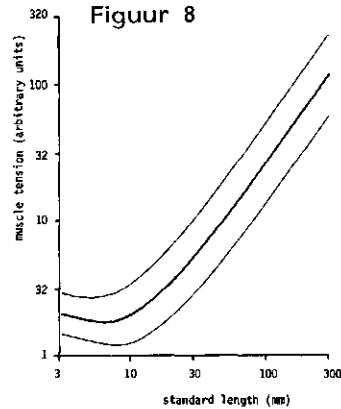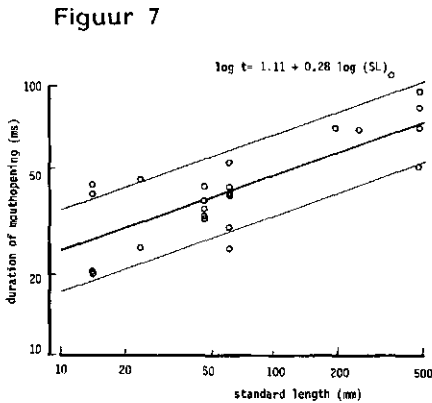log t= 1.11 + 0.28 log (SL)₀

Figuur 8

Fig. 7. The duration of the opening phase of the mouth aperture (time from 10% to 90% of maximal mouth apertures) as a function of the standard length for pike (Esox lucius). Times are measured from high speed films, framing speed ranged from 1000 fr/s for the 14 mm larvae to 200 fr/s for the 560 mm adults. At the thin lines the times differ by factor $\sqrt{2}$ of the values of the regression line (thickly drawn).

Fig. 8. Muscle tension (in arbitrary units) required to create an equivalent suction flow as a function of size. Form is held constant, i.e. isometric growth. The duration of the suction process is taken according to Fig. 7: thick line: $\log(t)=1.11+0.28$ SL, thin lines: duration within a factor $\sqrt{2}$, as measured for pike, Esox lucius. The influence of friction is calculated using the cylinder model (Fig. 4). The mouth radius was taken 3.3% of standard length, i.e. about half of the maximal radius. Most measured points fall within these boundaries. Note that in small larvae the required tension is low.

Starting from this minimum, the gradient with increasing size is much steeper than with decreasing size.

III PLATE MODEL

In the beginning of the suction process the walls of the mouth cavity are better described by two plates lying close together, than by a cylinder (Figs. 1,2). The reduced velocity distribution between two parallel plates of infinite length and width upon which an instantaneous pressure gradient is introduced, can be calculated analogously to the cylinder situation (see Appendix 2). The reduced

velocity distribution including the effects of friction ($U_{rf}(h,t)$) and ignoring the effects of friction ($U_{rp}(t)$) as a function of time and position between the plates are:

$$U_{rf}(h,t) = \xi.(2-\xi) - 4.\sum_{n=0}^{\infty} \frac{e^{-(\frac{\pi}{2} + n\pi)^2.\tau_p}}{(\frac{\pi}{2} + n\pi)^3.} \sin\{(\frac{\pi}{2} + n\pi)\xi\} \quad (4)$$

$$U_{rp}(t) = 2.\tau_p \quad (5)$$

$$\tau_p = \frac{\mu.t}{\rho.H^2}$$

The following reductions of the mouth cavity occur:
1. The walls are stationary.
2. The walls are parallel.
3. Obstacles in the flow are absent.
4. No entry flow occurs.
5. The side walls of the mouth cavity are neglected.

Simplifications 1-4 are treated in the section FLOWPIPE MODEL.

5. In the plate situation friction at the side walls of the profile is neglected: the width of the plates is taken to be infinite during the calculations. The ratio r_p is only used to calculate the height of the mouth cavity, from a given cross sectional area in the cylinder situation. If the ratio is high, the error due to neglecting the side walls is small. Two plates with a length- width ratio of π have the same surface area as a cylinder with the same cross sectional area. To make meaningful comparisons the ratio must thus be amply greater than π, e.g. a minimum value of $r_p=5$.

Simulations with the cylinder and plate model can be compared at equal cross sectional area (see Fig. 9) and equal time (thus in most cases $\tau_c \neq \tau_p$). In the plate situation the distance between the plates decreases with increasing ratio between width and height (under the boundary condition of equal cross sectional area). So for a plate situation corresponding to a given cylinder situation (τ_c) τ_p depends on the ratio between width and height of the mouth cavity (r_p).

Measurements showed that in the beginning of suction of larval carp
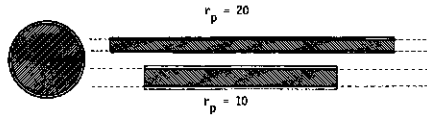
Fig. 9. Cross sections through the mouth cavity in the cylinder and the plate model. The cylinder and both plate sections have equal cross sectional areas (hatched). The plate configurations differ in ration r_p, between width and height. Circumference is $2 \cdot \pi \cdot R$ in the cylinder. Circumference in the plate depends on the ration r_p. For $r_p=20$ circumference S=15.9 R (2.5 times the circumference in the cylinder configuration); for $r_p=10$ S=11.8 R (1.9 times the cylinder circumference). N.B. the side walls are neglected in the plate model.
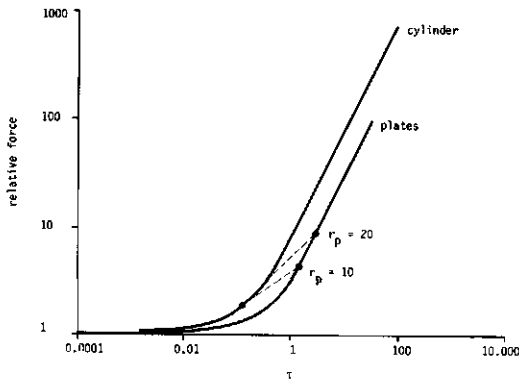
Fig. 10. Proportional increase due to friction of the force required to create a given flow rate relative to the force needed to create this flow ignoring frictional effects. Forces are a function of τ_c (reduced time: $\mu t/\rho R^2$). Forces are calculated using the cylinder model and the plate model. Required forces for cylinder and plates should be compared at equal cross sectional areas, so in most cases not at equal values of τ_c and τ_p. Cross sectional area for a cylinder depends only on its radius (R). For the plates it depends on the width between the plates and on the ratio (r_p) between the length and width of the profile (see Fig. 9). Indicated are the required forces for a given τ_c and the corresponding τ_p for r_p of 10 and 20. Required force in the plate situation is 2.5 times the cylinder force for $r_p=10$, for $r_p=20$ 5 times.
*-cylinder situation.

the ratio r_p of the width of the mouth cavity and its roof and bottom is 10 to 30. These values show that the plate model is a much better approximation of the mouth cavity than the cylinder model in the start of the section process. Relative flow rate and increase in required tension and power are calculated in the same way as for the cylinder.

Fig. 10 gives the tension-τ diagram for the cylinder and for the plate. For a given suction process (e.g. t=5 ms, r=0.21 mm) τ_c is 0.11 (Fig. 10: *). In the plate model the required tension for the same flow increases by a factor 2.5 relative to the cylinder model, assuming the ratio r_p=10; for a ratio of 20 by a factor 5.

IV DISCUSSION

In this paper the influence of size on the possible options to catch food is discussed. It seems conceivable that some feeding types are impossible at very small size due to viscous effects. One question in this research was whether such a minimum size does exist for fish larvae to use suction feeding (by muscular expansion of their mouth cavity).

The approach presented in this paper allows a first approximation of the relative importance of inertial and frictional forces during suction feeding as a function of larval size. The results can only be interpreted qualitatively, indicating trends.

The larvae of many fish species resemble eachother rather closely at hatching, except e.g. clupeids, (e.g. Russell, 1976). Feeding habits of most fish larvae are quite equal at first feeding, but they rapidly diverge during growth. Generally the length of fish larvae at first feeding is between 2 and 15 mm, although in viviparous fishes, like Embiotocidae (surfperches) and several chondrichthyan species much larger juveniles occur (see e.g. Blaxter, 1969 Table 1). It can be calculated that about this size friction becomes a major factor in swimming and suction. Apart from the larvae of most fishes, also the adults of some groups of fishes are very small (for a review see Miller, 1979).

To determine the accuracy of the plate and cylinder model we can compare their predictions of the influence of friction with values calculated with the model of Drost et al. (in prep). In this model

velocity and pressures in a radially expanding cylinder are calcu-
lated by solving numerically the Navier-Stokes equations in 2-D.
The volume increase of the cylinder was taken equal to the measured
flowrate of a snap of a 6 mm carp larvae. It was calculated that
60% of the energy is lost to friction, for a carp larva with a max-
imal mouth radius of 0.26 mm, reached in about 5 ms). So, $\tau_c=0.07$.
In the cylinder model this results in an increase in required ten-
sion of a factor 1.58 (Fig. 4). This is rather lower than the fac-
tor 2.5 of Drost et al. (in prep.) but clearly in the same order of
magnitude.

An absolute minimal size for fishes in order to be able to feed by
suction feeding is not found on the basis of the plate and cylinder
model. Although required tension for fish larvae increases with de-
creasing size (below about 5 mm, see Fig. 8) this increase is so
weak, that it does not impose a lower limit on fish size. It seems
that at least pike larvae hatch at a size that muscle tension re-
quired to create a suction flow is minimal. This gives them an op-
portunity have unfavorable configurations in the morphology of the
head and the body during the huge ontogenetical changes.

From Fig. 8 it is obvious that the muscle tension required during
suction feeding increases enormously during growth, almost a factor
20 between hatching larvae of about 10 mm and adults of 300 mm. It
is possible that the maximal tension per unit cross sectional area
increases during growth (development of the muscle fibers). I know
of no values in the literature, but it seems improbable that its
influence is more than a factor two. Another (partial) explanation
may be that fishes do not grow isometrically: e.g. the relative
proportion of muscle may increase during growth, or that the mo-
ment-arms increase. The negative pressure inside the mouth cavity
of a prey sucking fish can be reduced by an increased swimming
velocity (Muller & Osse, 1984). It is possible that the pike re-
duces the peak negative pressure during suction by increasing the
relative swimming velocity during growth.

The duration of the suction process will have a minimal value of
several ms, due to intrinsic properties of muscles, e.g. the twitch
contraction time. This will cause the suction velocities to de-
crease with decreasing size. For very small larvae this might im-

pair the possibility to catch relatively large (and mobile) prey. If previously stored elastic energy is used during the snap (Aerts et al., in prep.), this reasoning is not valid.

Especially in the small larvae there is a large influence of the total surface wetted area on the force required during suction feeding (see Fig. 11). In the plate situation with a width/height ratio of the mouth cavity (r_b^y) of 20 the required force increases with a factor 5 relative to the cylinder situation. Small larvae can reduce the needed power and tension spilled to friction by starting the suction process with a larger distance between roof and bottom of the mouth cavity. It would be interesting to know whether the ratio r_b^y, e.g. at the start of suction, increases during ontogeny. Unfortunately, this can not be investigated from serial cross sections of fixed larvae: the shrinkage in volume of carp larvae of 5.5 mm SL after fixation in Bouins fixative is 60% (Drost & Van den Boogaart, 1986a). The wall of the mouth cavity in larval fishes consists of intricately folded membranes, bone struts and some muscles. Therefore the volume of the cavity in the living fish can not be reliably estimated from the size of the cavity after fixation due to unknown movements of the wall during fixation.

Assuming that Fig. 2 gives a correct picture of the mouth cavity at the start of the suction process, the ratio r_b^y is very large in carp larvae at that moment and thus the increase in required power compared to a cylindrical mouth aperture. The power requirements are still low at the start of the suction process and are maximal at maximal flow rate through the mouth aperture (De Jong et al, in prep.; Drost et al., in prep.). So an increase in required power at the start of the suction process does not increase the maximal required power.

ACKNOWLEDGEMENTS

References

Aleyev, Y.G., 1977. Nekton. 435 pp. The Hague, Netherlands: Junk Publishers.

Andreu, B., 1960. Sobre la aparacion de las brachispinas en las formas juveniles de sardina (Sardina pilchardus). Real Soc. Espanola Hist. Nat. Bol. Sec. Biol. 58: 199–216.

Balon, E.K., 1975. Terminology of intervals in fish development. J. Fish. Res. Board Can. 32: 1663–1670.

Bayliff, W.H., 1963. The food and feeding habits of the anchoveta, Cetengraulis mysticetus in the Gulf of Panama. Inter-Amer. Trop. Tuna Comm. Bull. 7: 399–432.

Bird, R.B., Stewart, W.E. & Lightfoot, E.N., 1960. Transport phenomena. New York: Wiley.

Blaxter, J.H.S., 1969. Development: eggs and larvae. In: Hoar & Randall (Eds.) Fish Physiol. III: 178–252.

Blaxter, J.H.S. & Dickson, W., 1959. Observations on swimming speed in fish. J. Cons., Cons. Perm. Int. Explor. Mer 24: 472–479.

Blaxter, J.H.S. & Hunter, J.R., 1982. The biology of clupeoid fishes. Advances in marine Biology 20: 3–223.

Ciechomski, J.D. de, 1967. Investigations of food and feeding habits of larvae and juveniles of the argentine anchovy, Engraulis anchoita. Calif. Coop. Ocean. Fish. Invest. Rept. 11: 72–81.

Drost, M.R. & Boogaart, J.G.M. van den, 1986a. A simple method for measuring the changing volume of small biological objects, illustrated by studies of suction feeding by fish larvae and of shrinkage due to histological fixation. J. Zool. Lond. (A) 209: 239–249.

Drost, M.R. & Boogaart, J.G.M. van den, 1986b, in press. The energetics of feeding strikes in larval carp (Cyprinus carpio). J. Fish Biol.

Hand, C.H., & Berner, L., 1959. Food of the Pacific Sardine (Sardinops caerulea). Fish. Bull. 60: 175–184.

Hoda, S.M.S. & Tsukahara, H., 1971. Studies on the development and relative growth in the carp (Cyprinus carpio) (L.). J. Fac. Agricult. Kyushu Univ. 16: 387–509.

Janssen, J., 1976. Feeding modes and prey size selection in the Alewife (Alosa pseudoharengus). J. Fish. Res. Board Can. 33: 1972–1975.

June, F.C. & Carlson, F.T., 1971. Food of young atlantic menhaden, Breevoortia tyrannus, in relation to metamorphosis. Fish. Bull. 68: 493–512.

Lauder, G.V., 1983. Prey capture hydrodynamics in fishes: experimental tests of two models. J. exp. Biol. 104: 1–13.

Leeuwen, J.L. van, 1984. A quantitative study of the flow in prey capture by Rainbow Trout with general consideration of the actinopterygian feeding mechanism. Trans. Zool. Soc. Lond. 37: 171–227.

Leeuwen, J.L. van & Muller, M., 1984. Optimum sucking techniques for predatory fish. Trans. Zool. Soc. Lond. 37: 137–169.

Leong, R.J.H. & O'Connell, C.P., 1969. A laboratory study of particulate and filter feeding of the northern anchovy (Engraulis mordax). J. Fish. Res. Board Can. 26: 557–582.

Miller, P.J., 197?. Adaptiveness and implications of small size in teleosts. Symp. Zool. Soc. Lond. 44: 263–306.

Muller, M. & J.W.M. Osse, 1982. Hydrodynamics of suction feeding in fish. Trans. zool. Soc. Lond. 37: 51–135.

Muller, M., Osse, J.W.M. & Verhagen, J.H.G., 1982. A quantitative hydrodynamical model of suction feeding in fish. J. theor. Biol. 95: 49–79.

Muller, M, van Leeuwen, J.L., Osse, J.W.M. & Drost, M.R., 1985. Prey capture hydrodynamics in fishes: two approaches. J. exp. Biol. 119: 389–394.

Russell, F.S., 1976. The eggs and planktontic stages of British marine fishes.
    524 pp. London: Acadamic Press.
Stankovitch, S., 1921. Etude sur la morphologie et la nutrition des alevins de
    poissons cyprinides. Thesis, University of Grenoble.
White, F.M., 1974. Viscous fluid flow. New York: McGraw Hill Book Co.

APPENDIX 1

Symbols

h	relative position between the plates
H	distance between the plates
$J_0(\alpha)$ $J_1(\alpha)$	Bessel function of the first kind
L	length of the flow pipe
P	pressure
r	radial position in the pipe
R	radius of the pipe
Re	Reynolds number
r_p	ratio width/height of the mouth cavity in the plate model
SL	standard length of the fish
t	time
$U_{rf}(h,t)$	reduced velocity distribtion between the plates as a function of position between the plates and time, including effects of frictiob
$U_{rp}(t)$	reduced velocity between the plates as a function of time, neglecting effects of friction
$V_{rf}(r,t)$	reduced velocity distribution in the pipe as a function of radial position and time, including effects of friction
$V_{rp}(t)$	reduced velocity in the pipe as a function of time, neglecting effect of friction
x	horizontal coordinate
α_n	n-th value for which the Bessel function is zero
μ	viscosity of water
ρ	density of water
ξ	dimensionless postion between the plates dimensionless
ϕ	reduced velocity between the plates (used in appendix 2)
τ_c	reduced time, cylinder model $\frac{\mu t}{\rho R^2}$ dimensionless
τ_p	reduced time, plate model $\frac{\mu t}{\rho H^2}$ dimensionless .

APPENDIX 2

A fluid of constant ρ and μ is contained between two very long horizontal plates of length L and infinite width lying at a distance 2H. Initially the fluid is at rest. At t = 0, a pressure gradient $(p_0 - p_L)/L$ is impressed on the system.
It is assumed that $v_{2H} = v_0 = 0$ and that $v_x = v_x(h,t)$. The equations of continuity and motion may be combined to give

$$\rho \frac{\partial v_x}{\partial t} = \frac{p_0 - p_L}{L} + \mu \frac{\partial^2 v_x}{\partial h^2} \qquad (A1)$$

The initial and boundary conditions are
I.C. : at t = 0, $v_x = 0$ for 0 < h < 2H
B.C. 1: at h = 0, $v_x = 0$
B.C. 2: at h = 2H, $v_x = 0$

First we introduce the following dimensionless variables:

$$\phi = \frac{v_x}{(p_0-p_L)\frac{H}{2\mu L}}; \qquad \xi = \frac{h}{H}; \qquad \tau = \frac{\mu t}{\rho H^2} \qquad (A2, A3, A4)$$

The velocity is made dimensionless by dividing by the maximum velocity at t = ∞. When Eq. A1 is multiplied by $2L/(p_0-p_L)$, we get dimensionless variables

$$\frac{\partial \phi}{\partial \tau} = 2 + \frac{\partial^2 \phi}{\partial \xi^2} \qquad (A5)$$

This is to solved with the conditions that at $\tau = 0$, $\phi = 0$, and at $\xi = 0$, and $\xi = 2$, $\phi = 0$.
The system will attain a steady state at $\tau = \infty$.
Hence a solution of the following form must be sought:

$$\phi(\xi,\tau) = \phi_\infty(\xi) - \phi_t(\xi,\tau) \qquad (A6)$$

That is, we split up the solution into a steady-state limiting solution $\phi_\infty(\xi)$ and a transient function $\phi_t(\xi,\tau)$. The steady-state solution is obtained from Eq. A5 by setting $\partial\phi/\partial\tau = 0$ at $\tau = \infty$:

$$0 = 2 + \frac{\partial^2\phi}{\partial\xi^2} \qquad\qquad (A7)$$

for which the solution with $\phi = 0$ at $\xi = 0$ and $\xi = 2$ is

$$\phi_\infty = \xi(2-\xi) \qquad\qquad (A8)$$

This is, of course, just the Poiseuille velocity distribution. Substitution of ϕ_∞ into Eq. A16 and then inserting the result into Eq. A5 gives the following partial differential equation for the function ϕ_t:

$$\frac{\partial\phi_t}{\partial\tau} = \frac{\partial^2\phi_t}{\partial\xi^2} \qquad\qquad (A9)$$

This must be solved with initial and boundary conditions:

I.C. :   at $\tau = 0$, $\phi_t = \phi_\infty$
B.C. 1:   at $\xi = 0$, $\phi_t = 0$
B.C. 2:   at $\xi = 2$, $\phi_t = 0$

We now try a solution of the form

$$\phi_t(\xi,\tau) = Y(\xi) \cdot T(\tau) \qquad\qquad (A10)$$

Substitution into Eq. A9 and division by T gives

$$\frac{1}{T}\frac{dT}{d\tau} = \frac{d^2Y}{d\xi^2} \cdot \frac{1}{Y} \qquad\qquad (A11)$$

The left side is a function of τ alone, whereas the right side is a function of ξ alone. Hence both may be set equal to a constant, which we choose to designate as $-\alpha^2$.
We then get two ordinary differential equations:

E13/D

$$\frac{dT}{d\tau} = -\alpha^2 T \tag{A12}$$

$$\frac{d^2Y}{d\xi^2} = -\alpha^2 Y \tag{A13}$$

These equations have solutions as follows:

$$T = C_0 e^{-\alpha^2 \tau} \tag{A14}$$

$$Y = C_1 \sin(\alpha\xi) + C_2 \cos(\alpha\xi) \tag{A15}$$

B.C.1: $\xi = 0$, $Y = 0$, So $C_2 = 0$
    $Y = C_1 \sin(\alpha\xi)$
B.C.2: at $\xi = 2$, $Y=0$
    Y is symmetrical around $\xi = 1$
So: $\alpha = \frac{\pi}{2} + n\pi$ $n=0,1,2,...$

I.C.: We know that ϕ_t must equal ϕ_∞ at $\tau = 0$. Based eq. A10, we know that a superposition of the form

$$\phi_t(\xi,\tau) = \sum_{n=o}^{\infty} B_n \cdot e^{-(\frac{\pi}{2} + n\pi)^2 \tau} \cdot \sin\ (\frac{\pi}{2} + n\pi)(\xi) \tag{A16}$$

satisfies the boundary conditions and the partial differential equation.
Application of the initial condition then gives

$$\xi\ (\xi-2) = \sum_{n=o}^{\infty} B_n \sin\ \{(\frac{\pi}{2} + n\pi)\xi\} \tag{A17}$$

To get the B_n we multiply both sides by $\sin(\frac{\pi}{2} + m\pi)(\xi)$ and then integrate from 0 to 2:

$$\int_o^2 \xi(2-\xi) \sin\ \{(\frac{\pi}{2} + m\pi)\xi\}d\xi = \sum_{n=o}^{\infty} B \int_o^2 \sin\{(\frac{\pi}{2} + n\pi)\xi\} \sin\{(\frac{\pi}{2} + m\pi)\xi\}d\xi \tag{A18}$$

E13/D

After some algebra we get:

$$B_n = \frac{4}{(\frac{\pi}{2} + n\pi)^3} \qquad\qquad (A19)$$

Hence the final expression for the reduced velocity distribution is

$$\phi = \xi\,(2-\xi) - 4\sum_{n=0}^{\infty} \frac{1}{(\frac{\pi}{2} + n\pi)^3} \cdot e^{-(\frac{\pi}{2} + n\pi)^2 \tau} \cdot \sin\{(\frac{\pi}{2} + n\pi)\xi\} \qquad (A20)$$

A quantitative hydrodynamical model of suction feeding in larval fishes

M.R.Drost, M. Muller & J.W.M. Osse
Dept. of Experimental Animal Morphology and Cell Biology
Agricultural University, Marijkeweg 40, 6709 PG Wageningen.
The Netherlands

Synopsis
A model is presented for the suction flow during prey intake by larval fishes.
The mouth cavity is depicted as an expanding and compressing cylinder ('pro-
file'). The volume flow of the profile equals the volume flow in fish larvae
measured from a 1100 fr/s movie. The model is fully unsteady and takes viscous
effects into account. For a 6.5 mm carp larva calculated maximal power deliv-
ery during the strike is 7 μW (13 W/kg muscle) and total energy 20 nJ. At the
time of maximal water velocity (t=5 ms) only 40% of the total delivered energy
is present as kinetic energy. So 60% of the energy is spilled to friction.

I-Introduction

Suction feeding is applied by many adult fishes (Osse & Muller, 1980) and by

almost all fish larvae (Drost & van den Boogaart, 1986b). The suction flow is

generated by a rapid increase in volume of the buccal and opercular cavities

(together denoted as mouth cavity). The flow during suction is very unsteady.

Within 4-6 ms after the start of mouth opening of a 6 mm carp larva the prey

passes through the mouth aperture with a velocity of about 0.3 m/s (Drost & van

den Boogaart, 1986b). Most earlier approaches to suction feeding however ap-

plied however steady hydrodynamics. Exceptions are the model of Muller and

coworkers (Muller & Osse, 1978, 1984; Muller et al., 1982; van Leeuwen, 1984;

van Leeuwen & Muller, 1983, 1984) and a hydrodynamical improvement of this
model (de Jong et al., in prep.).

All present models neglect frictional effects, which is justified for adult
fish (Muller et al., 1982). Friction may be important during suction feeding by
larval fishes (Drost & van den Boogaart, 1986b; Drost & Verhagen, in prep.).
The present model is biologically very similar to the model of Muller, i.e. it
contains equal form parameters. Some important hydrodynamical aspects however
are different: friction is included and it is a finite element instead of an
analytical solution.

This paper is aimed to determine the effect of friction on the velocity of the
water sucked through the mouth aperture and on the energy spent during suction.
The flowfield in front of the profile will be dealt with in a separate paper
(Drost, in prep.b).

The suction process of larval carp and pike is described in detail by Drost &
van den Boogaart (1986b) and Drost (in prep.a). Here follow the mean features.

A typical attack sequence of a 6 mm carp larva lasts about 400 ms. Before
snapping, the larva directs both eyes towards the prey. The larva curves its
body and then darts forward with one or two vigorous oscillations of the body,
accompanied by vigorous movements of the pectoral fins. The increase in volume
of the mouth cavity starts. about 10 ms after the onset of swimming. The in-
crease is first due to the opening of the mouth, later to the depression of the
hyoid and abduction of the suspensoria and opercula. The prey enters the mouth
aperture at 4-6 ms (all times relative to the onset of suction). The opercular
valves open at about 8 ms. The opening of the opercular valves changes the
hydrodynamical conditions suddenly, because starting from that moment the
mouth cavity is open at both ends. During most snaps of fish larvae the yaw of
the head is very large (see Drost, in prep.a).

II.Model

II.1 General descsription of the program

The head of a fish while sucking prey is modelled as an expanding and compress-
ing hollow cylinder. The cylinder representation is a the simplest case of the
cone model of Muller et al. (1982). 'Profile' is used to denote the fish's head
and mouth cavity in the model. The water flow inside and in front of the pro-
file is calculated using the hydrodynamical model Odyssee from the Delft Hy-
draulic Laboratory and Laboratoire National d'Hydraulique France. In the model
the Navier Stokes equation is solved in 2-D (axial (x) and radial (r) direc-
tions), including the effects of friction. The Navier-Stokes equations in axial

and radial direction are:

$$\rho(\frac{\partial u}{\partial t} + v\frac{\partial u}{\partial r} + u\frac{\partial u}{\partial x}) = -\frac{\partial p}{\partial x} + \mu[\frac{1}{r}\frac{\partial}{\partial r}(r\frac{\partial x}{\partial r}) + \frac{\partial^2 u}{\partial x^2}] \qquad (1a)$$

$$\rho(\frac{\partial v}{\partial t} + v\frac{\partial v}{\partial r} + u\frac{\partial v}{\partial x}) = -\frac{\partial p}{\partial r} + \mu[\frac{\partial}{\partial r}(\frac{1}{r}\frac{\partial}{\partial r}(rv)) + \frac{\partial^2 v}{\partial x^2}] \qquad (1b)$$

in which u is velocity in axial direction, v velocity in radial direction, ρ density of water and p pressure and μ viscosity. Odyssee is a finite element method, with at present a maximum of 1700 calculation points. For an
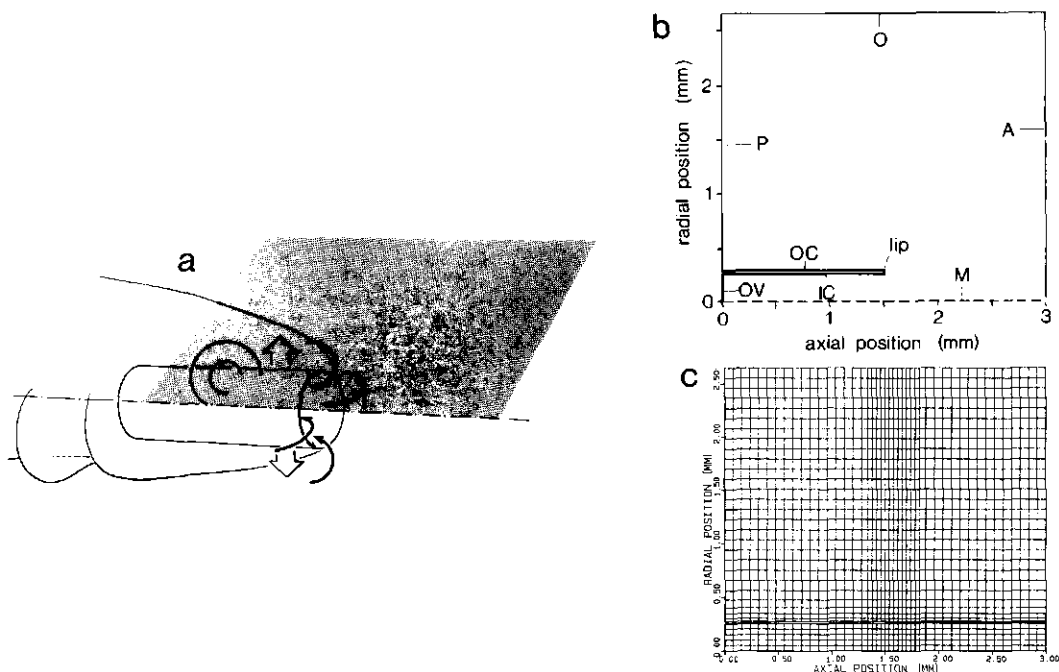
Fig. 1. Model approach of the head of a fish larva while sucking prey.
a-Impression of the fish head with the cylinder approximation of the mouth cavity. The calculation area is dotted.
b-Calculation area of the model and its dimensions. The profile (mouth wall=-'cheek') consists of an inner cheek (IC) and an outer cheek (OC). The symmetry-axis of the calculation area is M, the anterior border A, the posterior border P, the outer border O and the opercular valve OV. The calculation area is rotationally symmetrical.
c-Distribution of the calculation points over the calculation area at t=8 ms. In each point of intersection the velocities are calculated. The ratio of the length of the long and the short side of each calculation mesh is maximally 5 as well at the start position as in the ending position, exept just in front of the cheeks. At t=0 the radial distances inside the mouth cavity are much smaller (a factor 2.5), at the cheek much larger (a factor 2). At larger radial distances the mesh size is only slightly affected.

extensive description of Odyssee see Officier et al. (1986). The model was used
in the 'simple viscosity' mode, which is justified for Reynolds number (Re) up
to about 1000. Calculated maximal water velocity during the simulated snap was
about 0.7 m/s, but only very local (near the mouth aperture). For higher Re's
more cumbersome modes must be used.

The used calculation grid has the smallest meshes just in front of the mouth
aperture (see Fig. 1), because the accelerations and velocities are largest
here, besides this is biologically the most interesting area. The length ratio
between the long and the short side of each mesh must be between 1 and maximal-
ly 5. Therefore the total number of points limits the size of the calculation
area. Fig. 1 shows this area, its length is 3 mm, its width 2.65 mm. Inside the
mouth cavity, we have used radially only 6 calculation points. The length of
the profile is 1.5 mm, corresponding to a larva of 6.5 mm standard length.

The program calculates in each point of the calculation area the velocity
components in the axial and the radial direction and either the value of the
stream function or the pressure. Actually, pressure and stream function are
calculated half a mesh shifted relative to the calculation points of the veloc-
ity. The hydrodynamical calculations were made on a Cray 1 computer, pre- and
postprocessing on a CDC Cyber 205.

II.2 Definition of the profile

In order to keep the position of the profile stationary in the calculation area
the model calculations are made in a moving frame: i.e. positions and veloci-
ties are calculated relative to the fish and not in an earth bound frame.

The calculation area is given in Fig. 1. The inflow at the anterior border A is
prescribed, 'swimming velocity'. The outflow velocities through the posterior
border P are calculated by the program. The program can not deal standardly
with moving boundaries. Therefore the cheek of the profile was treated as a
combination of a moving inside (IC) and outside (OC) wall of the cheek. At IC
an outflow border was defined, at OC an inflow border. The radial position of
IC, $r_i(t)$, was given by Eq. 3. The radial position of OC, $r_o(t)$, was calculated
in such a way that the cross-sectional area of the cheek, $\pi \cdot (r_o^2 - r_i^2)$, was
kept constant. The (prescibed) water velocities at IC and OC were the deriva-
tives of their radial position to the time. So, at each time step in the
calculations the moving wall of the mouth cavity of the fish was treated as a
combination of two boundaries. The cheek itself was outside the calculation
area. The volume outflow through IC was at each time taken equal to the inflow
through OC.

In this way the calculation area behaves as if it contains a radially expanding cylinder skin.

II.3 Simplifying approximations

To get a hydrodynamical model of suction feeding with as few parameters as possible, simplifications of the biological complexity were made. The most important simplifications are stated explicitly and their validity is argued. Some reductions are necessary in using the model:

1-The prey is assumed to behave as an element of the water.

2-Rotational symmetry of the mouth cavity is demanded.

3-Swimming was assumed to occur only parallel to the axis of the mouth cavity.

4-Calculations are made only before the moment of opening of the opercular valves.

5-The wall of the mouth cavity must be given a prescribed thickness.

These reductions are discussed below:

The simplifying approximations 1 and 2 have been dealt with by Muller & Osse (1984).

3-If the swimming is not parallel to the length axis of the mouth cavity, even calculations in the cylinder approximation can not be made in pseudo 2-D, because no longer rotational symmetry is present. The swimming velocity during snapping by fish larvae however is often to a fairly large extent perpendicular to the axis (yaw of the head, see Drost & van den Boogaart, 1986b; Drost, in prep.a). This velocity is neglected. In the snap used as basis for this simulation total perpendicular displacement was about half of the forward displacement. The perpendicular velocity is neglected in the model.

4-After the opening of the opercular valves the outflow through the 'opercular slit' in the model must be prescribed. This is not known a priori. This boundary condition, however, determines the calculations. The most important biological events, i.e. prey capture and maximal power delivery, occur before the moment of opening of the opercular valves (see Muller et al., 1982 and later in this paper). The part where no reliable calculations can be made is thus the biologically less interesting part of the strike.

5-At the start of suction the mouth cavity (water) forms only a tiny fraction of the total volume of the head, about 5-10%, see Fig. 3. The stagnation effects due to the tissues of the the head of the fish are thus much greater than of the mouth cavity (water) itself, especially at the start of suction. In the model it is impossible to use walls of zero thickness, the minimum feasible wall thickness in our configuration was about 40% of the initial mouth radius.

Thicker walls, as are present in actual fish (Fig. 3) can be used in the calcu-
lations. However, in that case the wall effects depend on the shape of the
wall, which is difficult to prescribe accurately.

Other reductions are used that are not strictly necessary, but facilitate the
use of the model.

1-The walls are parallel at each instant: anterior and posterior part of the
profile move synchronously (cylinder-like motion).

2-No obstacles are present in the flow, the gill arches and the gill filaments
are thus neglected.

3-Swimming velocity was taken constant, in order to be able to calculate the
pressure. (In an accelerating frame it is difficult to calculate pressures,
which are by definition earth-bound quantities.)

4-The possible influence of mucus is neglected.

5-No slip is assumed at the walls.

6-Swimming starts instantaneously at t=0, no pre-flow of the profile is used.
The possible influences of these reductions of the actual situation are dealt
with below.

1-Fish open first their mouth and start later to abduct their opercula. In the
cylinder-like profile no phase difference between anterior and posterior expan-
sion occurs. However, at least in the snap used as input for the simulation,
the measured increase in volume of the head was distributed more or less equal
over the length of the head during the first 4.5 ms (see Fig. 2). Later the
volume increase occurred mainly in the posterior half of the head.
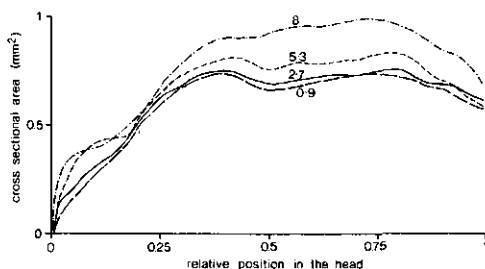
Fig. 2. Cross sectional area of the head as a function of its length of a 6.5
mm carp larva as determined with the ellipse method (Drost & van den Boogaart,
1986a). This is the same snap as in Fig. 4. Although the area consists for the
larger part of tissue (Fig. 3), the increase in area is completely due to
volume increase of the mouth cavity. At the start of the suction process the
increase in cross sectional area of the head is distributed more or less equal
over the length of the head (outlines at successive times parallel, according
to an expanding cylinder). Later the increase in the posterior part of the head
is much larger than in the anterior part.

2-The effect of gill resistance on the water flow in the mouth cavity of adult
fish while sucking prey is treated in Muller et al. (1985). In most fish the
influence seems to be small; in species with large gill bars and interdigitat-
ing rakers the influence may be profound. It is however possible that the
effect is larger in smaller fish, because a developing boundary layer between
the gill bars might obstruct the flow. However, gills are virtually absent in
young fish larvae and the gill arches do not yet bear branchiospines. We assume
that the effect of gill resistance is small.

3-Actually the swimming velocity first increases (from 0 to 0.056 m/s about at
t=5 ms, mean acceleration 10 m/s^2) and later decreases rapidly. This has some
effect on the earth bound velocities which must be used for calculating kinetic
energy.

NB. What we call swimming velocity does not result alone from swimming move-
ments. During the snap water and fish get equal but opposite momentum due to
suction.

4-The total volume of the layer of mucus present at the walls of the mouth
cavity of larval carp is estimated to be about half of the initial volume of
the mouth cavity (compare Fig. 3). We do not know if and how this influences
the flow.

5-No slip is a reasonable assumption for the walls, but in principle any other
value can be used. Mucus for instance might influence the slip at the walls.

6-In the first part of the suction process the larva rapidly increases its
swimming velocity. So a pre-flowed profile does not necessarily describe the
suction act of a fish larva better than a not pre-flowed one. Furthermore the
settlement of the flow happens during the first millisecond, where the move-
ments of the profile and the power delivery are still small.

Solid blocking occurs, because the outflow border is smaller than the inflow
border and the mean velocity thus higher. The effect is 2-3% for the cylinder
situation in the maximally expanded situation. This causes the earth-bound
velocity at the outflow border P to be about 0.001 m/s (instead of zero). The
influence of this too large velocity on the calculated kinetic energy is small.

II.5 Movement of the profile

Total volume of the head is estimated from high speed movie films (400-1250
fr/s) with synchronous lateral and ventral views by the ellipse method (Drost &
van den Boogaart, 1986a). If the form of an object is smooth, each of its
cross sections can be approximated by an ellipse. The entire object thus con-
sists of a series of ellipses. Total volume is the integral of the cross sec-
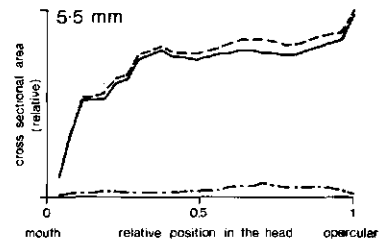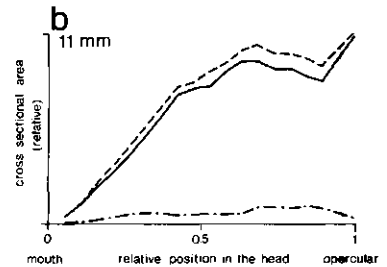
tional areas over the length of the head. Errors of the method have been esti-
mated to be less than 10%. By far the largest portion of this error was system-
atic.

a

b

11 mm

cross sectional area
(relative)

0   0.5   1
mouth   relative position in the head   opercular

5.5 mm

cross sectional area
(relative)

0   0.5   1
mouth   relative position in the head   opercular
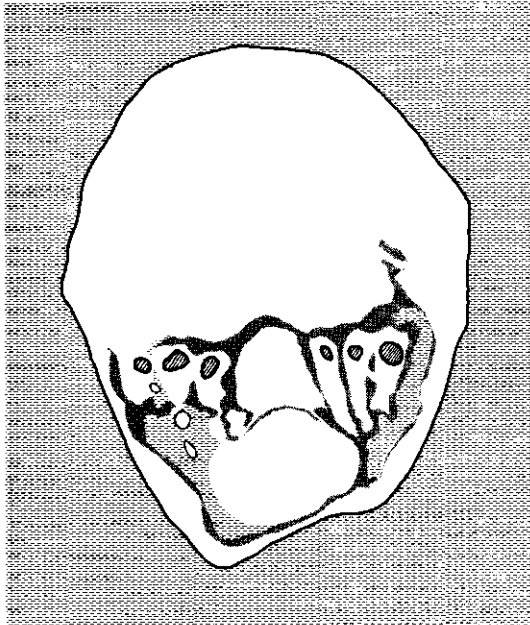
▨ water
▨ mucus
☐ tissue

0.5 mm

—.—water
——tissue
———total

Fig. 3. Determination of relative volume of mouth cavity (water plus mucus) and
tissue in the head of fish larvae, when it is in rest position (not expanded).
See the text for details of the technique.
a- Tracing of a microscopical cross section through the head of a 5.5 mm carp
larva just behind the eyes. The area of the tissue is much larger than the area
of the mouth cavity. About half of the mouth cavity is filled with mucus.
b-Distribution of tissue and water plus mucus in the head of carp larvae as a
function of axial position. Area on the Y-axis is in arbitrary units. Volume of
the mouth cavity is 4.5% (5.5 mm larva) resp. 7.6% (11 mm larva) of the total
volume of the head. These values must be considered with care because it is
impossible to decide how accurate the volume as measured on the sections equals
the volume at the onset of suction.

The ratio of the volume of the mouth cavity (water, including mucus) and the
volume of the tissues of the head of three carp larvae (SL 5.0, 9.2 and 11.0
mm) is determined (Fig. 3). The larvae first swam for 5 minutes in a diluted
(1:1) solution of indian inkt, were frozen in liquid nitrogen and sectioned (10
µm) on a Bright cryostat. The sections were examined with an Olympus Vanox

microscope, using pseudo dark field illumination. The mouth cavity was dark (inkt) and also the tissues were clearly visible (see Fig. 3). Negatives were projected and the outlines of mouth cavity and head were drawn. Relative volumes were determined by weighing the paper. The volume of the mouth cavity is 4.5-10% of the total volume of the head of carp larvae in the unexpanded situation (Fig. 3).
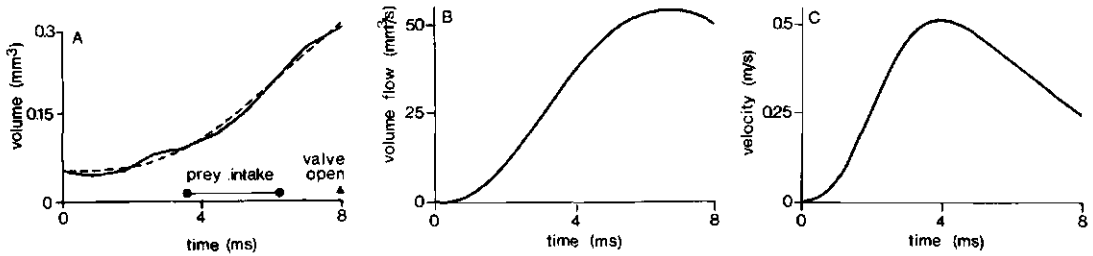
Fig. 4. a-Volume of the mouth cavity of a 6.5 mm carp larva while sucking prey (an Artemia nauplius). Total volume of the head is determined using the ellipse method (Drost & van den Boogaart, 1986a) from a 1125 fr/s movie with synchronous lateral and ventral views. It is assumed that the volume of the mouth cavity is 0.055 ml, i.e. 6.3% of the total volume of the head volume just before the onset of suction. The thick line is the measured volume, the dashed line is used as input in the model (Eq. 1).
b-Volume flow of the used movement.
c-Mean velocity at the mouth aperture.

Simulations are made using the data of an analysed snap. In a simulation the rate of expansion of the cylinder is chosen in such a way that the resulting volume flow closely resembles the measured volume flow (Fig. 4). The increasing volume of the mouth cavity is described with the formula (compare Muller et al., 1982):

$$V(t) = V_o + dV. \left\{ \frac{t}{t_m} \cdot e^{1-\frac{t}{t_m}} \right\}^\alpha \qquad t \geq 0 \qquad (2a)$$

$$V(t) = V_o \qquad t < 0 \qquad (2b)$$

V_o is the minimal volume of the mouth cavity, dV is the maximal increase in volume and t_m is the time that the maximal volume is reached. Alpha is the expansion coefficient, a physiological meaning of alpha cannot be given, the influence of the value of alpha on e.g. the pressure is given in Muller & Osse

(1984). The inner radius of the cylinder representing the mouth cavity is:

$$R(t) = \sqrt{\frac{V_o + dV.\left\{\frac{t}{t_m} . e^{1-\frac{t}{t_m}}\right\}^{\alpha}}{\pi . L}} \qquad t \geq 0 \qquad (3)$$

In this paper the measured flow of a 6.5 mm carp larva is used as basis for the curves, giving the following equations for the movement of the walls (it was assumed that the initial volume of the mouth cavity was 0.055 mm³, i.e. 6.3% of the initial volume of the head):

$$R(t) = \sqrt{0.0117 + 0.0849 . \left\{\frac{t}{13.5} . e^{1 - \frac{t}{13.5}}\right\}^{3.9}} \qquad t \geq 0 \qquad (4)$$

Measured and calculated volumes are indicated in Fig. 4, till the moment of opening of the opercular valve. Fig. 2 shows that at least in the first half of the strike the measured increase in cross sectional area of the simulated strike resembles an expanding cylinder.

II.6 Numerical problems

The program possesses the option to use the calculated velocities at a certain time, calculated in a previous run, as initial values in a continuation run. As the program took 30 min CPU time for a complete strike this option was used to obtain streamline pictures at certain times of a run which was made in pressure mode. During a restart the distribution of the meshes over the calculation area had to be recalculated. This introduced some error in the pressure and in the
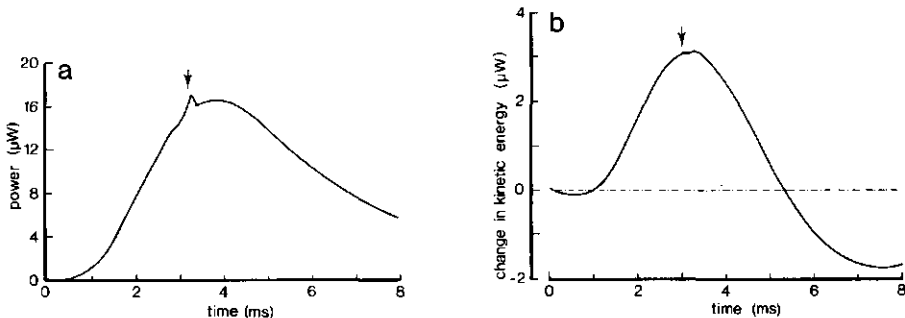
Fig. 5. Total power delivered by the cheeks (a) and change per unit time of the kinetic energy present in the total calculation area (b). After a restart of the program (arrow) 'jumps' occur resulting from inaccuracies in recalculating the calculation mesh. The error in power of the cheeks (calculated from the pressure) change is much more pronounced than the error in change in kinetic energy (velocity). These graphs are given only to show the influence of restarts, due to mistake the absolute values are not correct (for correct values see Figs. 14 and 15).
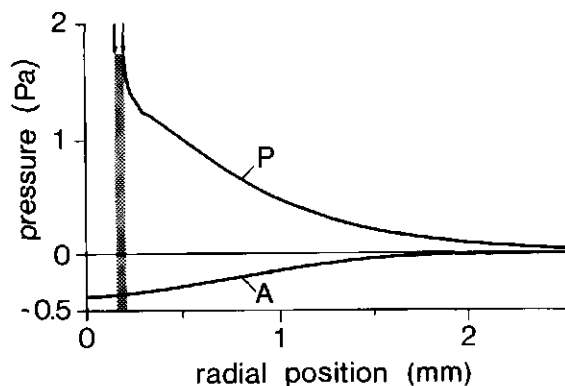
Fig. 6. Pressure distribution at t=4 ms at the anterior inflow boundary, A, and the outflow boundary, P (see Fig. 1 for the position of the borders). Ideally the pressure at A and P should be independent of radial position. The radial position of the cheeks is indicated with two arrows and shaded. The pressure in the right upper corner is taken as (undisturbed) zero pressure. This radial change is however very small (0.14 Pa) when compared with the pressure distribution at the mirror axis M (Fig. 11). The pressure at the outflow border P is higher than at A (order 0.1-1 Pa). The radial change is about 1 Pa. The radial change at P was expected to be larger than at A, because the smallest distance between profile and A is 1.5 mm, where P is directly adjacent to the profile (see Fig. 1).

velocities (see the bump in calculated change in total kinetic and potentential energy present in the calculation area, Fig. 5).

The size of the calculation area was large enough: the radial change in pressure at the anterior border A and the posterior border P (Fig. 6) was negligible compared to the axial pressure change at the symmetry axis M (Fig. 11). Also the flow near the outer boundary O is parallel to this boundary. The time step in the calculations was 0.025 ms. For larger values 'wiggling' of the velocity vector and the pressure occurred near the mouth aperture. It is also possible that the calculation mesh near the lips would better be smaller, because the pressure and velocity gradients are very steep near the lip.

III Results

III.1 Velocities

Fig. 7 shows a detail of the velocity distribution near the lip in the fish-bound frame. The boundary layer is obvious inside the mouth cavity at t=2 ms and later. The velocities are maximal near the mouth aperture. In front of the mouth they rapidly decrease with increasing distance, inside the mouth cavity they decrease slowly with increasing distance. The magnitude of the velocities in front of the mouth aperture is quite independent of the radial position. The
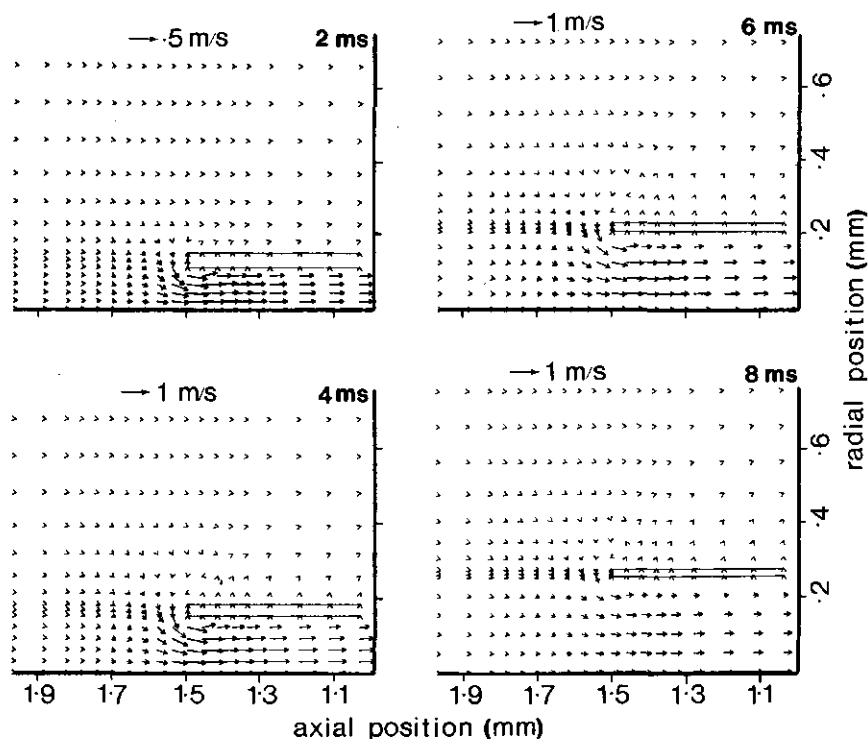
Fig. 7. Calculated water velocities in the moving frame near the mouth (see Fig. 1 for an orientation). Although the distribution of the calculation points inside and outside the mouth cavity does not change, their positions do (due to expansion): the same calculation points are drawn each time. The thickness of the cheek decreases with increasing radius. In this way the volume of the cheek is kept constant. Note the development of the boundary layer.

velocity is higher in the centre than near the lip but the differences are rather small. The slight wiggling of the velocity vector ·inside the mouth cavity near the lip is a result of the acute edge of the lip in the profile (in fishes the lips are rounded). Due to friction and no slip the water velocities near the walls are small (in the moving frame). Fig. 8 shows the radial distribution of the axial velocity at different times. The boundary layer is thin first (t=1 ms) and increases rapidly during the snap (compare e.g. t≈2 ms and t=8 ms, mean flow velocity being 4% higher at t=2 ms).

In a potential flow (no influence of friction) the velocity profile in a tube is flat, if friction is fully developed a parabolic velocity distribution is present (Poiseuille). Both the mean velocity near the mouth aperture (volume flow/cross sectional area) and the water velocity at the mirror axis (both at
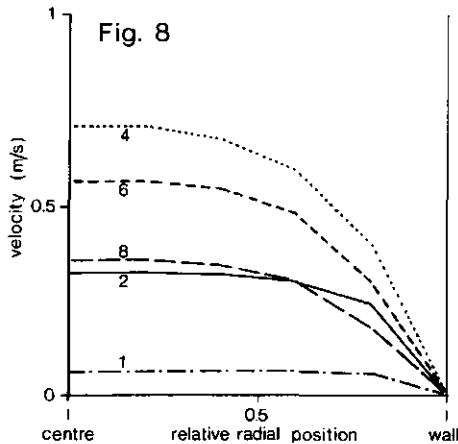
Fig. 8. Distribution of the axial velocity at 1.34 mm (89% of the length of the head) as a function of relative radial position (0 is the mirror axis, 1 is the inner cheek). Note that the radius of the mouth increases from 0.114 mm at t=2 ms to 0.256 mm at t=8 ms. So the increase in absolute size of the boundary layer is even larger than suggested in this figure. Mean (axial) velocity in the profile is maximal at t=4 ms (compare Fig. 4).
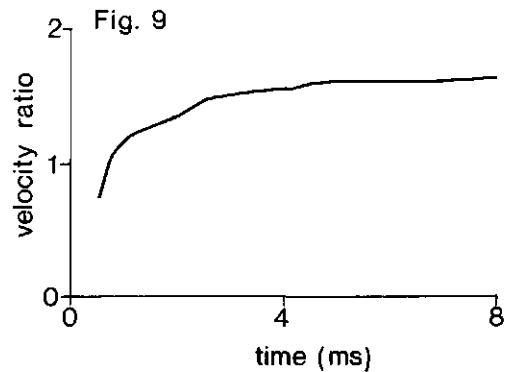
Fig. 9. Ratio of velocity at the symmetry axis and mean velocity over the cross sectional area. Theoretically this ratio is between 2 (Poiseuille flow) and 1 (frictionless flow). Because only 5 radial meshes are present in the mouth cavity and no slip at the wall is assumed the minimal ratio is 1/0.81=1.24. The ratio is determined at 90% of the length of the head. This gives an influence of the shape of the flow profile and the extra kinetic energy present compared to the frictionless situation (see discussion).

89% of the length of the head) are calculated. The ratio between these two is a measure for the form of the velocity profile. In a fully developed Poiseuille flow (parabola) the ratio is 2, in a flat velocity profile the ratio is 1. The ratio increases from below 1 at t=0.5 ms to 1.63 at t=8 ms (Fig. 9). Besides the increasing influence of friction, a second reason for the development of non-flat velocity profile does exist. Only water just in front of the mouth aperture is accelerated in axial direction. The radius of the mouth aperture increases in time. Water at a small radial distance of the mirror axis is thus accelerated during a longer time than water at a larger radial distance.

III.2 Pressures

Fig. 10 shows the calculated pressure as a function of time near the axis of the mouth cavity at the mouth aperture, halfway and in the opercular region. Peak negative pressure is most extreme in the opercular region (-276 Pa), and slightly higher halfway and at the mouth aperture (-250 and -243 Pa). Peak
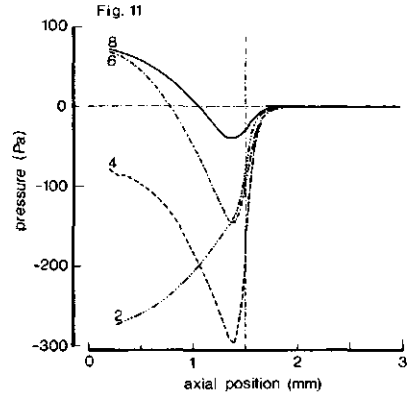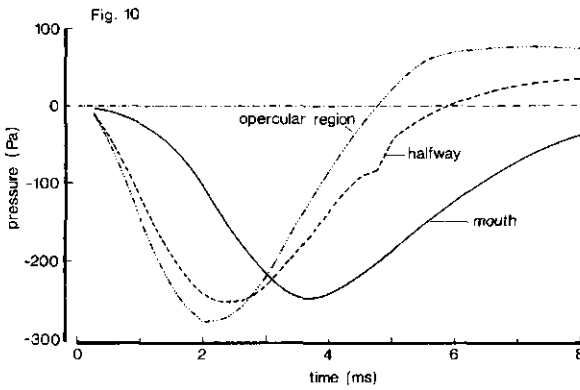
Fig. 10. Pressure as a function of time at three positions inside the profile at 10% of the radius of the mouth cavity from the axis: opercular region (13% of the length of the head), halfway (51%) and mouth aperture (99%).

Fig. 11. Pressure distribution at the symmetry axis as a function of axial position at four times (t=2, 4, 6 and 8 ms). Initially the pressure is posteriorly most negative, very early this peak moves to very near the mouth. The steepest pressure gradients are present just in front of the mouth, within about 0.25 mm the pressures are near ambient.
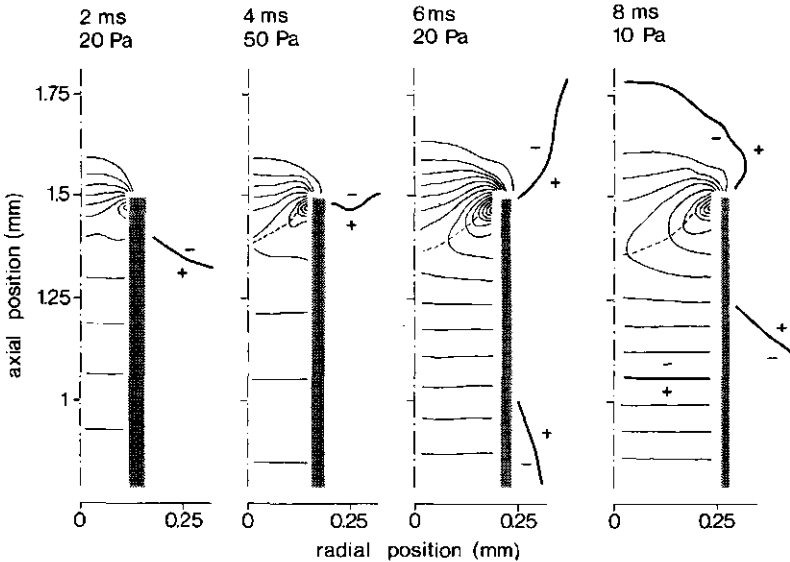
Fig. 12. Pressure distribution (isobars) in the calculation area at four times. Isobars do not reach the walls, because pressure is calculated half a mesh shifted to velocities. Isobar of ambient pressure is drawn thickly, the pecked line connects points of minimum pressure in axial direction. Except very near the mouth aperture pressure inside the mouth cavity is independent of radial position. The pressure gradient is most steep near the mouth aperture.
The pressure difference between each isobar is indicated above each drawing.
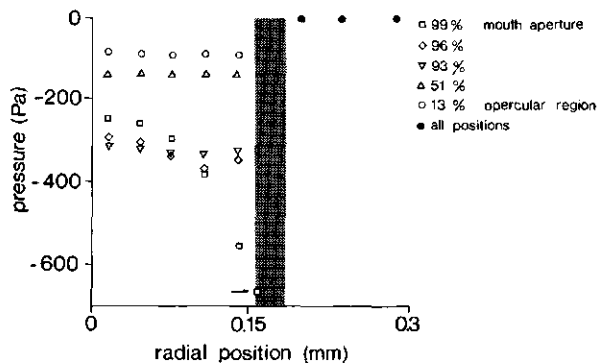
Fig. 13. Radial distribution of the pressure inside and outside the expanding profile at t=4 ms at six axial positions: 13% ('opercular region'), 51%, 77%; 93%, 96% and 99% ('mouth aperture') of the length of the head. For all axial positions the pressure outside the profile was ambient (within 3 Pa). The radial pressure gradient is very steep at the mouth aperture (99%), further inside the mouth cavity the pressure is independent of radial position. Pressures are calculated half a mesh away from the walls. At the mouth aperture (99%) the pressure exactly at the wall (arrow) is calculated using a three point differentiation formula, at all other radial positions the pressure at the wall is assumed to be the pressure half a mesh away from it.

negative pressure is reached first in the hindpart of the mouth cavity (at t=2 ms) and increasingly later in more anterior parts: at t=3.5 ms at the mouth aperture. Fig. 11 shows the axial pressure distribution near the central axis of the mouth cavity. The pressure is rather near ambient at distances larger than 0.2 mm in front of the mouth aperture. To the side of the profile the pressure is near ambient (see Figs. 12 and 13). The pressure inside the mouth cavity is independent of the radial position, except very near the mouth aperture (Figs. 12, 13). The extreme negative pressure near the lip is assumed to be due to the non-physiological (square) form of the lip: the acceleration of the water around the lips is very large (see Fig. 7). In real fishes the lips are rounded and most probably the radial pressure distribution at the mouth aperture will be more flat.

III.3 Energy

The total energy present in the calculation area at each moment is the sum of the potential and the kinetic energy.

Kinetic energy of each calculation point (E_{ki}) is given by:

$$E_{ki}=0.5 \cdot m_i \cdot vel_i^2 \tag{5}$$

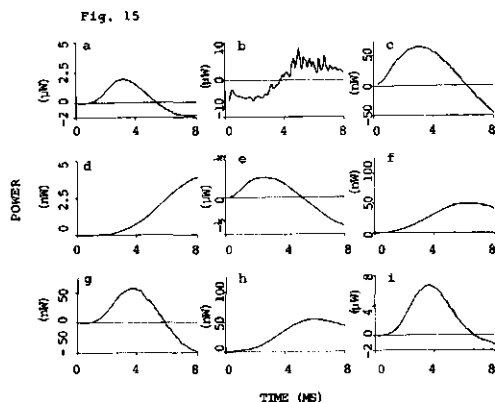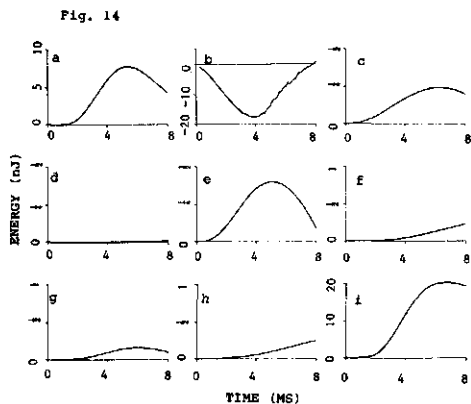m_i-mass of the calculation point i; vel_i-earth bound velocity in calculation point i.

Fig. 14. Kinetic and potential energy of the water in the calculation area. See Fig. 1 for the position of the borders. The changes in energy at the borders A and P are artifacts. Fortunately they are low compared to the change in potential energy at the cheeks (this is the biologically meaningful energy delivered by the muscles of the fish).
Change in kinetic energy at A is at all times zero: the earth bound velocity is there zero by definition.
a-kinetic energy present in the calculation area.
b-potential energy present in the calculation area.
c-cumulative change in potential energy at A.
d-cumulative change in kinetic energy at P.
e-cumulative change in potential energy at P.
f-cumulative change in kinetic energy at OC.
g-cumulative change in potential energy at OC.
h-cumulative change in kinetic energy at IC.
i-cumulative change in potential energy at IC.

Fig. 15. Kinetic power and potential power of the water present in the calculation area, i.e. change in kinetic and potential energy. See Fig. 1 for the position of the borders. The changes in energy at the borders A and P are artifacts. Fortunately they are low compared to the change in potential energy at the cheeks (this is the biologically meaningful energy delivered by the muscles of the fish).
Change in kinetic energy at A is at all times zero: the earth bound velocity is there zero by definition.
a-change in kinetic energy present in the calculation area.
b-change in potential energy present in the calculation area.
c-change in potential energy at A.
d-change in kinetic energy at P.
e-change in potential energy at P.
f-change in kinetic energy at OC.
g-change in potential energy at OC.
h-change in kinetic energy at IC.
i-change in potential energy at IC.

The potential energy, E_{pi}, is given by:

$$E_{pi}=V_i \cdot P_i \tag{6}$$

V_i-volume of calculation point i; P_i-pressure in calculation point i. It is assumed that the pressure in the upper right corner of the calculation area is unaffected by the movement of the profile. All pressures are calculated relatively to this pressure. Total kinetic and potential energy are calculated by summation over all calculation points.

Total amount of energy present in the calculation area can change by (see Fig. 1 for the position of the borders):

1-change of kinetic energy at A, OC, P and IC

2-change of potential energy at A, OC, P and IC;

3-energy losses to friction (heat).

Energy changes at IC and OC are delivered by the fish, energy changes at A and P are artifacts due to the configuration of the calculation area.

The pressure is calculated half a mesh shifted to the velocities. The pressure at the borders (A, P, IC and OC) is thus not known exactly. The pressure gradient in the wall of the profile (cheek) is very steep. In the water the pressure gradients perpendicular to the wall are not steep, except near the mouth aperture inside the mouth cavity (see Fig. 13). So the pressure at the wall is assumed to be the pressure half a mesh away from it. Only at the mouth aperture the pressure is calculated at the wall. The direction coefficient, dP/dR is calculated in the nearest point (using a three point differentiation formula) and the pressure at the wall is extrapolated (see Fig. 13). Total force acting on each side of the wall is the pressure times the area summated over all meshes of the wall.

Fig. 14 shows the change in energy, Fig. 15 the cumulative change in energy present in the calculation area and at its borders. The change in kinetic energy at the borders is very low, the change in potential energy at OC, A and P is larger but still an order of magnitude smaller than the change of energy at IC.

The calculation of the potential energy present in the calculation area is not accurate enough to calculate a meaningful change in potential energy (Fig. 15b). Kinetic energy is calculated more accurate and the change in time in kinetic energy (Fig. 15a) shows a smooth curve. Total energy delivered by the cheeks is 20 nJ, maximal power delivery 6.7 μW.

IV-Discussion

IV.1 Errors due to the form of the profile

The estimation of initial volume of the mouth cavity and volume flow of the simulated snap is more accurate than in previous simulations (e.g. in Muller & Osse, 1984 and van Leeuwen & Muller, 1983). The volume flow is measured quite accurately (error about 10%, Drost & van den Boogaart, 1986a). The error in initial volume may be a factor 2 (compare Fig. 3). Calculated mean velocity at the mouth aperture is increase in volume divided by cross sectional area. An error of a factor 2 in the initial volume causes an error of a factor 2 in the initial cross sectional area, and thus initially in calculated velocities, accelerations and pressures. This error decreases with increasing volume of the mouth cavity. Assuming that the absolute size of the boundary layer is not affected, its relative size is affected and so the amount of energy spilled to friction.

In the snap used in the model simulation the centre of prey passed the mouth aperture at t=4.4 ms (frame 6). The velocity measured between two frames of a 1125 fr/s movie was 0.34 m/s. We assume that the velocity of the prey is equal to the water velocity at the position of its centre of mass. This water velocity is determined over calculated fluid path particle paths (Drost, in prep.b). The calculated mean velocity of the prey over 0.89 ms, time between two film frames, when it is half outside the mouth and half inside, equals 0.5 m/s. The difference between these two velocities (a factor 1.5) could result from an error of the cross sectional area of the mouth or to the large size of the prey (see below). The measured cross sectional area of the mouth aperture at t=5.3 ms is about 1.8 times the value used in the model (prescribing the correct volume flow in a cylinder may involve a wrong mouth radius). This difference is larger at earlier times and almost disappeared at t=8 ms. Much attention is paid to the estimation of the accuracy of the velocities. This is done because the calculated kinetic energy is proportional to velocity squared. Also the calculated pressures are more or less proportional to velocity squared, but here friction might influence the values in an unpredictable way.

The approximation of the mouth cavity by an expanding cylinder is worse than the much more versatile movement of a cone (Muller & Osse, 1978, 1984). In the snap used as basis for the simulation the increase in volume of the mouth cavity was distributed equally over the length of the head during the first 4 ms (Fig. 2). Later the posterior end expanded strongly while the anterior end only slightly expanded. The underestimation of the posterior expansion of the fish by the cylinder-like movement of the profile caused (at least partly) the positive posterior pressure after t=5 ms (Fig. 10). Also the constant swimming

velocity was not optimal. It seems safe to suppose that the model adequately describes the suction flow, despite the cylinder form and the constant swimming velocity.

At the start of suction a representation of the mouth cavity by two parallel plates lying close together appears to be a better approximation of the mouth cavity than a cylinder. Drost & Verhagen (in prep.) calculated that friction causes an increase in required power of a factor 2.5 when plates with a width/- heigth ratio of 10 are compared with a cylinder having an equal cross sectional area. We assume that the influence on the energy spilled to friction is much lower, because the power at the start of suction is low (Fig. 15) and the length/width ratio in the plate configuration rapidly increases during the suction.

IV.2 Pressures

The calculated peak negative pressure (-276 Pa) for this strike of a 6.5 mm carp larva is much smaller than peak negative pressures measured for adult predatory fishes (van Leeuwen & Muller, 1984 and references therein: -5 to -65 kPa depending on species and intensity of attack). The pressure gradient dP/dx is in larval carp in the same order of magnitude as in adult fishes (see Muller et al., 1982), as are the resulting accelerations: 800 m/s^2 in larval carp (Drost, in prep.b) and 1000 m/s^2 in adult pipefishes (Muller & Osse, 1984). Furthermore the absence of bone and the delicacy of construction seems to exclude real low pressures. Unfortunately, it is however impossible to measure the pressure in the mouth cavity of a carp larva (mass about 1 mg at first feeding). The water velocities as measured from the film (Drost & van den Boogaart, 1986a) were in the same order of magnitude as the calculated values. The difference of about a factor 1.5 can easily be attributed to differences in intensity between a series of snaps. The times in which these velocities were reached were equal. The calculated accelerations are thus also in the correct order of magnitude.

In adult fish often an initially positive pressure peak is present in the opercular region: this was called acceleration pressure, originating from the acceleration of the fish (Lauder, 1980; Muller et al., 1982; Muller & Osse, 1984; van Leeuwen & Muller, 1984). This is absent is this calculation because the profile had a prescibed constant speed in our calculations. The maximal acceleration of the larva during the snap used as the basis for this calcula- tion was estimated to be 17 m/s^2. So the pressure gradient due to the accelera- tion is 17 Pa/mm, giving an acceleration pressure at the hind part of the

profile of 25 Pa. This is about 10% of peak negative pressure (compare Fig. 11).

In the simulation the pressure outside the cheeks was always near ambient (within 1-3 Pa), even during peak radial acceleration of the outer cheek (about 8 m/s^2 at t=2.3 ms). The situation might be different in a more fish like situation: an cone-like profile accelerating forward. In a carp larva the half top angle of the cone frustrum is about 10^0, before valve opening and the maximal acceleration of the fish is 17 m/s^2. To us it seems improbable that this will cause a large (positive) pressure at the outer cheek. We estimate it to be less than 10 Pa.

The radial pressure gradient inside the mouth cavity near the mouth aperture is very steep. Part of this may result from the 'square' lips. Even if the lips were rounded, a very low pressure near the lip is necessary to account for the very large accelerations near the lips. At a distance of 10% of head length the pressure is independent of radial position (Fig. 13), as was tacitly assumed by previous researchers measuring buccal and opercular pressure (e.g. van Leeuwen & Muller, 1983).

Previous workers have put emphasis on the peak negative pressure during suction feeding of fish (e.g. Alexander, 1967; Lauder, 1983), as these pressures may impose constructional demands on the head of the fish. Pressures in the mouth cavity are related to forces exerted by muscles. Due to the complicated kine-matic couplings and moment-arms in the fish head it is difficult to deduce required tension of particular muscles in the head from measured pressures in the mouth cavity. Also the power used during suction is a biologically meaning-ful parameter. Power can be estimated from the increase in energy present in the water (plus the energy converted to heat) or by the work exerted by the walls of the mouth cavity against a pressure gradient. Power can be calculated as wall area times pressure difference over the wall times radial velocity of the wall summated over the length of the head. Power during a snap can be calculated from accurate motion curves (Drost & van den Boogaart, 1986a) com-bined with pressure measurements in at least two positions of the mouth cavity. Eventually, the wall of the mouth cavity transmits the power (velocity and pressure difference) to the water. The velocity and pressure at the wall are coupled to the velocity and tension of muscles by transmission coefficients, the power delivered by the wall is equal to the power of the muscles, unless energy is used which was stored as e.g. elastic energy. Power is independent of geometry and inertial effects are already included in the pressure.

IV.3 Effects of friction

Friction influences the energy required to create a given suction flow in two ways. First, more (33%) kinetic energy is present in a fully developed Poiseuille profile, than in a flat velocity profile (assuming equal flowrate); secondly energy is converted to heat. In the fish-profile the extra 'Poiseuille' energy is lower for two reasons: 1- in the mouth aperture (where the highest velocities occur) the velocity profile is rather flat and 2- outside the profile (where also high velocities are present) no Poiseuille profile occurs.

Power spilled to heat by friction may be calculated from the change in kinetic and potential energy present in the calculation area and the changes of energy at the borders. As the total volume of the mouth cavity is only 0.5% of the total volume of the calculation area, slight fluctuations of the pressure outside the mouth cavity have a profound influence on the total potential energy. This precludes the calculation of the effect of friction as a function of time. The calculation of the kinetic energy is much more accurate: 1- earth bound velocities are very low at some distance of the profile and 2- velocities are squared to calculate kinetic energy. Another way to determine the influence of friction is to subtract the maximal kinetic energy present in the calculation area from the total energy delivered by the moving wall of the profile. According to Fig. 14 maximal kinetic energy is 8 nJ, total energy delivered by the cheeks is 20 nJ, so 60% is spilled to friction. The rest of the energy is also converted into heat, but it has been useful first. Muscle mass of a carp larva of this size is 0.53 mg (Drost & van den Boogaart, 1986b). Maximal power delivered by the cheeks is 6.7 μW (Fig. 15 g,i, t=3.65 ms). Assuming that all muscles contract synchronously, specific power for suction is 13 W/kg muscle. This value is somewhat lower than the value of 30 W/kg muscle calculated more crudely by Drost & van den Boogaart (1986b) for the snap of a 5.8 mm carp larva. These values are in close agreement with values in the literature (Johnston et al., 1985). Energy required for swimming is neglected in this reasoning.

Total energy delivered by IC might be underestimated, because the pressure at the inner lip might be lower than calculated. As the mesh of the lip is only 2.7% of the total wall area, the error will surely be less than 10%.

Total energy delivered by the cheeks is almost 20 nJ (t=7 ms). After that time negative power is delivered by the cheeks. Muscles however cannot gain energy from negative power. At the time negative power is delivered, water is actively

decelerated by the cheeks. This occurs first in the opercular region (Fig. 10). Prey suction is defined as: 'the ingestion of water and prey by expansion and compression of the mouth, eventually coupled with opening of the opercular valve' (Muller & Osse, 1984). If a large swimming velocity is obtained by movements of body and tail, an always positive pressure may be present in the mouth cavity, and suction may thus entirely passive. Although to our opinion it might be better to restrict the term 'suction' to active movements, in practice model calculations would be necessary to decide whether feeding is suction or not.

IV.4 Influence of large prey

The velocity gradients are steep, both near the mouth aperture and inside the mouth cavity at the outer half of the mouth radius (i.e. near the wall). Larvae often feed on large prey, e.g. the diameter of an _Artemia_ nauplius is 0.22 mm, the maximal mouth diameter of a 6.5 mm carp larva 0.54 mm. The velocity gradient is least steep near the axis. The prey is forced to the centre of the mouth aperture by centrifugal effects: prey are slightly denser than water and the water velocity is highest at the centre (see Merzkirch, 1974). So, prey uptake is a self-centering·process. The prey itself will not or only negligibly be deformed by the flow. So, if the prey enters the mouth aperture the velocity field is disturbed. If the diameter of the prey is 0.5 times the mouth diameter the velocity gradient near the wall need to steepen hardly; if the prey is 0.75 times the mouth diameter the velocity gradient between the prey and the wall steepens and thus viscous forces.

References
Aerts, P. & Osse, J.W.M., in prep. Title still unknown.
Alexander, R.McN., 1967. The functions and mechanisms of protrusible jaws of some acanthopterygian fish. J. Zool. Lond. 151: 43-64.
Drost, M.R., in prep.a. The relation between aiming and catch success in larval fishes.
Drost, M.R., in prep.b. Prey capture by fish larvae, water flow patterns and the effect of escape movements of prey.

Drost, M.R. & Boogaart, J.G.M. van den, 1986a. A simple method for measuring the changing volume of small biological objects, illustrated by studies on suction feeding by fish larvae and of shrinkage due to histological fixation. J. Zool. Lond. (A) 209: 239-249.

Drost, M.R. & Boogaart, J.G.M. van den, 1986b, in press. The energetics of feeding strikes in larval carp, Cyprinus carpio. J. Fish Biol.

Drost, M.R. & Verhagen, J.H.G., in prep. Hydrodynamic limitations of feeding in larval fish.

Johnston, I.A., Sidell, B.D. & Driedzic, W.R., 1985. Force-velocity characteristics and metabolism of carp muscle fibres following temperature acclimation. J. exp. Biol. 119: 239-249.

Jong, C de, Sparenberg, J.A. & Vries, J. de, in prep. On the hydrodynamics of suction feeding of fish.

Leeuwen, J.L. van, 1984. A quantitative study of flow in prey capture by Rainbow Trout Salmo gairdneri, with general consideration of the actinopterygian feeding mechanism. Trans zool. Soc. Lond. 37: 171-227.

Leeuwen, J.L. van & Muller, M., 1983. The recording and interpretation of pressures in prey-sucking fish. Neth. J. Zool. 33: 425-475.

Leeuwen, J.L. van & Muller, 1984. Optimum sucking techniques for predatory fish. Trans. zool. Soc. Lond. 37: 137-169.

Lauder, G.V., 1980. The suction feeding mechanism of sunfishes (Lepomis): an experimental analysis. J. exp. Biol. 88: 49-72.

Merzkirch, W. 1974. Flow visualisation. New York: Academic Press.

Muller, M & Osse, J.W.M., 1978. Structural adaptations to suction feeding in fish. In: Proceedings of the ZODIAC symposium on adaptation, pp. 57-60. Pudoc: Wageningen, The Netherlands.

Muller, M. & Osse, J.W.M., 1984. Hydrodynamics of suction feeding in fish. Trans. zool. Soc. 37: 51-135.

Muller, M., Osse, J.W.M., Leeuwen, J.L. van & Drost, M.R., 1985. Prey capture hydrodynamics in fish. J. theor. Biol. 95: 389-394.

Muller, M., Osse, J.W.M. & Verhagen, J.H.G., 1982. A quantitative hydrodynamical model of suction feeding in fish. J. theor. Biol. 95: 49-79.

Officier, M.J., Vreugdenhil, C.B. & Wind, H.G., 1986. Applications in hydraulics of numerical solutions of the Navier-Stokes equations. In: C.T. Taylor (ed.). Computational techniques for fluid flow. Swansea, U.K.: Pineridge Press.

Prey capture by fish larvae,
water flow patterns and the effect of escape movements of prey

M.R.Drost
Dept. of Experimental Animal Morphology and Cell Biology
Agricultural University, Marijkeweg 40, 6709 PG Wageningen.
The Netherlands

Abstract

Streamlines and fluid particle pathlines during suction feeding of a 6.5 mm carp larva, calculated with the hydrodynamical model of Drost et al. (in prep.) are presented. Also the path lines of actively accelerating fluid particles ('escaping prey') are calculated. The shape of the parcel of water sucked into the mouth cavity is almost spherical, due to the low swimming velocity and entirely in front of the initial position of the larva. It is hypothesized that the low swimming velocity and the absence of protrusion are coupled with the high aiming inaccuracy of young fish larvae. For a prey starting from the centre of the parcel of water sucked into the mouth cavity the best escape direction is foreward. If escaping radially the required velocity is doubled. Optimum sucking techniques for fish larvae are discussed. Accelerations of the water near the mouth aperture up to 800 m/s^2 are calculated.

I-Introduction

Almost all fish larvae feed on relatively large prey (Blaxter, 1969) which they capture by a combination of swimming and suction (i.e. a rapid increase of the volume of buccal and opercular cavities, together denoted in this paper as mouth cavity). The flow during this feeding is highly unsteady, within 4-6 ms after the start of mouth opening of a 6 mm carp larva the prey passes through

the mouth aperture with a velocity of 0.3 m/s (Drost & van den Boogaart, 1986b). A quantitative hydrodynamical model has been made to simulate the flow inside and around the mouth cavity of fish larvae while sucking prey (Drost et al., in prep.). The model is unsteady and takes viscous effects into account.

The catch success during the ontogeny of larval fishes increases rapidly (Drost, in prep.a and references therein). Beyer (1980) made a model relating catch success to aiming inaccuracy (see also Drost, in prep.a). In this aiming model radial flow during prey intake and escape movements of the prey are neglected (so it resembles a filter system). Escape movements of the prey may influence the catch success profoundly. Drenner et al. (1978) determined capture frequency of a siphon with a constant flowrate on various prey. Capture probability, relative to heat killed zooplankters, was about 0.9 for clado-cerans, 0.25 for cyclopoid - and less than 0.1 for calanoid copepods. The interaction between the movements of an accelerating (i.e. escaping) prey and the rapidly changing flow during suction feeding by fish larvae has not previously been investigated. This interaction determines the strategy a fish should adopt to optimize its movements to catch prey of different types.

In this paper calculated streamlines and particle path lines are presented. The purpose is to determine the fate of fluid particles in different positions around the mouth during suction feeding and to translate these data to possible fates of prey in these positions. The shape of the parcel of water sucked into the mouth cavity is shown from these path's, as was done previously by van Leeuwen (1984), Muller & van Leeuwen (1985) and de Jong et al. (in prep.). Also the path of an escaping prey in the suction flow of a larva are calculated.

II Material and methods

II.1 Streamlines and path lines

The curves described by fluid particles in time are called path lines. Stream-lines are everywhere tangential to the instantaneous velocity in the fluid. Path and streamlines are identical in steady flow, but different if the flow is unsteady, as in suction feeding by fish (Muller et al., 1982; Muller & Osse, 1984; see also Fig. 8). The dividing streamline is the streamline separating the water tending to enter the mouth from the water tending not to enter the mouth.

The flow field around a prey sucking fish larva was calculated using the model of Drost et al. (in prep.). In this model the mouth cavity is depicted as a cylinder, expanding first and compressing later. The anterior end, 'mouth', is open; the posterior end, 'opercular region', is at first closed by the opercu-

lar and branchiostegal valve. This valve opens at a certain time. The cylinder moves forward with a certain velocity, 'swimming velocity'. The flow field of a prey sucking (adult) fish relative to its mouth looks like a combination of a parallelstream (resulting from its translation: 'swimming') and a bound vortex (resulting from suction by enlarging the mouth cavity). This flow has been visualised by van Leeuwen (1984). For frictionless flow an extensive treatment of the form of the flow field as a function of the relative strength of swimming and suction is given in Muller & Osse (1984).

For the present simulation the data of a snap of a 6.5 mm carp larva were used, filmed at 1125 fr/s. Swimming velocity was taken constant (0.035 m/s), actually it varied from almost rest to 0.056 m/s. For details see Drost et al. (in prep.). The water velocities in the axial and radial directions were calculated in the simulation as a function of position and time. By multiplying the velocity of a certain water particle with the time between two calculation steps the new position of the water particle can be calculated. So fluid particle path's from t=0 to t=8 ms were constructed. To determine the volume of water sucked into the mouth cavity a reverse calculation was used (van Leeuwen & Muller, 1984; Muller & van Leeuwen, 1985). The positions of 6 fluid particles being at the mouth aperture at t=2, 4, 6, and 8 ms, radial position about 0, 20, 40, 60, 80, and 96% of the mouth radius were back calculated to t=0 (actually all times were 0.025 ms later due to clumsy output statements). The same was done for 3 points just outside the outer cheek: approximately 0.05, 0.1 and 0.5 mm in a radial direction. Path's are indicated with the time at which they enter the mouth (2 ms path etc.) and according to the radial position they enter the mouth (0% path etc.). Reverse calculations were done in ten steps of 0.025 ms, followed by 6-8 steps of 0.125 ms and 10-15 steps of 0.25 ms, the remainder (if present) was calculated in steps of 0.5 ms. The change in used time interval is barely visible in Figs. 3 and 4, showing path's, but clearly in Fig. 8, showing accelerations. So, near the mouth aperture the path's were calculated with the time step used in the simulation, further away the velocity gradients are less steep and an increasingly larger time step was used. Although the change in time step from 0.025 to 0.125 ms is rather large, I suppose the resulting error in the path is small.

The flow can be described in two frames of reference: the earth bound frame and the moving, "fish bound" frame (relative to the centroid of the mouth aperture of the moving fish) (see Muller et al., 1982; Muller & Osse, 1984; van Leeuwen, 1984). The earth bound frame must be used to calculate forces and

energies. For prey capture the flow with respect to the moving frame is most useful, because it describes the flow with respect to the mouth of the predator. Water flow is called backward if it is moving towards the hindpart of the profile (i.e. opposite to the swimming velocity of the fish).

II.2 Prey movement in the flow field

To simulate the movement patterns of actively moving (escaping) preys in the flow field of a prey sucking larva, preys were treated as fluid elements of infinitesimal size. So the flowfield of the sucking larva is not disturbed, otherwise also a hydrodynamical model of the moving prey would be needed. Their active velocity was varied sinusoidally (Fig. 1). This choice is argued in the discussion. The active movement started generally at t=0. To determine the influence of the timing of the start of the movement also earlier starts were used (t=-2 ms and t=-5 ms). The direction of the active movement (forward, radial and forward under 45°), time to peak velocity (10 ms and 20 ms) and the peak velocity itself were varied. Water velocity at the position of the particle due to suction and its active velocity were added to get the total velocity. Path's were calculated till the moment of definite escape or passage through the mouth aperture. The prey was taken to start moving at approximately the centre of the parcel of water sucked into the mouth cavity before the moment of valve opening (Fig. 5). The exact position was chosen quite arbitrarily to be 0.35 mm in front of the centre of the mouth aperture at t=0. If the escape movement started before t=0, the position of the prey was calculated using only its active movements, i.e. stagnation and swimming of the fish was neglected before t=0.
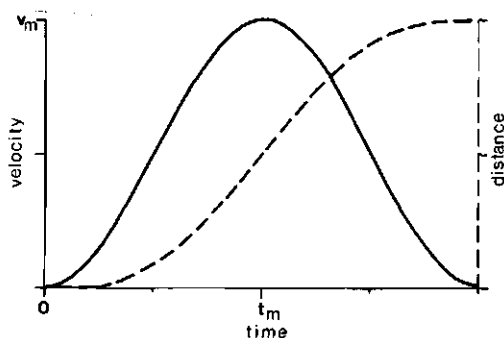

Fig. 1. Velocity and cumulative distance travelled as a function of time of accelerating particles with a sinusoidal movement.
t_m=time of maximal velocity
v_m=maximal velocity

III Results

III.1 Streamlines

Fig. 2 summarizes the variable streamline pattern of the simulation of one snap of a 6.5 mm carp larva in the moving frame. At all four times the flow in the moving frame resembles a combination of a bound vortex lying at the lips of the fish (created by suction) and a parallelstream (created by swimming). Near the mouth aperture however large deviations of a vortex occur: in an approximation with a vortex lying on the lips maximal velocities occur near the lip, in our calculations maximal velocities occur in the centre of the mouth and the velocity (in the fish-bound frame) near the lips is zero (see e.g. Drost et al., in prep.: Fig. 13). The dividing streamline rapidly moves radially outward, its radial position being 0.31 mm at t=2 ms, 0.58 mm at t=4 ms, 0.70 mm at t=6 ms and 0.68 mm at t=8 ms. The dividing streamline contracts towards the mouth. Near the lip the dividing streamline is almost perpendicular to the mouth axis at t=2, at later times a slight forward flow occurs near the lip (in the moving frame!). Pushing occurs only before t=2 ms. At t=8 ms the opercular and branchiostegal valve opens and after this time no reliable calculations can be done. The flow patterns closely resemble those which van Leeuwen (1984) has drawn tentatively for an expanding cylinder, neglecting the influence of
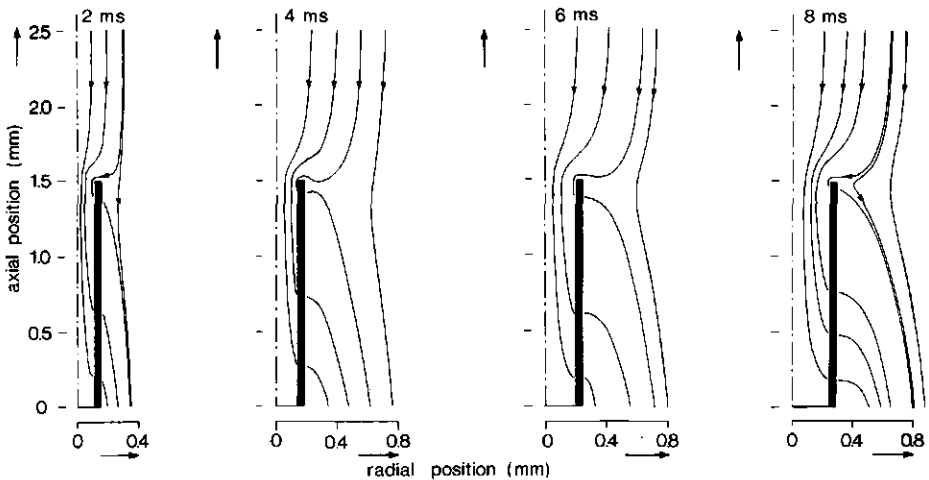
Fig. 2. Streamline pattern in the moving frame (relative to the mouth aperture of the fish larva), calculated with the model, using the data of a snap of a 6.5 mm carp larva. The streamline pattern is rotation symmetric around the central axis (-.-).The opercular valve is drawn thinly, the cheek thickly. The decrease in thickness which actually occurs during the simulation is not indicated. The position of the dividing streamline can be seen most accurate at t=2 ms and t=8 ms.

friction (friction is negligible for adult fish).

III.2 Fluid particle path's

Particle paths in the moving frame are given in Fig. 3. Particles passing through the outer half of the mouth aperture are sucked from radial distance much larger than the mouth aperture. The 2 ms-98% path is directed principally backward over its total length. At later times (t=4-8 ms) the direction of the 98% path's is principally radially and even forward (in the moving frame). Particles just outside the mouth move radially outward, they are pushed away by the cheeks. Particles radially further away move radially towards the mouth; they may move forward or backward depending on their exact position.

The form, but not the length, of the 0-98% particle path's is much alike between t=4 ms and t=8 ms. The 2 ms-path's deviate from the others by the relatively large effects of pushing.
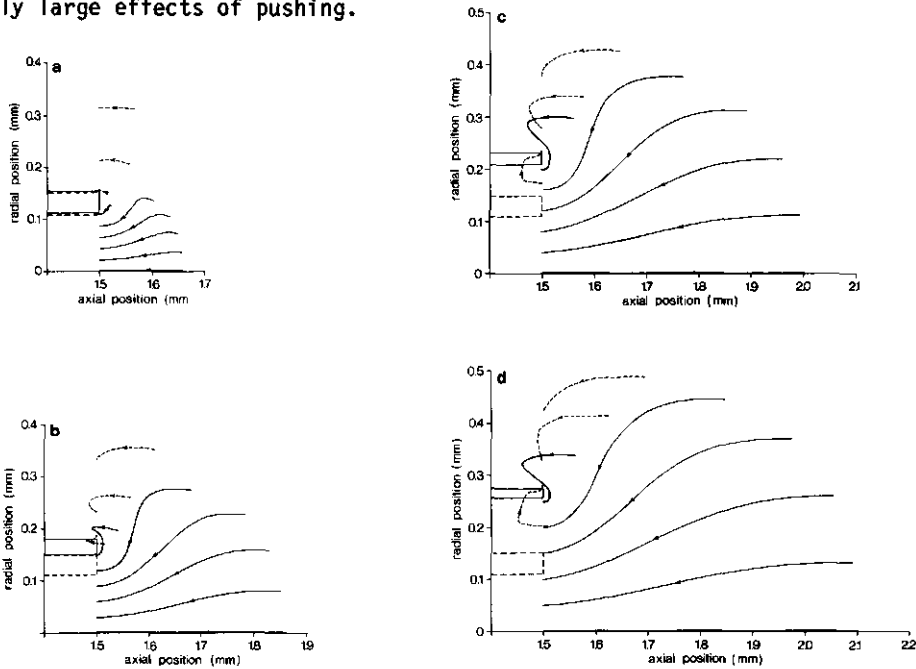
Fig. 3. Calculated fluid particle path's in the moving frame. The radial position of the mouth wall at t=0 (pecked line) and at the time the particles are entering the mouth (drawn line) is indicated. The axial position of the mouth aperture is 1.5 mm, the opercular valve is at x=0. Only the most anterior 0.1 mm of the mouth cavity is drawn. Path's of particles entering the mouth are drawn, of particles not entering the mouth pecked. Note the wide field from which particle enter the mouth.
a-Fluid particles entering at t=2 ms.
b-Fluid particles entering at t=4 ms.
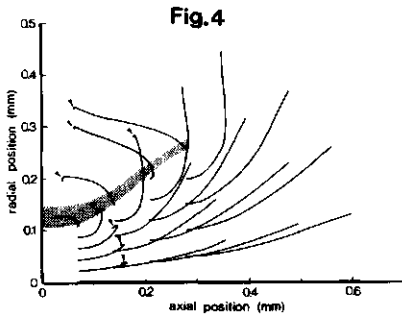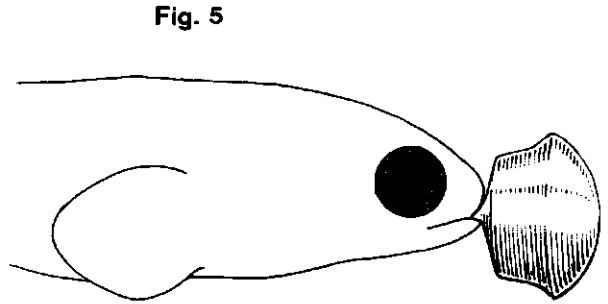c-Fluid particles entering at t=6 ms.
d-Fluid particles entering at t=8 ms.

Fig. 4. Calculated fluid particle path's in the earth bound frame. The path of the moving inner and outer lip is also indicated (dotted area). During the snap the lips becomes thinner. The lips move 0.28 mm forward due to swimming. Path lines may cross eachother or the cheek, because they do not have the same position on the same time. Positions were pushing occurs are indicated with arrows.

Fig. 5. A reconstruction of the carp larva at the start of the suction process and the parcel of water that will be ingested before t=8 ms (time of opening of the opercular valves). Water entering the mouth after the opening of the valves is neglected. The parcel of water is based on Fig. 4.

At each time the radial position of the diving streamline is larger than the maximal radial distance from which the water was sucked (compare Figs. 2 and 3). This is caused by the smaller radius at earlier times.

The path's of the same particles in the earth bound frame are given in Fig. 4. Only particles entering the mouth are drawn. Pushing is rather obvious in the 2 ms-particle path's (being initially at a distance of about 0.15-0.20 mm of the mouth aperture). In particles entering the mouth aperture at a later moment the effects of stagnation are almost invisible, except for the 98%-4 ms-particle path. The 98% particles move forward in the boundary layer of the outer cheek.

The form of the parcel of water sucked into the mouth before the moment of opening of the valves is given in Fig. 5. Only water that was in front of the mouth aperture before the start of suction is sucked into the mouth. This was not expected because the swimming velocity was very low (0.035 m/s), compared to the mean suction velocity at the mouth aperture, which was (earth bound) over 0.3 m/s between t=2.4 and t=6.7 ms.

The water sucked into the mouth cavity at t=8 ms was at t=0 ms maximally at an axial distance of 0.62 mm (40% of the length of the head) and maximally at a radial distance of 0.45 mm (twice the mouth radius at t=8 ms). All water entering through the edges of the mouth aperture was initially (t=0) less than 0.1 mm in front of the mouth (in axial direction, see Fig. 4).
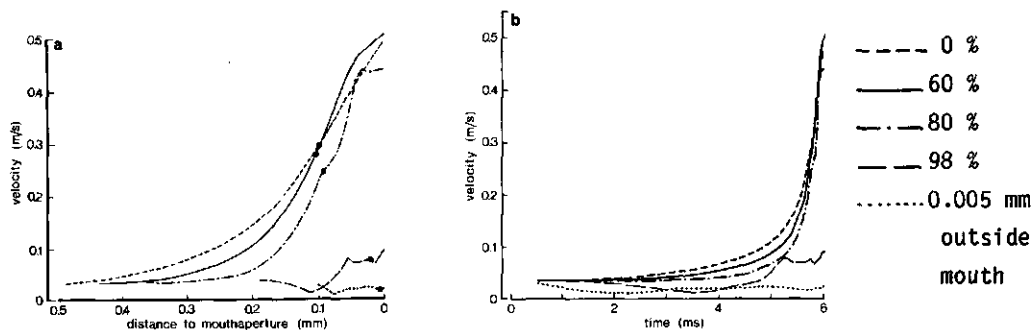
Fig. 6. Velocities (moving frame) of some calculated fluid particles moving over the 6 ms-path's of Fig. 3c, as a function of distance to the mouth aperture (a) and time (b). Note that the swimming velocity is 0.035 m/s. Symbols in the curves of a denote t=5.75 ms.
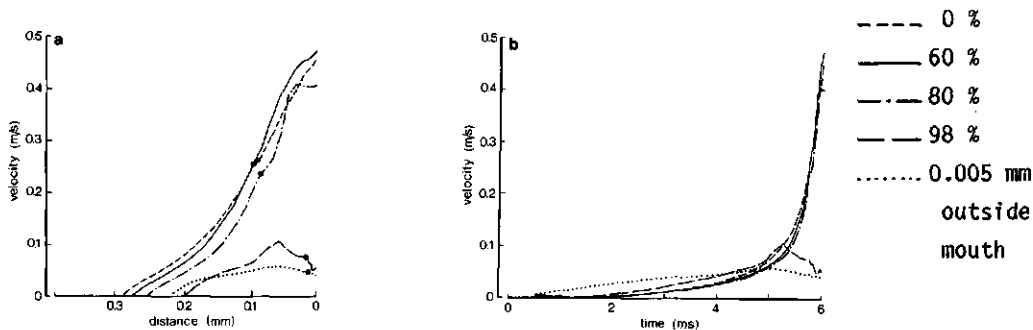

Fig. 7. Velocities (earth bound frame) of some calculated fluid particles moving over the 6 ms-path's of Fig. 4c, as a function of distance travelled (a) and time (b). Symbols in the curves of a denote t=5.75 ms.

The velocity of the particles moving over the 6 ms-particle path's of Fig. 3c is given in Figs. 6 (fish-bound frame) and 7 (earth-bound frame). The velocities in the moving frame of the 0, 20 and 40% path's are much alike. The velocity over the 60% path is initially somewhat lower, but at ingestion somewhat higher than the more central path's. This higher velocity of the 60% path is caused by the large radial velocity, the axial velocity is maximal at the central axis. The velocity over the 80% path is much lower. The velocity at the 98% path is initially comparable to the others, later the path is caught in the boundary layer of the lips and the velocity is much lower. As the path's all span 6 ms, their length is proportional to the mean velocity at the path. The length of the path is maximally at the central axis. The mean velocity at the 60% path (fish-bound frame) is 90%, at the 98% path only 39% of the velocity at the 0% path (see Fig. 6).
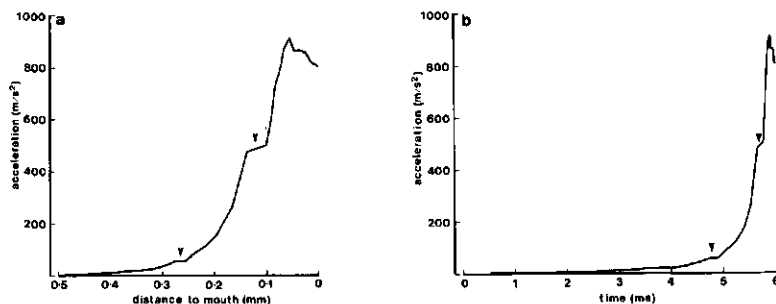
Fig. 8. Calculated acceleration of the particle moving over the 0%-6 ms- path (Fig. 3) as a function of distance to the mouth aperture (a) and time (b). The acceleration was calculated using an ausgleich spline (sd=0.001 m/s), the velocities were calculated by the model Odyssee (and used during the reverse calculation to reconstruct the particle path). The jumps in the curves (arrows) are caused by a change in time step in the reverse calculation.
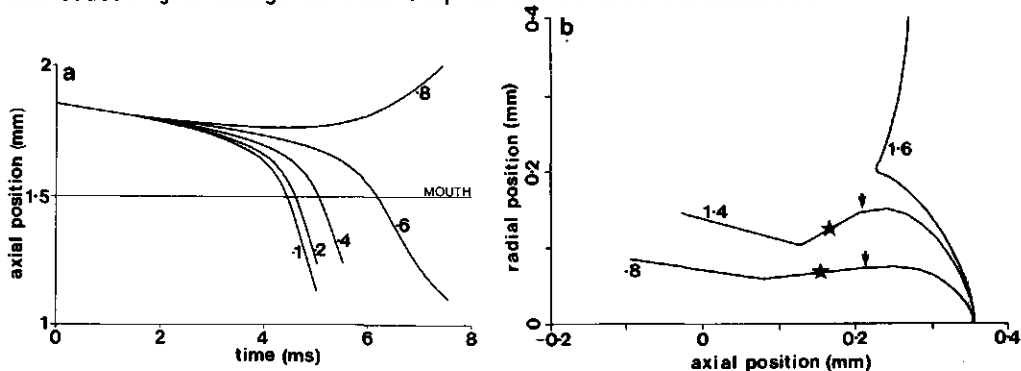

Fig. 9. Calculated movements of actively accelerating particles in the suction flow. The direction of acceleration is constant, the active velocity varies sinusoidally. All particles are taken to start escaping from the centre of the parcel of Fig. 5 (at the symmetry axis at 0.35 mm in front of the larva at t=0).

a-Axial position of axially accelerating particles as function of time in the fish-bound frame of reference. The axial position of the mouth aperture is 1.5 mm. Particles all start to move at t=0 and maximal velocity (v_m of Fig. 1) is reached at t=20 ms. The value of the maximal velocity is indicated near each curve. Particles enter the mouth if their axial position equals 1.5 mm.

b-Axial and radial position (in the earth bound frame) of particles accelerating radially. The lip is at t=0 at the axial position 0 and moves forward due to swimming. The position where a path enters the mouth is indicated with x, while entering the mouth the velocity increases enormously. Near the mouth they can be sucked inward (decreasing radial position, indicated with arrows). The mouth aperture is at t=0 at axial position zero. Maximal velocity (v_m in Fig 1) is indicated near each path. All particles start to move at t=0, time to maximal velocity is 20 ms. Note that initially some pushing occurs (the axial distance increases slightly and that also the escaping particle (v_m=1.6 m/s) is stongly effected by the suction flow. Inside the mouth cavity no strong radial suction flow exists. This is the reason that the particles inside the mouth cavity move radially outward. This is biologically not relevant, because they can not pass through the cheeks.

In Figs. 6 and 7 it is shown that the increase in velocity over the path's occurs mainly during the last 0.5 ms and the last 0.1 mm before entering the mouth. The acceleration over the 0%-6 ms-path is given in Fig. 8. From t=5 to t=6 ms the acceleration rapidly increases from 80 to about 800 m/s^2. At a distance of about 0.25 mm the acceleration becomes to high for any zooplankter to escape, although the acceleration is already at t=1 ms over 2 m/s^2.

III.3 Calculated movements of escaping prey

All statements are based on the simulated snap. Note that all prey were assumed to start their escape from the centre of the parcel of water sucked into the mouth. Some calculated escape movements are given in Fig. 9. The best strategy for a prey to escape is to escape in the axial direction. When escaping under an angle the required acceleration is higher, e.g. when changing only the direction of the active escape (from forward to sideward) the maximal velocity required to escape increases by about a factor two (compare Figs. 9a and b). Starting the escape movement earlier decreased the required escape velocity strongly, e.g. starting at t=-2 ms with almost a factor 2.5, starting at t=-5 ms with a factor 5, both relative to starting at t=0.

IV Discussion

In the preceding part the results of one simulation of the snap of a carp larva are discussed quite in detail. In total about 20 snaps of carp larvae smaller than 10 mm were filmed and the films were carefully looked at. Although all parameters that can be looked at (e.g. swimming velocity, time of the opening of the valve) differed between the snaps, the snap used for the simulation looked like a normal, though not very intensive snap. The results obtained with the model will be interpreted in biological terms. I am aware of the fact that using another snap would have given in different quantitative results. I suppose however that the results adequately describe most snaps of small carp larvae and in fact of most fish larvae.

IV.1 Pushing

Due to the difference between a real larva and the simulated profile the initial effect of pushing the prey away caused by the approach of the predator may be underestimated. In the simulation profile cavity and wall have an almost equal volume at the start of suction, in fish larvae the wall is 10 to 20 times larger than the initial cavity (Drost et al., in prep.). The form of the fish head however is much more streamlined than the profile. I therefore suppose that although pushing will be larger than calculated here, its effect will be unimportant in most snaps.

Van Leeuwen (1984) argued that pushing should be avoided. I agree that pushing is unfavorable, because if it occurs the flow rate could be increased by opening the valves. With a given flow rate, pushing has only effect on the distance from which water is sucked into the mouth (increasing the axial and decreasing the radial distance). The effects of the form of the parcel of water sucked into the mouth on prey capture chance are discussed later.

IV.2 Distortion of the flowfield by large prey

In all calculations of actively moving particles, they were of infinitesimal size. Their path's are considered to be the path's of the centre of mass of a prey. Prey of larval fish generally are relatively large, the prey used for the carp larvae had a length of about 0.72 mm and a greatest radius of about 0.15 mm. These dimensions are very large compared with the parcel of water sucked into the mouth mouth cavity before valve opening (Fig. 5). At the moment the head-end of the prey passes the mouth aperture (t=3.6 ms, frame 5) the calculated velocity at the axis of the mouth aperture is 0.606 m/s (earth-bound). The velocity 0.72 mm away (near the 'tail' of the prey) is only 0.030 m/s. Owing to the rigidity of a prey the flowfield around a prey sucking larva must be considerably distorted. According to Fig. 4 water initially at an axial distance of 0.62 mm enters the mouth aperture. The initial axial distance of the 'tail' of the prey was 0.92 mm, and it passed the mouth aperture at t=6.2 ms (frame 8). This difference between calculated and measured value is not really surprising if we realise that the volume of the prey is about 5-10% of the total volume sucked into the mouth before valve opening. The influence of a non deformable large prey on the energy and the resulting flowfield is still unpredictable.

IV.3 Acceleration of large prey

It is generally agreed upon that the minimal prey size is determined by energetic considerations and that the maximal prey size is determined by the mouth size (e.g. Hunter, 1977). Mouth width increases by about 20% during prey intake (by abduction). Due to the very steep velocity gradients elongated prey items are always taken in with their long side parallel to the axial direction. So, depending on their initial position, considerable rotation of the prey can occur during intake. The acceleration is so high that appendages (e.g. antennae) become pressed against the body, or stretched foreward or hindward, depending on their initial position. The critical size for prey is thus the width, excluding appendages. This conclusion from hydrodynamical considerations explains the results of Hunter (1977), which were based on the size of prey

actually found in the intestine of fish larvae.

It is reasonable to assume that larger prey can escape with higher velocities and that they can perceive a potential predator at a larger distance. This causes that larger prey are more difficult to catch than smaller prey. In the next section I will discuss the relation between the size of a prey and its acceleration in the flow field of a prey sucking fish larva.

To determine which size of prey can be sucked into the mouth cavity, I will consider the acceleration of a large, cylindrical prey, positioned parallel to the axis of mouth. The reasoning is restricted to prey of a 'normal' size, i.e. longer than 5%, but shorter than 75% of the length of the head (these values are chosen quite arbitrarily). The pressure at the front and hind side is assumed to be independent of radial position. The acceleration of a water particle is proportional to the pressure gradient. The acceleration of the large prey is dependent on the pressure difference (hind-fore) divided by its length (rewriting the second law of Newton). The pressure in front of a prey sucking larva is near ambient·at a distance of at most 0.15 to 0.3 mm (i.e. 10 to 20% of the head length) in front of the mouth aperture (see Fig. 10 and Drost et al., in prep.: Fig. 12). It is thus reasonable to assume that the pressure at the hind part of a large prey will be near ambient, until the centre of mass has far entered the mouth cavity. The acceleration of the prey
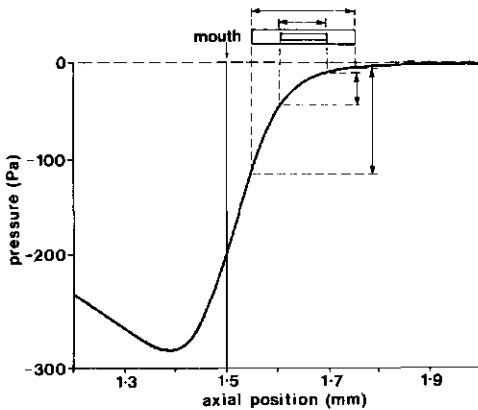

Fig. 10. Calculated pressure distribution at the central axis at t=4 ms. Outside the mouth aperture the pressure rapidly becomes ambient. The centre of mass of a large and a small prey are at the same position. The pressure difference (hind-front) increases more than linearly with size. So the force per volume (and thus acceleration) is larger on the large prey than on the small prey.is thus proportional to the pressure (relative to ambient) at its front end.

divided by its length. In this reasoning the effects of friction and flow disturbance at the side walls of the prey and of the too low velocity of the front part and the too high velocity of the hind part of the prey are neglected. I cannot predict the net effect of this phenomenon.

If we consider prey of different lengths, but with their front end at the same (axial) position, their accelerations are inversely proportional to their length. If we consider two prey of unequal length, and with their centres of mass at equal position, their accelerations are besides inversely proportional to their length also proportional to the (negative) pressure at their front ends. As the pressure very rapidly decreases near the mouth aperture, I suppose the latter effect is much stronger than the former (see Fig. 10). So I suppose that the shorter prey accelerates slower than the longer at that place in the suction flow, i.e. if the front end of the larger prey has entered the low pressure area just in front of the mouth aperture.

So, the acceleration of a prey in the suction flow is quite independent of its size. The smaller catch success on larger prey might thus be solely due to a perception of the predator at a larger distance and a higher escape velocity.

Copepod prey generally are obtuse anteriorly and tapering posteriorly. Their acceleration will thus be much higher if they are taken front end first than in the opposite direction.

IV.4 Form of the water sucked into the mouth cavity

The parcel water drawn in Fig. 5 does not give the total parcel of water sucked through the mouth aperture, because also water enters the mouth after the valves have been opened. This will tend to elongate the parcel. The water velocity is assumed to slow down rapidly, due to the large effects of friction, which even in this short time (several milliseconds) are very important (Drost et al., in prep.). Further more a prey passing through the mouth at a late time, is sucked only to the anterior end of the mouth cavity and may be able to escape due to the low velocities which occur during the end of the suction (this has been actually observed in 15 mm carp feeding on Daphnia). I therefore assume that the estimation of the water sucked into the mouth before valve opening may be a good approximation of the volume of which prey can be caught.

Total distance covered from t=0 to t=8 ms was in the simulation 0.28 mm; the fish moved 0.22 mm in axial direction and in total 0.26 mm. Mean swimming velocity is thus quite accurate, the velocity is first overestimated and later underestimated. So, initially a small volume of water might be sucked from behind the mouth opening, later the parcel should be a bit elongated. In the

simulation the size of the mouth aperture is underestimated, mainly initially. As the volume flow is accurate, the velocities are overestimated. The influence on the form of the parcel water is not clear to me.

This calculated shape for larval carp differs from the shapes calculated (neglecting the influence of friction) for adult fish. If the swimming velocity is large, only water in front of the mouth is taken in and the parcel is long and thin (van Leeuwen, 1984; Muller & van Leeuwen, 1985; de Jong et al., in prep.). If the swimming velocity is small, also water initially behind and lateral to the mouth aperture is taken in and the parcel is more or less spherical (de Jong et al., in prep.). As friction causes the water velocity near the lip to be low and in the centre thus relative high, the amount of water sucked from behind and lateral will be diminished.

IV.5 Optimum sucking techniques

As energetic considerations seem unimportant in suction feeding (Drost & van den Boogaart, 1986b), optimizing suction feeding is maximizing the chance that a prey is captured. An unsuccessful attack may result from bad aiming or from an escape movement of the prey (or a combination). Aiming accuracy (in 3-D) required to catch a prey depends on the shape of sucked the parcel of water and on its total volume. The success of a particular escape movement of a prey depends on the same factors, but also on the duration of the snap and thus on the velocities.

Maximizing the total volume flowed through the mouth aperture during one suction act, can be done by minimizing the initial volume of the mouth cavity, as we see in the initial slitlike mouth cavity and by maximizing the final volume of the mouth cavity (I assume that outflow through the opercular slit will be relatively unimportant in larval fishes, due to frictional effects (Drost et al., in prep.)). Generally, a maximal volume is obtained by a mouth cavity with a circular cross sectional area at each longitudinal position (Osse, 1969). Carp larvae (5.8-9 mm) increase the volume of the mouth cavity relatively much compared to their wet weight (13-19 cm^3/100 g, calculated from data from Drost & van den Boogaart, 1986b: table 1) compared to adult fish (5-8 cm^3/100 g, Alexander, 1970; Casinos, 1973). The influence of parameters as the closure of the mouth edges by maxillaries, protruding praemaxillae and long flexible branchiostegal rays is discussed in Muller & Osse (1984).

The question which shape is optimal for increasing prey capture chance, compare the long and thin parcel of adult trout (van Leeuwen, 1984) with the more spherical parcel for larval carp (Fig. 5), is difficult to answer.

The influence of parameters of form and movement on the total volume flow (before the opening of the opercular valves) can be determined with simple geometric formulae (i.e. the changing volume of a cylinder or cone). Complicated hydrodynamical programs (e.g. Muller & van Leeuwen, 1985; de Jong et al., in prep.; Drost et al., in prep.) must be used to determine shape of the parcel of water sucked into the mouth cavity. The effect of the changing mouth radius on maximal distance of which a prey can be captured (van Leeuwen & Muller, 1984: Fig. 11), may in fact be due to a change in total volume sucked through the mouth aperture.

According to van Leeuwen & Muller (1984) a fish should optimize its sucking during attack by maximizing the prey (i.e. water) velocity at the mouth aperture at the moment that the mouth radius is maximal, because at that moment the prey generally enters. Given the volume flow of the snap, no optimization of mean velocity over time is possible, except by swimming when still at a large distance or by protrusion. Near the mouth aperture the acceleration of prey is very large, because the pressure gradient is generally steepest near the mouth (see Fig. 10 and Drost et al., in prep.) (this is only true if the flow is contracting towards the mouth, i.e. suction is relatively large compared to swimming). Also the velocity is very high. The calculated acceleration of water entering the mouth equalled 800 m/s^2 during suction by larval carp. Maximizing this acceleration seems useless in increasing catch success, unless it is correlated with another, useful, feature, see later. If a prey enters the pressure gradient just in front of the mouth of the predator, it will be caught. If it stays at a (even small) distance of this gradient, it is is able to escape by a relatively small acceleration. So, in my opinion, maximization of water velocity during peak gape (when the prey generally enters the mouth), does not necessarily increase the chance of prey capture. Prey capture chance will by optimized by manipulating the flow in such a way, that acceleration, in the fish bound frame, starts at a larger distance from the mouth aperture. The pressure dip in front of the mouth can be thought to result from a vortex filament, lying near the lips. The form of this pressure dip is always very similar, but its magnitude is dependent on the strength of the vortex. In order to be able to enlarge the acceleration at a certain distance of the mouth the fish must enlarge the acceleration of the mouth aperture itself. I suppose that an acceleration in the moving frame over a large distance can be obtained only by manipulating the swimming (when still at a large distance) and protrusion velocity (i.e. accelerating the mouth aperture).

If the prey can perceive the predator at a distance larger than the attack distance of the predator, the prey will always be able to escape. This happens for example when 15 mm pike larvae are feeding on calanoid copepods. During the formation of the S-shaped attack posture by the larva (which takes about 1 second), the copepod nearly always darts away.

If the prey can perceive a predator from a distance smaller than the attack distance, the prey has to escape within the time of the duration of the snap.

Fast swimming causes the parcel of water sucked into the mouth cavity to be narrow and elongated, slow swimming to be wide and shorter. In adult fishes many feeding types exist with variable contributions of swimming, protrusion and suction (Muller & Osse, 1984; van Leeuwen, 1984). Both swimming and protrusion cause a highly directed waterflow towards the mouth. Small larvae generally are very bad in aiming at their prey (see Drost, in prep.a) and therefore need a rather undirected waterflow, i.e. swimming velocity must be low compared to suction velocity. Protrusion is thus not very useful for larvae till the time they can aim rather accurate. In first feeding carp larvae no protrusion is visible. At a length of 9 mm already a considerable protrusion does occur. The low swimming speed and thus the wide shape of the parcel of water sucked into the mouth cavity (Fig. 5) may also be advantageous for a larva because of the large yaw of the head during prey suction (Drost & van den Boogaart, 1986b): the prey is sucked towards the centroid of the mouth aperture also at moments it is at a large radial distance from the length axis of the mouth cavity. Protrusion might be difficult if the yaw during suction is still high.

So, during their ontogeny a very rapid decrease in aiming inaccuracy is very important for larvae, because bad aiming precludes the use of swimming and protrusion during prey capture, which both are important in increasing the distance from which a prey can be attacked.

IV.6 Escape movements

Maximal velocity required to escape was strongly dependent on the exact timing of the start of the escape movement. This is a consequence of the sinusoidal distribution of velocity in time and the chosen time to peak velocity (20 or 10 ms, rather longer than the duration of the snap (8 ms)). A start several milliseconds before the onset of suction is however not unreasonable because e.g. carp larvae start to swim about 10 ms before the onset of suction (Drost & van den Boogaart, 1986b).

If the acceleration had been taken constant in time, required maximal escape velocity would have been less dependent on exact time of starting the escape.

The most important prey taxa for larval fish are cladocerans, copepods and rotifers. The first two actually have a sinusoidal distribution of the velocity in time (Lehman, 1977; Strickler, 1977; Kerfoot, 1978). Rotifera have an erratically changing velocity with no clear trend in time (Gilbert, 1985). So it seems more important for a fish larva to postpone the moment of its detection by a (cladoceran or copepod) prey, than to maximize the velocity during suction. This conclusion is only valid if the acceleration phase of the zooplankter is longer than the duration of the suction process. At early times the cumulative distance (see Fig. 1) increases (percentually) very rapidly with time, later the increase occurs much more slowly: between t=0.1 tm and 0.2 tm with a factor 7.9, between t=0.6 tm and 0.7 tm by a factor 1.5 (t_m is the time of maximal velocity, see also Fig. 1). Carp larvae however, feed on prey of a much smaller size, than the size of the zooplankters of which the velocity data were determined. The only data about the relation between size and 'escape properties' of copepods are given by Rosenthal (1972). The duration of the jump of Cyclops strenuus seems to be not or only very slightly dependent on size (Rosenthal, 1972), although the filming rate was too low to get unequivocal results. I assume therefore that smaller zooplankters have the same duration of the accelerational phase (10-20 ms). First feeding pike larvae (SL 12-14 mm) do feed on the size of prey of which the velocities were measured. The duration of their suction process is about 25 ms. In this timescale the influence of starting several milliseconds earlier on the distance covered may be much less (see Fig. 1).

According to Kerfoot (1978) cyclopoid copepods can perceive objects at a distance of 2-3 body length. If a carp larva tries to approach a prey to a distance of about 0.35 mm (centre of the parcel of water of Fig. 5), then a maximal prey size would be about 0.1 mm length, because larger prey have perceived the fish before suction has really started and thus can escape. With increasing aiming accuracy larvae get the possibility to swim faster during prey capture and the initial prey distance can rapidly increase. For large fish filterfeeding on copepods or cladocerans the required escape distances are so large, that escape is almost impossible irrespective of the escape possibilities of preys.

In order to escape a prey must avoid to come too close to the mouth of the predator (about 0.25 mm is the boundary in this snap). If the swimming velocity of the predator is low compared to the suction velocity, the best escape direction of the prey is straight forward parallel to the axis of the predator, in

order to avoid to get caught in the pressure dip in front of the mouth. If the swimming velocity is high compared to the suction velocity, the best escape direction is perpendicular to the axis of the predator, the pressure dip near the mouth is then very small. This is the cause in adult trout.

Conclusions

1-Swimming and protrusion, which both increase the distance from which prey can be attacked, become possible options during suction feeding only at the moment that fish larvae can aim accurately at the prey. So, decrease of aiming inaccuracy early during the ontogeny of larvae is of the utmost importance, both for increasing catch success on stationary prey and for feeding successfully on mobile prey.

2-The possible increase in mouth cavity volume in carp larvae is larger than in most adult fish. So a large volume of water can be sucked into the mouth cavity before the moment of opening of the valves. This may compensate for the high aiming inaccuracy.

3-An escape movement parallel to the axis of the predator seems to optimize escape from the centre of the parcel of water sucked into the mouth, if the suction velocity is high compared to the swimming velocity, as occurs in larval carp; a radially directed escape movement seems optimal if swimming is strong relative to suction, as occurs in adult trout.

4-During suction feeding of carp larvae enormous accelerations do occur near the mouth aperture (800 m/s^2).

5-If a prey enters this area of high acceleration it will be caught. So, the escape strategy of a prey should be to stay outside this area of low velocity.

References

Alexander, R.McN., 1970. Mechanics of the feeding action of various teleost fishes. J. Zool. Lond. 162:145:156.
Beyer, J.E., 1980. Feeding success of clupeoid fish larvae and stochastic thinking. Dana 1: 65-91.

Blaxter, J.H.S., 1969. Development: eggs and larvae. In: W.S. Hoar & D.J. Randall. Fish Physiol. 3: 177-252. New York: Academic Press.

Casinos, A., 1973. El mecanisme de deglucio de l'aliment a Gadus callarius L. 1758 (Dades preliminars). Bull de la Soc. Catalana de Biologia I: 43-52.

Drenner, R.W., Strickler, J.R. & O'Brien, W.J., 1978. Capture probability: the role of zooplankter escape in the selective feeding of planktivorous fish. J. Fish. Res. Board Can. 35: 1370-1373.

Drost, M.R., in prep. The relation between aiming and catch succes in larval fishes.

Drost, M.R. & Boogaart, J.G.M. van den, 1986a. A simple method for measuring the changing volume of small biological objects, illustrated by studies on suction feeding by fish larvae and of shrinkage due to histological fixation. J. Zool. Lond. 209: 239-249.

Drost, M.R. & Boogaart, J.G.M. van den, 1986b, in press. The energetics of feeding strikes in larval carp, Cyprinus carpio. J. Fish Biol.

Drost, M.R., Muller, M. & Osse, J.W.M., in prep. A quantitative hydrodynamical model of suction feeding in larval fish.

Drost, M.R. & Verhagen, J.H.G., in prep. Hydrodynamic limitations of feeding in larval fish.

Gilbert, J.J., 1985. Escape respons of the rotifer Polyarthra: a high speed cinematographic analysis. Oecologia (Berl) 66: 322-331.

Hunter, J.R., 1977. Behavior and survival of northern anchovy Engraulis mordax larvae. Cal. Coop. Oc. Fish. Invest. Rept. 19:138-146.

Jong, C de, Sparenberg, J.A. & Vries, J. de, in prep. On the hydrodynamics of suction feeding of fish.

Kerfoot, W.C., 1978. Combat between predatory copepods and their prey: Cyclops, Epischura, and Bosmina. Limnol. Oceanogr. 23: 1089-1102.

Lauder, G.V., 1983. Prey capture hydrodynamics in fishes: experimental tests of two models. J. exp. Biol. 104: 1-13.

Leeuwen, J.L. van, 1984. A quantitative study of flow in prey capture by Rainbow Trour Salmo gairdneri, with general consideration of the actinopterygian feeding mechanism. Trans zool. Soc..Lond. 37:171-227.

Leeuwen, J.L. van & Muller, 1984. Optimum sucking techniques for predatory fish. Trans. zool. Soc. Lond. 37: 137-169.

Lehman, J.T., 1977. On calculating drag characteristics for decelerating zooplankton. Limnol. Oceanogr. 22: 170-172.

Muller, M. & Leeuwen, J.L. van., 1985. The flow in front of the mouth of a prey-capturing fish. In: H.R. Duncker & G. Fleisher (Eds.). Vertebrate Morphology. Gustav Fisher Verlag. Stuttgart, New York. Fortschritte der Zoologie 30.

Muller, M. & Osse, J.W.M., 1984. Hydrodynamics of suction feeding in fish. Trans. zool. Soc. 37: 51-135.

Muller, M., Osse, J.W.M. & Verhagen, J.H.G., 1982. A quantitative hydrodynamical model of suction feeding in fish. J. theor. Biol. 95: 49-79.

Osse, J.W.M., 1969. Functional morphology of the head of the perch (Perca fluviatilis L.),: an electromyographic study. Neth. J. Zool. 19: 289-392.

Rosenthal, H., 1972. Ueber die Geschwindigkeit der Sprungbewegungen bei Cyclops strenuus. Int. Revue. ges. Hydrobiol. 57: 157-167.

Strickler, J.R., 1977. Swimming of planktontic Cyclops species (Copepoda, Crustacea): patterns, movements and their control. In.: T.Y.T. Wu, C.J. Brokaw & C. Brennen (Eds.). Swimming and flying in nature (2): 599-613. 917 pp. PLenum Press. New York, London.

Summary

The food uptake of larval carp and pike is described from high speed movies with synchronous lateral and ventral views.

During prey intake by larval fishes the velocities of the created suction flow are high relative to their own size: 0.3 m/s for carp larvae of 6 mm.

Starting from the first feeding carp larvae have morphological adaptations to suction feeding: the suspensorium and opercula can be abducted, the hyoid lowered, the mouth edges can be sealed by a rotating maxillary and the opercular keeps the opercular slit closed till the moment of prey uptake.

A model has been extended to calculate catch success of larval fishes from aiming inaccuracy (article 3). The absolute aiming inaccuracy (mm) increases during growth, the relative aiming inaccuracy (relative to the standard length) decreases. No causal relation exists between catch success and prey size (unless the prey is too large to pass the mouth aperture)

During the time fish larvae cannot yet aim accurately, they must suck the water undirectedly. By swimming and protrusion a directed field of flow is created. Both are thus unfavorable in this respect, but they are the best ways to catch prey from larger distances. Film analysis showed that protrusion is absent in 6 mm carp larvae, but already 3.8% of the head length in 9 mm larvae. Young larvae have a larger relative increase (to body weight) during suction feeding than adult fishes. This is an optimization of suction feeding by enlarging the volume flow.

A quantitative hydrodynamical model of suction feeding by larval fishes has been made. In the model the mouth cavity is treated as an expanding cylinder. the flow in and around the cylinder is calculated by numerically solving the Navier-Stokes equation in 2-D. Energy costs of suction feeding by larval fishes are negligible compared to the gains: 0.01% for large prey and 10% for very small prey. In an optimal foraging model energetic considerations during suction will be unimportant.

The relation between muscle tension required for suction and fish size is determined. The relation between duration of the suction process, as measured from high speed films from 12-485 mm pikes, was used as input. The required muscle tension appeared to be minimal at hatching and increased with increasing size. Also at sizes smaller than hatching the calculated tension increased (with decreasing size), but the slope was much weaker. So on the basis of this relation no minimal size for the use of suction feeding seems to exist, at small size a freedom for architectural changes seems to be present.

The interaction between suction flow and active escape movements of the prey

determine which types of prey can be caught. For young larvae it is more important to postpone the moment of detection by the prey, than to maximize the water velocity. If the snap lasts longer (e.g. 20 ms) the velocity is important. The reason is that it takes 10 to 20 ms for a copepod or cladoceran to reach maximal velocity.

During suction by carp larvae enormous accelerations of the water do occur (800 m/s^2 in the mouth opening of a 6 mm larva). If a prey enters this region of high accelerations it is impossible to escape.

Curriculum vitae

Maarten Robert Drost werd op 16 maart 1957 geboren in Eindhoven. Het gymnasium B diploma behaalde ik in 1975. Vanuit een populatie gerichte en plantkundige belangstelling ben ik in 1975 aan de Landbouwhogeschool biologie gaan studeren. Het kandidaatsexamen heb ik in 1979 'met lof' behaald. In de loop van de studie is mijn belangstelling naar beestjes en naar een lager integratieniveau veschoven, zoals blijkt uit mijn doctoraal onderwerpen:

1. Bewegingsanalyse van de zuigende prooiopname bij beenvissen, o.l.v. drs. M. Muller.
2. Biosystematiek van graslandcicaden, o.l.v. ir. C.F.M. den Bieman.
3. Bloembezoek bij paardebloemen, o.l.v. dr. A.A. Sterk en ir. C.F.M. den Bieman.

Het ingenieursdiploma is in 1982 'met lof' behaald. Daarna heb ik tot juni een part time aanstelling gehad op de vakgroep EDC. Van 1 juni 1983 tot 1 juni 1986 ben ik bij BION-ZWO in dienst geweest voor dit promotie onderzoek.